A STUDY ON BREEDING PERFORMANCE OF COMMERCIAL LIQUID METAL COOLED FAST BREEDER REACTOR

by

NANAMI KOSAKA

Department of Nuclear Engineering

Faculty of Engineering

University of Tokyo

Japan

A STUDY ON BREEDING PERFORMANCE OF COMMERCIAL LIQUID METAL COOLED FAST BREEDER REACTOR

by

NANAMI KOSAKA

Department of Nuclear Engineering

Faculty of Engineering

University of Tokyo

Japan

Academic Advisers

Professor SHIGEHIRO AN

Associate Professor YOSHIAKI OKA

A thesis submitted in partial fulfilment
of the requirement for the degree of

DOCTOR OF ENGINEERING

at the

University of Tokyo

February , 1981

ABSTRACT

Breeding and safety characteristics of large fast breeder reactors were evaluated with primary emphasis on minimizing doubling time.

The Super-Phenix, 1200 MWe, reactor design was taken as reference reactor in this study and several design parameters which affect breeding performance were changed around this reference design to analyze their effect on doubling time. The best value for doubling time achieved with oxide fuel was 19 years.

Carbide fuel was also considered as future potential LMFBR fuel due to its high density and high thermal conductivity. Carbide fuel provides a reactor doubling time around 12 years. Since the homogeneous core configuration presents a high positive sodium void reactivity a heterogeneous core is recommended to ensure high breeding performance and low positive sodium void reactivity.

TABLE OF CONTENTS

LIST OF FIGURES

page

page

LIST OF TABLES

Page

CHAPTER 1

INTRODUCTION

The world demand for energy grows as man-power is replaced more and more by machine power. It is known that the oil and natural gas are going to decline in the near future, hence to solve the energy problem in future assiduous efforts should be made to develop a new energy system. Among them the most promissing alternative energy is nuclear energy and various kind of thermal reactor system have been developed and are in operation now.

Even considering the vast amount of energy produced by fission of ^{235}U ,uranium-235 atoms are used up, being converted to other atoms during the process. Since there is only a finite reserve of uranium in the earth, it is an exautible, nonrenewable fuel source, just like the fossil fuel.

Nuclear energy strategy calculations have shown that the uranium consumption can be markedly reduced by the large future fast breeder reactors introdution. Present fast breeders under development utilize mixed uranium-plutonium oxide fuel and they present a doubling time ranging from 20 to 30 years.

CHAPTER 1

INTRODUCTION

The world demand for energy grows as man-power is replaced more and more by machine power. It is known that the oil and natural gas are going to decline in the near future, hence to solve the energy problem in future assiduous efforts should be made to develop a new energy system. Among them the most promissing alternative energy is nuclear energy and various kind of thermal reactor system have been developed and are in operation now.

Even considering the vast amount of energy produced by fission of ^{235}U ,uranium-235 atoms are used up, being converted to other atoms during the process. Since there is only a finite reserve of uranium in the earth, it is an exautible, nonrenewable fuel source, just like the fossil fuel.

Nuclear energy strategy calculations have shown that the uranium consumption can be markedly reduced by the large future fast breeder reactors introdution. Present fast breeders under development utilize mixed uranium-plutonium oxide fuel and they present a doubling time ranging from 20 to 30 years.

In the case of uranium supply difficulties or higher energy demands, a reactor with short doubling time will be required. The fast breeder reactors with carbide fuel have a specially greater potential on this respect than one with oxide fuel. Therefore the carbide fuel introduction is the future goal of fast breeder reactor development.

Some researchs concerned with carbide fuel were evaluated in Germany, France and USA. A Germany study has evaluated the feasibility of carbide fuel utilization in SNR/43/ whereas USA reseaxch has investigated the applicability in FFTF/44/ and CRBR/65/ without large modification in the fuel assembly design .

The applicability of the carbide fuel in large commercial reactors has been evaluated by the Argonne National LAboratory/66/ and Combustion Engineering,Inc.,/67/. These works have concentrated on analytical study of nuclear properties for homogeneous core configurations. In order to evaluate the future potential of carbide fuel for LMFBR, the characteristics of several carbide fueled reactor configurations will be investigated in this work. Also heat transfer,nuclear and safety studies are performed and compared with those of the oxide fuel.

Objectives of this work include these three itens:

(1) - To perform several comparative studies around a 1200 MWe reference reactor LMFBR configuration.

(2) - To achieve an improved reactor core design that produces a short doubling time.

(3) - To analyze the inherent safety characteristics of the cores considered.

The first item refers to the analyse of the effect of the several basic design parameters which change breeding performance of reactor. The parameters considered are axial and radial blanket thicknesses, cladding thickness, fuel density and plutonium isotopic composition. The reference reactor design was based on that of the Super-Phénix, the first large fast breeder under construction now.

This study also involves oxide and carbide fuels as well as homogeneous and heterogeneous core configurations.

Outline of the work.

Chapter 2 is introduced as a summary of the requirements for electrical power for a long term and the role of the nuclear power. The uranium demand and resource available are mentioned. The breeder introduction need is emphasized.

In Chapter 3 a brief historical development of FBRs and world program are mentioned.

The model and methodology applied for a reactor performance calculations are described in Chapter 4. Definitions for breeding ratio, doubling time, sodium void reactivity and Doppler coefficient are done.

Chapter 5 describes the nuclear, safety and thermal characteristics calculated for the conventional reactor. A series of oxide designs are studied in which the blanket thicknesses, cladding thickness, fuel density and plutonium isotopic composition are varied around the reference.

Carbide presents some attractive properties like high fuel density and high thermal conductivity to be used as LMFBR fuel. Chapter 6 analyzes the performance of carbide fuel in a large breeder reactor and the results are compared with those of the reference oxide reactor.

Chapter 7 describes all study data for three heterogeneous core configurations with carbide fuel. The advantages of this configuration are analyzed. A summary of carbide fuel development programs are mentioned specifying the areas that require attention.

Chapter 8 provides an analysis about breeding ratio improvement verified due heterogenization. The fertile material inventory and neutron spectrum effects on breeding ratio are analyzed.

Chapter 9 summarizes major conclusions of this work.

CHAPTER 2

PERSPECTIVE ON NUCLEAR POWER

2.1 WORLD ELECTRICAL ENERGY GROWTH

Demand of energy will continue to grow even with vigorous policies to conserve energy adopted by countries. There is general agreement that, with respect to fossil fuels the oil and natural gas reserve are so restrictive that before the end of this century a marked decline in the supply of these fuels will be observed. Thus the balance between supply and demand requires that new energy sources be developed quickly. The uranium was chosen today as source of electrical energy to save the fossil fuels which are needed for transport and as row material for pharmaceuticals, plastics and other important commodities.

The projections of total energy demand and distribution of demand between different sources for a long time are surrounded by uncertainty. Accoding to preliminary assessment of electricity demand prepared for the World Energy Resource Conservation Commission /1/, the world energy demand in the year 2020 is expected to be between three and four times present consumption if average

economic growth is between 3.0 and 4.1 per cent year. The world electrical demand is estimated to be 39.8 EJ(*) by 1985, rising to 98.5 EJ by 2000 and 237.7 EJ by 2020. On the other hand, according to WAES studies /5/, total primary energy demand in the year 2000 ranges from 344 to 445 EJ. Another report, OECD-Nuclear Energy Agency/International Atomic Energy /2/ predicts 285 EJ by 1985, 360 EJ by 1980, 559 EJ by 2000 and 1,088 EJ by 2025 for world primary energy requirements, while the electrical power share will be about 34 per cent of primary energy by 1985, 37 per cent by 1990 and 43 per cent by 2000.

Although different energy growths are predicted it is clear that new sources of energy must be developed to substitute the fossil fuels. Nuclear energy continues to be one of the attractive ways to generate the required electrical power. Another sources as solar energy and nuclear fusion cannot contribute too much substantialy in the next half century.

2.2 GROWTH OF NUCLEAR POWER

The projected increase in world electricity demand would not met without a major contribution from nuclear power. The estimates of nuclear power growth presented here are based on WEC report /1/ and OECD-NEA/IAEA /3/ works.

(*) EJ = 10^{18} joules

WEC forecasts show that the nuclear share of world electricity output could be almost 45 per cent by the year 2000 and might be as higher as 65 per cent by 2020. The world total nuclear generation capacity implied by these percentage would be between 1,300 and 1,900 GWe in the year 2000 and between 3,200 and 5,500 GWe in the year 2020, provided the mining and production facilities could be developed in time. On the other hand, OECD-NEA/IAEA prediction for the year 2000 is 1,200 GWe for the high forecast and 833 GWe for low forecast. The future nuclear power growth estimates adopted by INFCE for 1800-2000 are shown in Tab. 2.2.1.

Nuclear power is viable and commercially compepetive now and its contribution is most conveniently supplied in form of electrical power. At present the most of nuclear power reactor is based on non breeding cycle where only U-235 is the principal fissioning isotope.

In September 1980, the world installed capacity was 122 GWe, within this total light-water reactors represent 84.10 per cent, gas-cooled graphite moderated reactors represent 9.1 per cent and heavy-water reactors 5.1 per cent /4/. The INFCE estimation for the world reactor distribution up to 2000 is listed in Tab. 2.2.2.

In the future there will be an increasing incentive in many other application areas, for example, for process heat in industry. Other potential area of use includes

district heating and manufacture of syntetic fuel.

To support this continuous growth of nuclear power a substantial addition to uranium reserves or a new technology for efficient usage of fuel will be necessary.

2.3 URANIUM RESOURCE AND DEMAND

2.3.1 Uranium Resource

If nuclear power is to play a major role in nation's electric energy economy and thereby important contribute to the world overall energy needs, adequate supply of uranium must be available at acceptable cost.

The most recent world resource of uranium survey has been published by OECD Nuclear Energy Agency/IAEA. According to this report /2/ the reasonable assured uranium resources at cost up to $130/kgU are measured in 2.60 million tonnes U. The world wide uranium resources position at 1st January 1979 is summarized in Tab. 2.3.1 for the cost ranged up to $130/kgU.

In addition to these resources there are higher cost, generally lower grade resources. In evaluating the uranium resources it is important to considered whether all this material could be available at a rate sufficient to satisfy demand. In next sections the balance between uranium demand and supply is analyzed.

2.3.2 Uranium Production Capabilities

In conformity with OECD-NEA/IAEA report /2/ the uranium production was amounted about 38,000 tonnes in 1979 while the maximum attainable production capacity is about 44,000 tonnes/year. This capacity would increase to 119,000 tonnes/year by 1990 based on currently estimated uranium resources. After the year 2000 uranium production from known resources will decrease and uranium supply will come to dependent more and more on resources which will be explored. Tab. 2.3.2 shows the future projections for uranium production and it is essentially an estimate of the maximum rate of production that can be expected from known resources.

2.3.3 Uranium Demand

Nuclear power will grow in different ways in different countries, thus the energy supply as well as demand prediction for a long time faces many uncertainties.

Most of energy planners would probably agree that nuclear energy appears to be the most practical energy source for a long range perspective. However, the naturally occurring fissile isotope U-235 is not sufficiently abundant to support, by itself, a nuclear power program for more than a few decade, specifically, 15 to 20 years according to the OECD report.

To arrive at a plausible overall energy demand scenario for the 1980-2025 period, a number of fore-

casts and predictions have been examined. The strategies discussed in the literatures /1,2,5,6,7,8/ include a contribution of the several reactor types, namely light-water reactor (LWR), fast breeder reactor (FBR), heavy-water reactor (HWR) and advanced converter reactor (ACR).

The WAES/5/ estimates the future installed nuclear capacity about 2,000 GWe by the year 2000 at an annual growth rate of about 15 per cent. This nuclear growth correspond an estimates cumulative uranium requirements of about 3.0 million tonnes of uranium. According to OECD-NEA/IAEA report, on the other hand, the cumulative requirements for the period of 1980 to 2025 could be in the range 3.4 million to 12.0 million tonnes U depending on the rate of growth of nuclear power, the choice of reactors and the treatment of spent fuel.

Tab. 2.3.3 summarize the cumulative uranium requirements for four nuclear reactors stratey considered by INFCE and Fig.2.3.1 and Fig. 2.3.2 show the annual world uranium supply and demand to 2025 for low and high growth projections, respectively. The nuclear reactor strategy until 2000 will be principally based on the Ligth Water Reactor. It is expected that commercial introduction of FBRs will become significant in the mid-1990.

Analyzing uranium demand and supply data, one can see that fast breeder introduction is essential if nuclear energy is to be sustained as a substantial source of

world energy much beyond the end of this century /9/.

2.4 BREEDER PRINCIPLES AND FBR INTRODUCTION

Of the fissionable isotopes, U-233,U-235 and Pu-239,only U-235 occurs in nature where it makes up about 0.71 per cent of the natural uranium. Though the over two fissionable isotopes do not exist in nature they can be manufactured.

In reactors as LWR the fuel used is enriched uranium with 3.0 to 3.5 per cent uranium-235 and less than 5 per cent of the total weigh of fuel in the core is fissioned before the fuels are removed. Furthemore, a large amount of natural uranium has been used,whereas in fast breeder reactor, by its characteristics, a large fraction of natural U or Th ores can be fissioned /12/ multiplying, perhaps more than 50 times, the usability of natural uranium resources.

The breeding principle consist of transforming the fertile material into new fissile material, consequently a fast breeder produces more new fissionable material then it consumes. It provides a way to use most of the 99 per cent of natural uranium that is the nonfissionable U-238 or the thorium ore.

In the case of fission reactors,two kinds of reaction lead to breeding. The chain for the production of plutonium from uranium ($^{239}Pu/\ ^{238}U$) and uranium from

thorium (^{233}U/ ^{232}Th) are described by following chains:

a) $$_{92}U^{238} \xrightarrow{(n,\gamma)} {}_{92}U^{238} \xrightarrow[23.5\ min]{\beta^-} {}_{93}Np^{239} \xrightarrow[2.85\ d]{\beta^-} {}_{94}Pu^{239}$$

b) $$_{90}Th^{232} \xrightarrow{(n,\gamma)} {}_{90}Th^{232} \xrightarrow[23.4\ min]{\beta^-} {}_{91}Pa^{233} \xrightarrow[27.0\ d]{\beta^-} {}_{92}U^{233}$$

The more complete chains are shown in Fig. 2.4.1 and Fig.2.4.2.

As shown in Tab.2.4.1 a number of fast breeder concepts could be considered with various types of fuel and fertile material, coolants and reactor arrangement. The main type of fast breeder presently under construction for power reactor is Liquid Metal Cooled Fast Breeder Reactor (LMFBR) type. It is a liquid metal (Na) cooled reactor with (UO_2-PuO_2) fuel in the core and depleted UO_2 in the blankets.

The LMFBR by its characteristics can produce energy and simultaneously produce fuel in the greater quantities than it is consumed. The plutonium produced by existing LWR will be used in LMFBR and thermal reactor and fast breeder will probably coexist for a number of years till FBR-FBR self fuel cycle will become possible.

TABLE 2.2.1

INFCE ESTIMATES OF NUCLEAR POWER GROWTH IN THE WORLD /2/ , /3/

	INSTALLED CAPACITY , GWe						
year	1980	1981	1985	1990	1995	2000	2025
Low growth	144	163	257	433	617	833	1,800
High growth	159	181	303	533	805	1,206	3,900

TABLE 2.2.2

WORLD REACTOR DISTRIBUTION (1980-2000) /2/ , /3/

(GWe)

	LWR (Light water reactor)		HWR (Heavy water reactor)		AGR (Advanced gas cool.reac)		CG (Graphite gas reac)		HTR (High temp. gas reactor)		FBR (Fast breeder reactor)		TOTAL	
year \ growth	L	H	L	H	L	H	L	H	L	H	L	H	L	H
1980	126.0	140.8	7.6	7.8	2.9	2.9	7.1	7.1	0.3	0.3	0.5	0.5	144.4	159.4
1981	141.7	159.5	8.2	8.4	4.9	4.9	7.1	7.1	0.6	0.6	0.5	0.5	163.0	181.0
1985	228.0	273.1	14.9	15.7	4.9	4.9	6.7	6.7	0.6	0.6	2.0	2.4	257.1	303.4
1990	387.7	483.7	25.9	29.0	8.0	8.0	4.2	4.2	1.6	1.6	5.4	6.9	432.8	533.4
1995	544.7	717.6	43.6	55.8	12.4	12.4	0.8	0.8	2.6	2.6	12.7	15.8	616.8	805.0
2000	716.8	1,040	73.5	101.0	16.8	23.0	0.0	0.0	3.6	3.6	21.8	38.2	823.5	1,205.6

L: low growth

H: high growth

TABLE 2.3.1

WORLD URANIUM RESOURCES /2/

(1,000 tonnes U)

	(*) $80/kgU ($30/lbU_3O_8)	$80-$130/kgU ($30-50/lb$U_3O_8$)	Total at $130/kgU
Reasonable assured resources	1,850.0	740.0	2,590.0
Estimated additional resources	1,480.0	970.0	2,450.0

(*) defined as "Reserve"

TABLE 2.3.2

PRODUCTION OF MAXIMUM ATTAINABLE URANIUM PRODUCTION CAPACITIES (1980- 2020) /2/

(1,000 tonnes U)

Year	Total World
1980	50.1
1985	98.0
1990	119.3
1995	123.0

Year	Total World
2000	114.8
2005	94.0
2010	82.9
2020	57.8

TABLE 2.3.3

CUMULATIVE URANIUM REQUIREMENTS FOR DIFFERENT FUEL CYCLE STRATEGIES FOR THE WORLD /2/

(1,000 tonnes U)

	LWR		FBR		LWR/FBR Mixed strategy			
	Once-through cycle		U/Pu fueled advanced FBR		10% in 2025 oxide fueled FBR		60% in 2025 advanced FBR	
	L	H	L	H	L	H	L	H
1980	29	32	28	32	28	32	28	32
1990	499	617	447	561	455	568	454	568
2000	1,520	2,080	1,270	1,763	1,280	1,780	1,250	1,690
2015	4,620	6,810	2,730	3,759	3,370	5,400	2,740	3,990
2025	6,710	12,040	3,420	4,590	5,180	9,240	3,690	5,790

L: low growth

H: high growth

TABLE 2.4.1

DESIGN VARIABLES FOR FAST BREEDERS

Fissile material	U-235,Pu mixtures
Fertile material	U-238, depleted U,Th-232
Types of fuel	metal,oxide,carbide
Reactor coolant	liquid metal(Na,NaK) gas (He,CO_2)
Reactor arrangement	integrated concept (pool) loop design

FIG 2.3.1 /2/

COMPARISON OF ANNUAL WORLD[1] URANIUM
SUPPLY AND DEMAND TO 2025
(modified INFCE diagram)
LOW GROWTH PROJECTION - ILLUSTRATIVE STRATEGIES

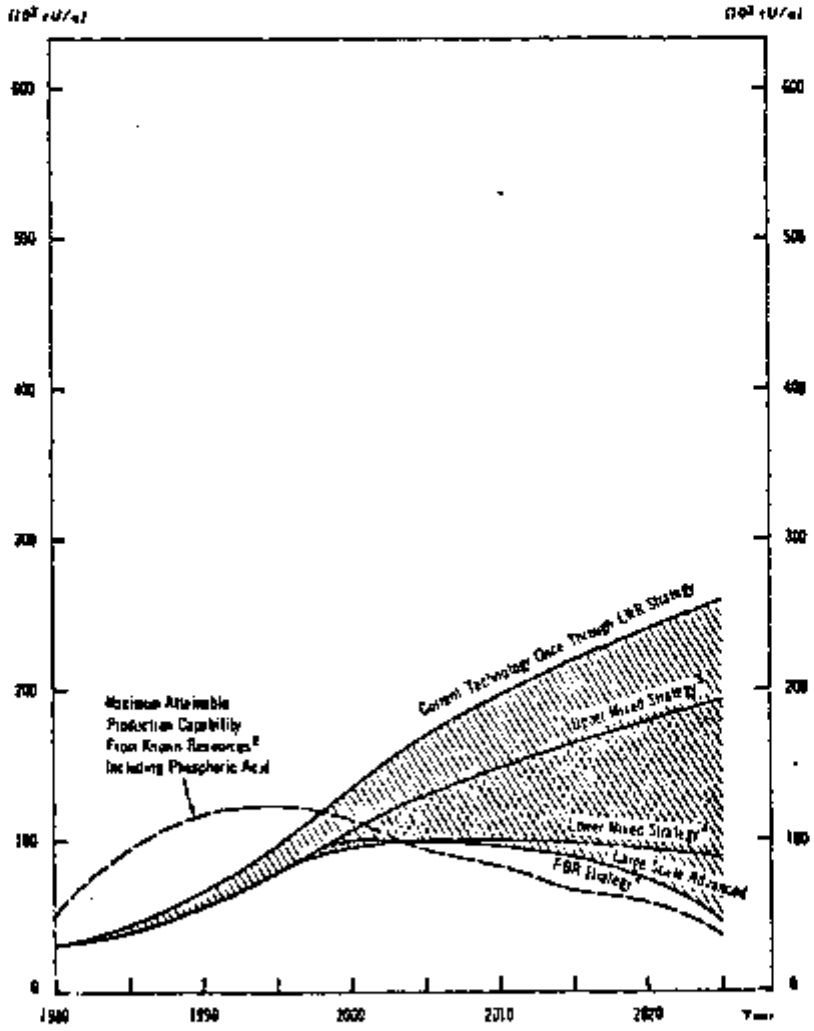

1. Data were not supplied nor included for USSR, Eastern Europe nor China.
2. Reasonably Assured plus Estimated Additional Resources.
3. With Oxide-fuelled FBRs.
4. With Carbide-fuelled FBRs.

FIG 2.3.2 /2/

COMPARISON OF ANNUAL WORLD[1] URANIUM
SUPPLY AND DEMAND TO 2025
(modified INFCE diagram)
HIGH GROWTH PROJECTION - ILLUSTRATIVE STRATEGIES

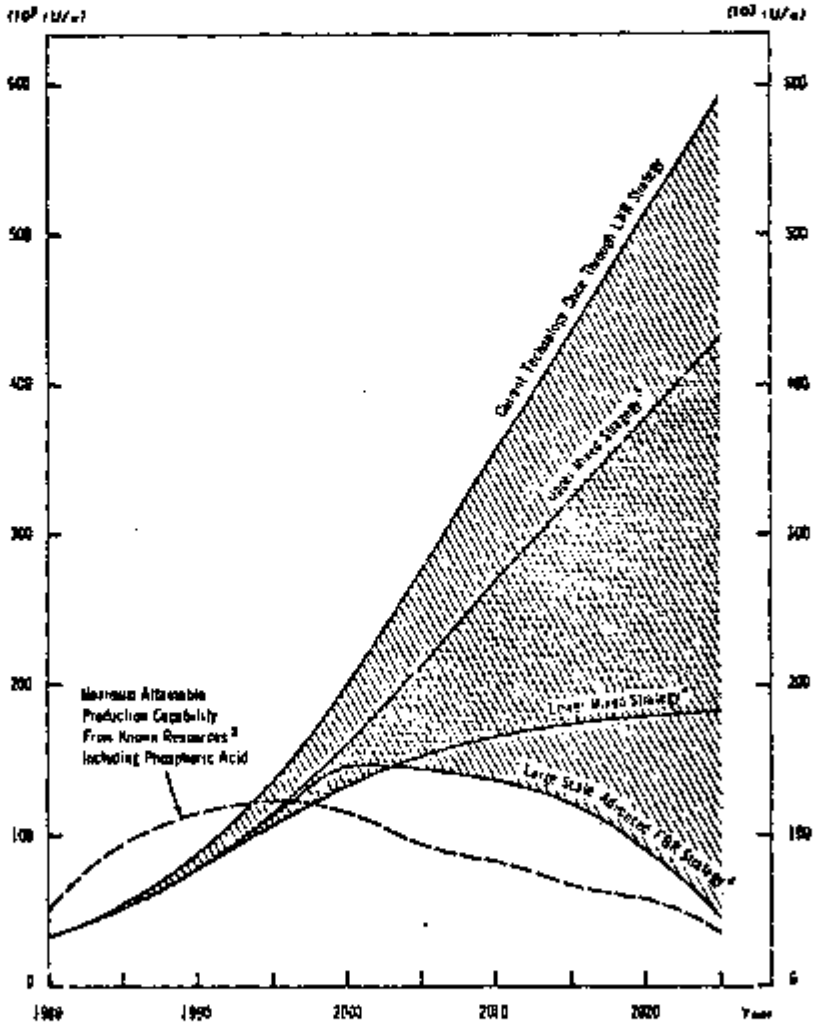

1. Data were not supplied nor included for USSR, Eastern Europe nor China.
2. Reasonably Assured and Estimated Additional Resources.
3. With Oxide-fuelled FBRs.
4. With Carbide-fuelled FBRs.

FIG 2.4.1

URANIUM-PLUTONIUM CONVERSION

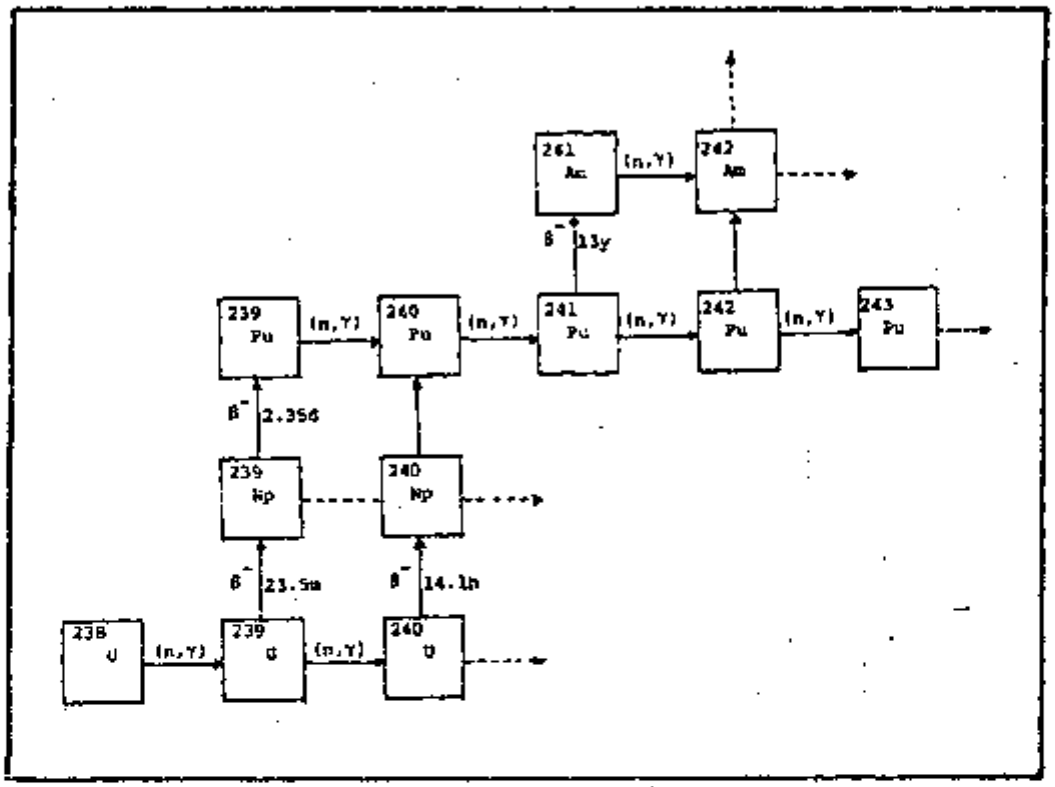

FIG 2.4.2

THORIUM -URANIUM CONVERSION

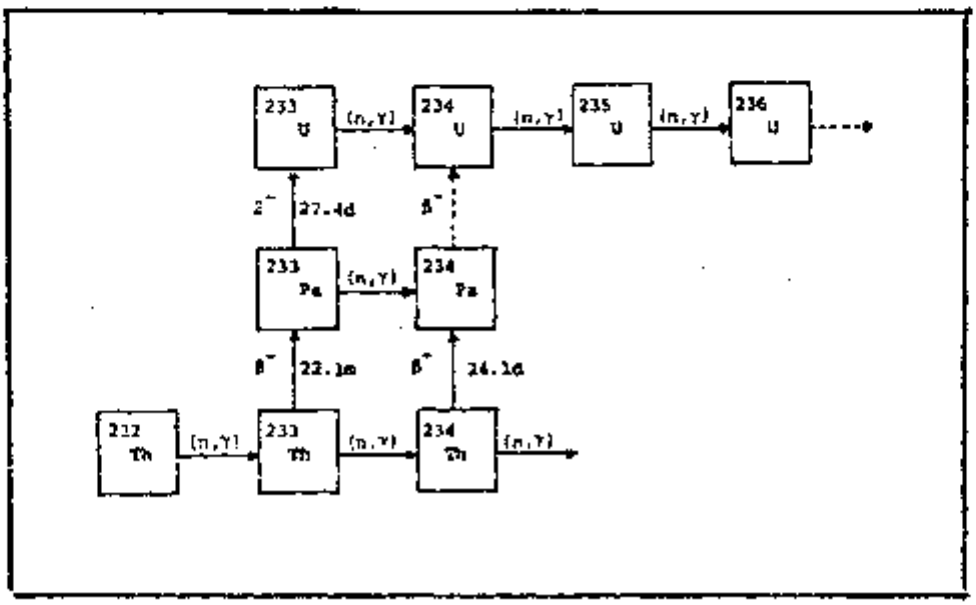

CHAPTER 3

FAST BREEDER REACTOR

3.1 HISTORICAL FBR DEVELOPMENT AND WORLD PROGRAM

The development of fast breeder reactors first followed the line of metallic fuel element and their power was only few hundred megawatts. It is represented by early concepts such as that of the first generation fast breeder reactor. As matter of fact, the first fast breeder reactor, CLEMENTINE, was operated in 1946 at Los Alamos (USA) with mercury coolant. The first power reactor, EBR-I, was started in 1951 generating 100 kWe.

Since 1950 a large amount of research and development has been carried out around the world in the fast breeder field, mostly in USA, USSR, France, Germany , Italy, UK and Japan.

The second line of fast breeder development is distinctly different in terms of fuel technology, reactor physics, safety and as well as power plant characteristics. Mixed plutonium-uranium dioxide is used as reactor fuel. This phase is known as " Second Generation Fast Breeder " and one can mention Joyo, SEFOR, FFTF. The characteristics these

reactors are listed in Tab. 3.1.1 /10/.

Design and costruction of reactor of the 300 MWe class began between 1965 and 1970. The reactor size of 300 MWe is considered a first step towards to the construction of large commercial size breeder of the 1000 to 1500 MWe class. Some of the 300 MWe LMFBRs are alredy in operation such as the Soviet BN-350 that became critical in 1972; the French prototype fast breeder Phenix has been operating since 1974. The British PFR and the Soviet BN-600 are also in operation now; the German prototype SNR-300 is still under construction while US Clinch River Breeder Reactor and the Japan Monju construction are expected to start soon. The Tab.3.1.2 shows the demonstration reactors characteristics, while Tab.3.1.3 shows the future commercial fast breeder reactors planned, only the French Super-Phenix with 1200 MWe is under construction / 13,14,15 /. Table 3.1.4 gives the time schedule for FBR development in the world.

Generally the development and evaluation of new major technologies is seen to follow a pattern that distinguishes three degree of feasibility, as:

- scientific feasibility ;
- engineering feasibility ;
- commercial feasibility.

In case of fast breeder development the technologies for liquid sodium as coolant and for mixed oxide as fuel are essentially in hand. It can ,therefore, be

considered that the phases of scientific and engineering feasibility have almost passed, the commercial feasibility however has not yet passed.

The success and the early commercialization of the LMFBR will depend on the success of Super-Phenix operation and performance. Commercial feasibility of LMFBR also includes the remaining part of the fuel cycle such as fuel fabrication plant, fuel reprocessing plant and their waste disposal must be fully developed.

The energy crisis has reemphasized the importance of achieving a short doubling time in a FBR to save world uranium resources. The next target then will be develop an advanced FBR fuel with thermal and neutronic properties superior to those of mixed oxide. Carbide fuel can satisfy above conditions and will achieve a shorter doubling time than oxide fuel.

3.2 CORE DESIGN PARAMETERS SPECIFICATION PROCEDURE

3.2.1 Core Design Procedure

The various parameters that contribute to core design generally are not indepedent but form an interrelated matrix in which the degree of influence of one parameter on another may vary considerably. The desired reactor core parameters are generated from trade-off envolving a lot of parameters interdependent.

The primary analytical areas are: nuclear

design, thermal-hydraulic desig, material design,safety design and economic related design, and the desired design specifications are determined by considering all the analytical areas. Fixed conditions,together with data needed for the analysis, such as cross sections, thermal and material properties, serve as input in each analytical areas. The required fuel loading, flux and power distribution are obtained from the nuclear design, and some feedback to both the nuclear data and thermal-hydraulic design.

The coolant temperature,flow and velocity and geometric arrangement evolve from the thermal-hydraulic design. Thermal conditions also contribute some feedback to the material specifications. The thermal condition is also taken as the limiting criteria for the core design. This representation emphasizes some important interdependencies among the design parameters.

In this study only nuclear design and thermal design are considered with safety design analysis. Since fast reactors are important primaly because of their potentially high breeding ratio, the design objective is to obtain a high breeding ratio or specifically a short doubling time. So, the parameters associated with the production of new fissile fuel from fertile material are of interest. However the core breeding ratio tends take a dependent variable rather than a primary design objective since the design is also related with reactor size and configuration

from the heat-removal view point, coolant characteristics and perhaps various safety requirements.

The sequence of a design approach taken in this study is showed in Figs. 3.2.1, 3.2.2 and 3.2.3. First the homogeneous core design was taken into account and later the heterogeneous core was considered. Some design parameters are taken fixed and the fuel center temperature and cladding surface temperature were considered as limiting criteria.

3.2.2 Nuclear Analysis

The design decision concerned with selecting fuel element composition and diameter are critical to fuel cycle economics. Design data on the thermal conductivity and limiting temperature of the fuel are used to compute the design limit linear power rating on the fuel element.

Fig. 3.2.1 shows a flow diagram for a core design approach considered where each step is described bellow:

- Fuel pellet diameter is specified ;
- Cladding thickness and gap are specified ;
- With wire diameter defined and space between pins fixed the pin pitch is determined ;
- With core power and core heigh specified, the total number of pin fuel in the core is calculated ;
- Number of subassemly is determined as well as the

subassembly pitch ;

- After definition of the assembly, the core material volume fraction is determined. The coolant volume fraction is a dependente parameter deduced from coolant velocity ;
- Core sizing is determined. ;
- Reactor size is defined and geometric parameters are specified. The axial and radial blanket thicknesses are fixed ;
- Neutronic calculations are evaluated. The fuel enrichment is determined taking into account the peaking factor and k_{eff} at EOEC ;
- Power density distribution is calculated and linear power is determined ;
- Nuclear characteristics calculated are :
    - breeding ratio, doubling time, fuel inventory and power distribution ;
- Axial linear power profile is determined for the maximum power channel and thermal analysis is evaluated .

3.2.2 Thermal Analysis

In this process, thermal analysis begins with primary coolant inlet temperature and mean outlet temperature specifications (see Fig.3.2.2) and

- The coolant temperature profile in the maximum power channel is determined ;
- The axial profile of the cladding temperature is calculated

using axial power profile and empirical correlations for the surface heat transfer coefficient ;

- Cladding inner surface temperature profile is computed;
- With gap conductance specified the fuel surface temperature is computed ;
- Using empirical correlation for thermal conductivity the fuel center temperature is calculated ;
- Coolant mass flow rate necessary to mantain the difference between inlet and outlet temperatures equal to 150 °C is calculated ;
- From coolant flow area determined in design specification the coolant velocity is calculated.

The calculated maximum fuel center temperature and maximum cladding outer surface temperature are compared with allowable temperatures specified from material properties. The coolant velocity is also compared with the permitted value.

If the temperature at the fuel center or at cladding surface is superior than that the allowable temperature the new fuel pin diameter is considered and the calculations are performed again. If the coolant velocity is too high the coolant volume ratio is reconsidered and the calculations are repeated.

The limiting criteria adopted are ;

- Maximum allowable temperature at fuel center

for oxide fuel : 2400 °C

for carbide fuel : 1800 °C

- Maximum permitted temperature at cladding surface: 620 °C
- Coolant velocity recomended : 5-7 m/sec

3.2.4 Safety Analysis

In the safety analysis the remote possibility of a total voiding in the core (total loss of coolant) is accepted. Doppler coefficient and sodium void reactivity are calculated in this condition (Fig.3.2.3).

The severity of the reactivity change perhaps can be reduced by proving a enhanced Doppler coefficient or reducing the void coefficient. The second option can be obtained in modifying the reactor core configuraton, for example, to heterogeneous one.

TABLE 3.1.1 SECOND-GENERATION EXPERIMENTAL FAST REACTORS

Reactor	USA		Japan	France	Germany	Italy	USSR
	SEFOR	FFTF	JOYO	RAPSODIE	KNK-II	PEC	BOR-60
Reactor Power							
Thermal (MWth)	20	400	100	40	58	130	60
Electrical (MWe)	0	0	0	0	20	0	12
Core							
Fual	PuO_2/UO_2	PuO_2/UO_2	PuO_2/UO_2	PuO_2/UO_2	PuO_2/UO_2 +UO_2	UO_2	PuO_2/UO_2 or UO_2
Core Volume (l)	500	1030	280	45	320	420	53
Max. Linear Power (W/cm)	650	500	430	400	430	400	590
Coolant Temp. (°C)							
Inlet	370	320	370	410	360	375	360
Outlet	430	480	500	530	550	525	600
Coolant Material	Na	Na	Na	Na	Na	Na	Na
Date of OPeration	1969	1978	1977	1970	1977		1969

TABLE 3.1.2 FAST BREEDER DEMONSTRATION REACTORS

Reactor	France	FRG	Japan	UK	USA	USSR	
	Phenix	SNR-300	Monju	PFR	CRBR	BN-350	BN-600
Reactor Power							
Thermal (MWth)	563	736	714	600	950	1000	1480
Electrical (MWe)	250	312	300	270	360	350	600
Core							
Height (cm)	85	95	90	91	91	106	75
Diameter (cm)	139	178	178	147	188	158	205
Fuel Pin Diameter (mm)	6.6	6.0	6.5	5.84	5.84	6.1	6.9
Max. Linear Power (W/cm)	430	460	457	450	475	470	530
Burnup (MWD/T)	50,000	55,000	80,000	70,000	80,000	50,000	90,000
Coolant Temp. (°C)							
Inlet	400	377	390	400	387	300	380
Outlet	560	546	540	562	540	500	550
Breeding Ratio	1.16	1.0	1.2	1.2	1.23	1.4	1.3
Operation Data	1973	1982	1986	1975	?	1973	1979

TABLE 3.1.3

COMMERCIAL REACTOR DESIGN PARAMETERS

Reactor	Super Phenix France	CFR-1 UK	SNR-2 FRG	GCFR FRG
Power				
Thermal (MWth)	2910	2900	3420	2780
Electrical(MWe)	1200	1320	1300	1030
Core dimension				
Height (cm)	100	100	100	
Volume (cm^3)	10.2		8.8	10.2
Fuel pin diameter (mm)	8.5	6.0	7.5	8.2
Peak linear power (W/cm)	450	420	450	
Max. burnup (MWD/T)	70,000	85,000	80,000	100,000
Coolant	Na	Na	Na	He
Coolant temperature				
Inlet (°C)	395	370	380	273
Outlet(°C)	545	540	550	555
Specific fissile inventory (kg Pu/MWe)	4.6	2.3	3.1	3.3
Breeding Gain	0.18	0.16	0.18	0.45
Doubling Time (y)	42	37	41	
Status	under construction	planned	planned	planned

TABLE 3.1.4 TIME SCHEDULE FOR FBR IN THE WORLD /10,11/

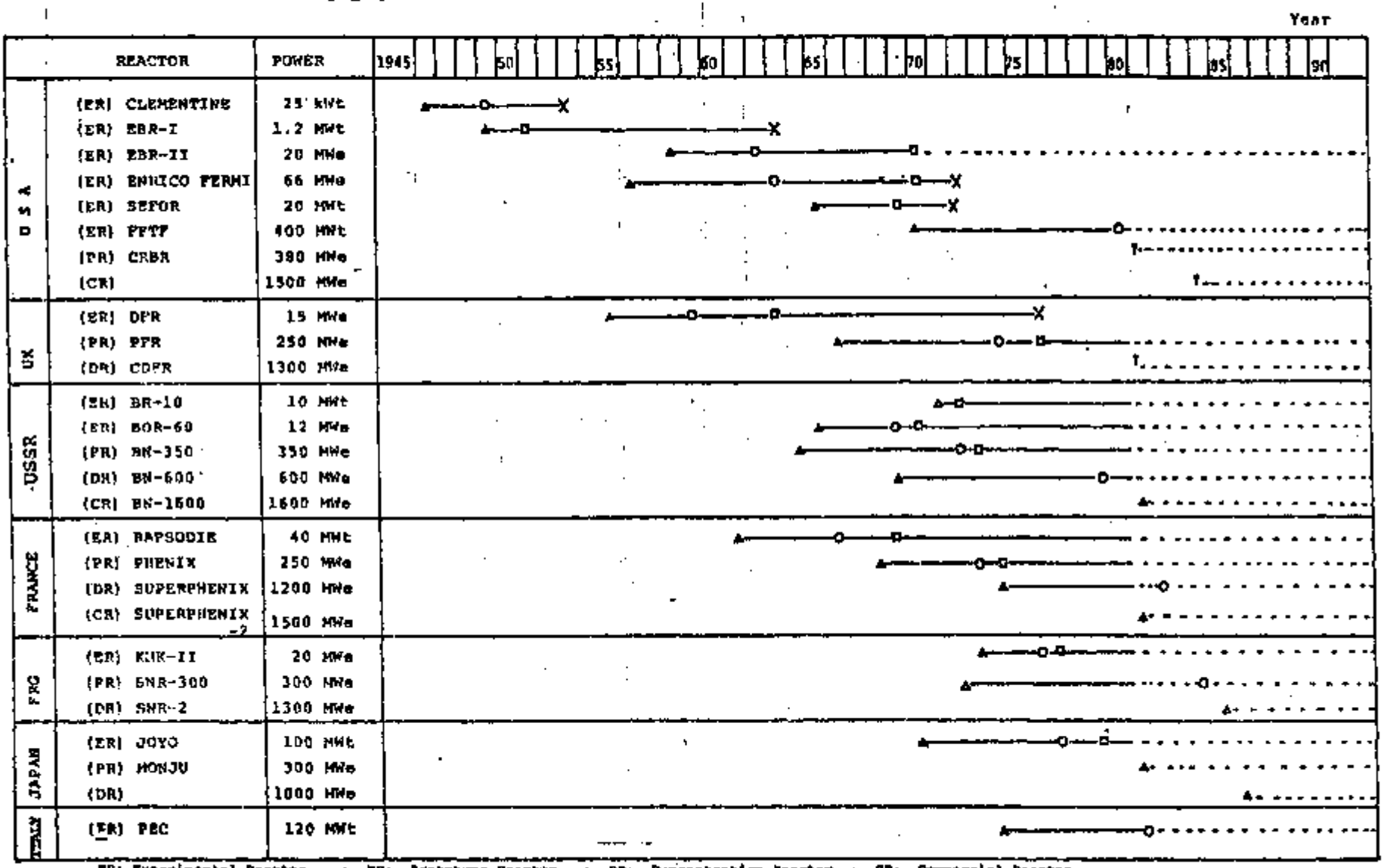

ER: Experimental Reactor , PR: Prototype Reactor , DR: Demonstration Reactor , CR: Commercial Reactor

A: Construction O: Criticality □: Full power operation X: Shut-down

FIG 3.2.1 NUCLEAR ANALYSIS

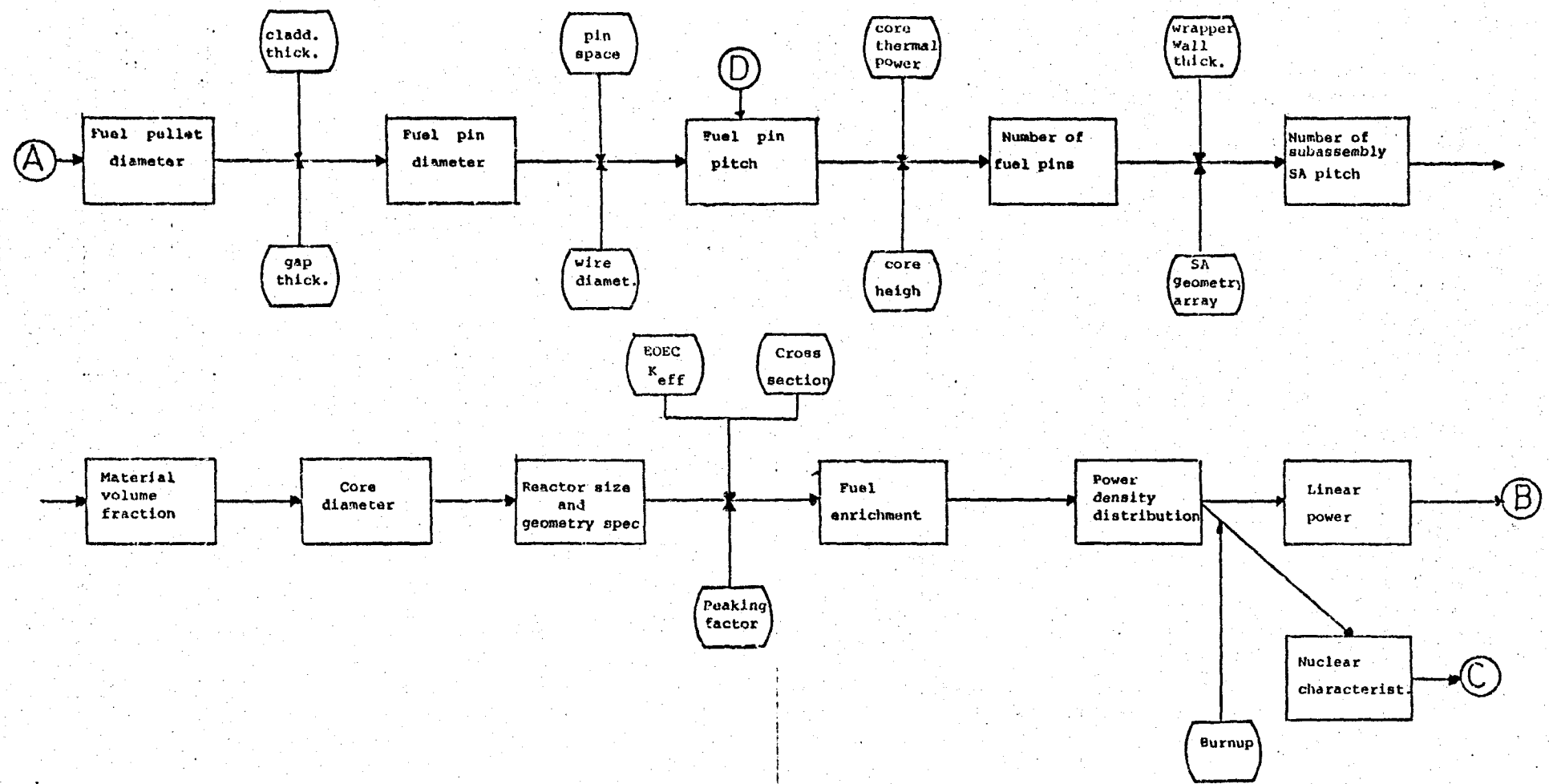

FIG 3.2.2 THERMAL ANALYSIS

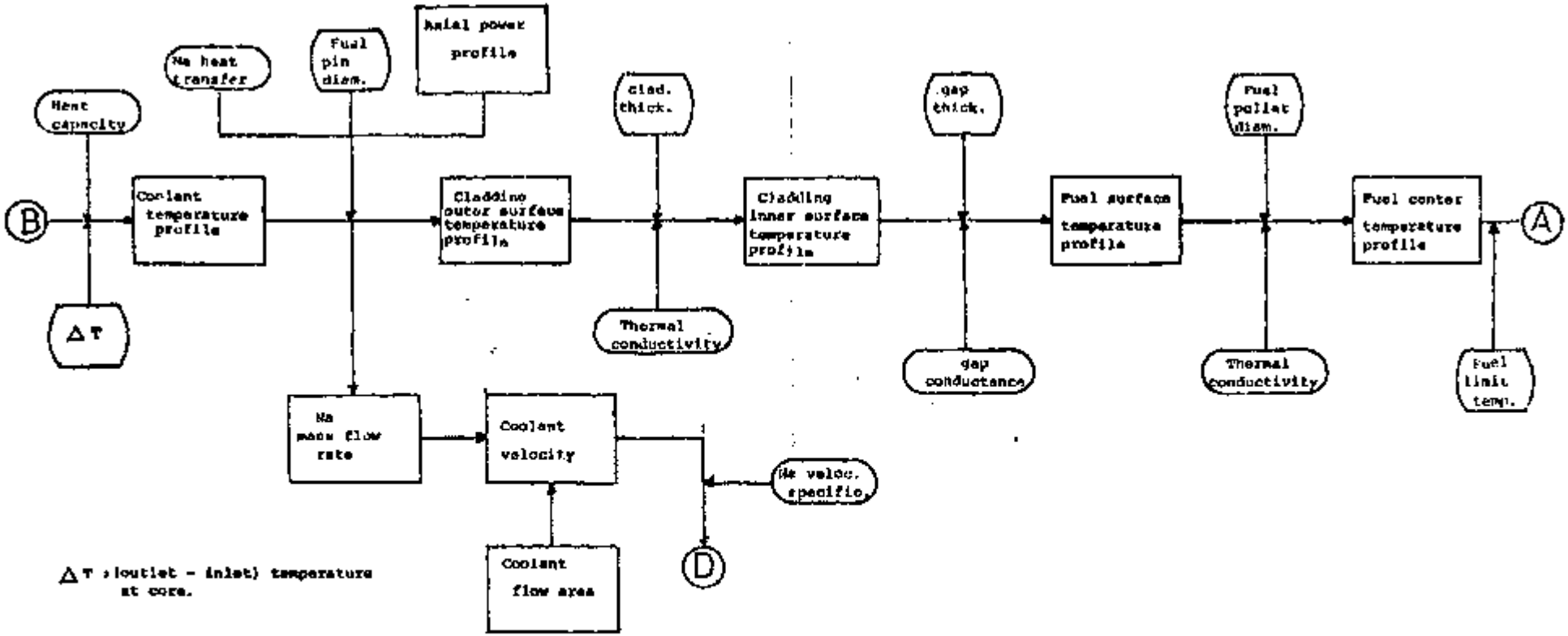

FIG 3.2.3

SAFETY ANALYSIS

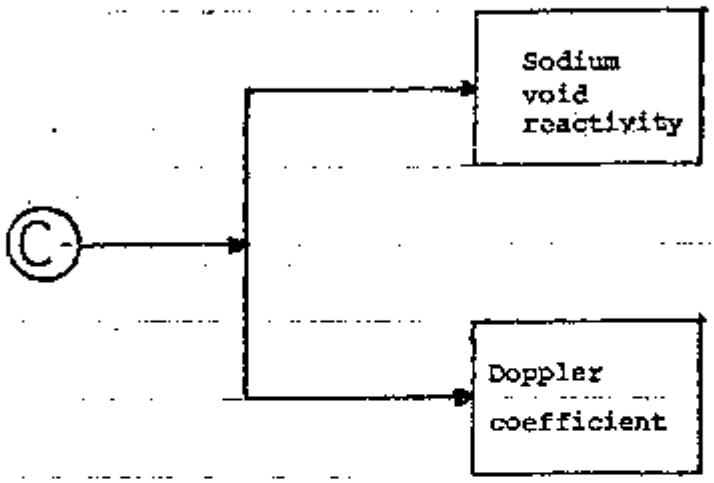

OBS:

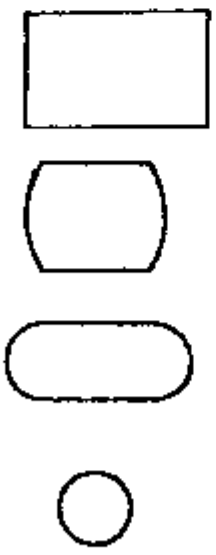

CALCULATED PARAMETERS

DESIGN SPECIFICATIONS

DESIGN DATA

STAGE LINK

CHAPTER 4

CALCULATIONAL METHODOLOGY

4.1 PHYSICAL MODEL

The homogeneous reactor configuration analyzed in this study is shown in Fig. 4.1.1. In the plutonium-uranium fueled fast breeder homogeneous reactor the core consists of plutonium-uranium mixed fuel pins and it is subdivided into two enrichment zones to minimize the radial power peaking factor. Surrounding the core is a blanket of depleted uranium which absorbs neutrons leaking from the reactor core and produces additional plutonium. Blanket consists of two parts, axial and radial. Cooling is accomplished by means of liquid sodium in the case of LMFBR and the plutonium loaded in the core is supplied from light water reactor.

For the calculations the reactor was modeled in R-Z geometry with two core zones, a radial blanket zone, a radial reflector zone, an axial blanket zone and an axial reflector zone and each zone was homogenized into equivalent annular rings as indicated in Fig.4.1.2. The control rods were negleted. The heterogeneous configuration will be described in Chapter 7.

4.2 NUCLEAR PROPERTIES CALCULATIONS

4.2.1 Cross Section Set

Two computer codes were used to determine the reactor physics parameters. APOLLO /16/ a two-dimensional, multigroup diffusion theory code and ANDROMEDA /17/ a one-dimensional diffusion code.

All calculations were performed with 3 or 6 neutron energy groups collapsed from 25-group data library, the JAERI-FAST-SET 2. The collapsed energy groups were corrected for resonance self-shielding and spacial flux weighting. The 3 and 6 group strucutures are shown in Tab. 4.2.1 .

4.2.2 Methodology

The iterative scheme represented in Fig.4.2.1 was used to determine the beginning of life (BOL) fuel enrichment and the physical parameters of reactor. The calculation procedure aimed at minimizing the power peaking factor while keeping reactor criticality condition at end-of-equilibrium cycle (EOEC).

The scheme starts with a guess of BOL fuel composition and minimum peaking factor survey is realized with one dimension calculation. With minimum peaking factor determined burnup is proceeded till the equilibrium cycle is achieved and the EOEC effective multiplication factor

(k_{eff}) is checked. If it is not equal to 1.005 $\pm$ 0.002 the BOL enrichment is revised. The iterations are repeated till BOL fuel enrichment obtained results in EOEC reactor composition that satisfies both criticality and flat power distribution.

In the burnup calculations the following sequence was considered in order to achieve the equilibrium cycle. A reactor fuel at BOL was burned one cycle, then 1/3 of core and axial blanket as well as 1/5 of radial blanket were reloaded and the fuel was burned for another cycle. This operation is repeated till equilibrium cycle is obtained.

4.2.3 Breeding Ratio and Doubling Time

Breeding ratio and doubling time are important parameters to characterize breeder reactors. The breeding ratio is a measure of the production of fuel and doubling time is a measure of the time that it takes to produce fuel sufficient to start up another identical reactor.

Breeding Ratio

The breeding ratio is derived from reaction rates integrated over the equilibrium cycle. For the region $\underline{k}$ breeding ratio is defined as

$$BR_k = \frac{\sum_{m2} \sum_{n} \int_{Vk} N_k^m \; \bar{\sigma}_{c,k}^{m,n} \; \phi^n(\bar{r}) \, d\bar{r}}{\sum_{k} \left(\sum_{m1} \sum_{n} \int_{Vk} N_k^m \; \bar{\sigma}_{a,k}^{m,n} \; \phi^n(\bar{r}) \, d\bar{r} \right)}$$

Where

m1 : ^{235}U, ^{239}Pu, ^{241}Pu

m2 : ^{238}U, ^{240}Pu, ^{242}Pu

N_k^m : effective concentration of nuclide m in the region k

n : energy group

σ : microscopic cross section

ϕ : neutron flux

The total breeding ratio is the summation over all regions

$$BR = \sum_{k} BR_k$$

Doubling Time

A wide variation of expressions are currently used to calculate the doubling time /18,19,20/. In this study the doubling time is calculated according to the definition presented in reference 19. The reactor doubling time (RDT) is defined according to

$$RDT(year) = \frac{\text{fissile BOEC}}{(\text{fissile gain}) \times (\text{fuel cycle/year})}$$

Where:

Fissile material considered are ^{235}U, ^{239}Pu, ^{241}Pu;

Fissile BOEC : all fissile amount in the core and blankets at beginning of equilibrium cycle (Kg) ;

Fissile gain : net increase in quantity of fissile during one fuel cycle (Kg).

The reactor doubling time provides information about the breeding capacity of a particular reactor. As such it is useful in comparing various reactors breeding performance. On the other hand a full-cycle-inventory-doubling time (IDT) is defined to examine a reactors performance in terms of its overall fuel cycle. In addition it includes a term of fuel loss during fuel fabrication and reprocessing. Then the definition for IDT is

$$IDT\ (year) = \frac{M_{in} + M_{ex}}{(G - L_p - L_d) \times \text{cycles/year}}$$

With

M_{in} : reactor fissile inventory at BOEC

M_{ex} : external cycle fissile inventory

G : fissile gain/ cycle

L_p : fuel cycle loss (fabrication and reprocessing)

L_d : ^{241}Pu decay loss for the external cycle.

The components of above expression are defined as :

- External cycle fissile inventory

$$M_{ex} = M_{in} \times RF \times T_{ex} / T_{cycle}$$

with

RF : refueling fraction

T_{ex} : external cycle time

T_{cycle} : cycle length

- Fuel cycle loss

$$L_p = \text{fissile at MOEC} \times RF \times 0.02$$

- ^{241}Pu decay loss

$$L_d = {}^{241}Pu\ (MOEC) \times RF \times 0.0462$$

with

^{241}Pu (MOEC) : $\frac{1}{2}$ (BOEC + EOEC) ^{241}Pu inventory

In the case of a system containing a large number of breeders it would be convenient to define fuel-cycle-compound-system-doubling time (CSDT) related as

$$CSDT(\text{ year }) = 0.693 \times IDT$$

4.2.4 Sodium Void Reactivity and Doppler Coefficient

The transient characteristics of large plutonium fueled fast reactor core depend on two important parameters, the Doppler coefficient and Sodium void reactivity.

In large plutonium fueled reactor the void effect usually adds positive reactivity whereas the Doppler effect is able to add prompt negative reactivity. A general problem of commercial LMFBR core design is to reduce the sodium void reactivity as low as possible.

Sodium Void Reactivity

In accident situations due to the sodium voiding the fuel temperature is drastically increases and the reactivity is increased due to following effects:

(a) - Less neutrons are captured in sodium ;

(b) - Neutron leakage from core is increased as a consequence of less scattering ;

(c) - Spectrum hardening .

Effect (b) diminishes, effect (a) and (c) normally increase the reactivity.

A set of six neutron energy group cross section was used in two dimensional configuration and sodium void reactivity was determined from direct eigenvalue calculations. The effective multiplication factor (k_{eff}) was calculated with sodium-in and with sodium-out conditions at end-of-equilibrium cycle.

$$\text{Sodim void reactivity} = \rho_1 - \rho_0$$

where

ρ_0 : reactivity at normal condition ;

ρ_1 : reactivity at sodium voided condition .

Doppler Coefficient

In the case of the Doppler coefficient, broadening of fission resonance in fissile material increases the reactivity whereas broadening of capture resonance in both fissile and fertile materials decrease the reactivity. For large fast reactors, in which the ratio of ^{238}U to ^{239}Pu is high, the broadening with fuel temperature increasing results in a significant negative value to the Doppler coefficient.

For Doppler coefficient calculation the core temperature was changed and the variation in the

reactivity was computed.

4.3 FUEL ELEMENT TEMPERATURE PROFILE

The LMFBR has a higher inlet temperature and higher specific heat generation rate than a LWR. Both factors tend to yield higher fuel temperature. The coolant sodium, however, has a good heat transfer characteristics which permit to remove the heat produced without producing local boiling or significant changes in its physical properties at normal operation condition. Table 4.3.1 lists the main thermo-hydraulic properties of sodium /21/.

The temperature profile in the maximum power channel is the prime importance in reactor design due to the fact that reactor power capacity is limited by its thermal transport capacity. A reactor core must be operated in such way that the temperature of the fuel and the cladding anywhere in the core must not exceed safe limits. The temperature calculations were performed using the program TASS (Thermohydraulic Analysis at Steady State) /22/ and the following conditions were assumed :

- Reactor power fix ;
- The coolant is in the steady-state ;
- The coolant does not suffer changes in phase.

4.3.1 Axial Temperature Distribution

Energy is generated in the fuel volume at a rate depending on the fission rate. The variation of the power density in the axial direction is a pure cosine function. The axial coolant temperature distribution changes along the channel in response to both the change in energy source distribution along to the fuel pin rod, and the rise in coolant temperature through the core.

In a fuel the peak temperature tends to follow the heat generation pattern with the maximum occuring at the mid-height of the fuel pin rod. However the coolant flows from botton to upper core, so the coolant temperatures increase along the rod and its maximum occurs at the top of the channel. The axial variation of the power density is given by the equation

$$q''' = q_o''' \cos (\pi z/H)$$

where q''' and q_o''' are the volumetric heat source at any point and at center of the fuel element, respectively.

The numerical solution for steady-state heat transfer in rod bundle was evaluated using a triangular lattice model (see Fig.4.3.1) and the lumped parameters method /23,24/ . In the lumped parameters method, often referred to as subchannel analysis, the subassembly is divided

in a number of subchannels whose boundaries are defined arbitrarily by surfaces of fuel element. Axial coolant temperature in each subchannel is evaluated by solving equations of continuity, conservation of energy and the entalphy definition, as follow :

(a) Equation of Continuity

$$\frac{\partial(\rho v)}{\partial z} = 0$$

(b) Equation of Conservation of Energy

$$\rho v \times \frac{\partial h}{\partial z} = q'''$$

(c) Entalphy

$$\int_{100}^{T} \varepsilon_p (T_o)\, dT_o = h$$

Where

ρ =	density of coolant	(kg/m^3)
v =	velocity of coolant	(m/sec)
z =	axial position	(m)
h =	entalphy	(Kcal/Kg)
q''' =	power density	($Kcal/m^3$ sec)
c_p =	specific heat	(Kcal/Kg °C)

The power density was obtained from the neutronic calculations described in section 4.2.2. The coolant density and specific heat were considered dependent of temperature as are shown by following equations /25/ :

(a) Density

$$\rho\ (T) = 949.0 - 0.223\ T - 1.75 \times 10^{-5}\ T^2$$

(Kg/m^3)

T ⟶ K

(b) Specific Heat

$$C_p(T) = 0.3893 - 1.9908 \times 10^{-4} T - 11.0542 \times 10^{-8} T^2$$

(Kcal/Kg °C)

T ⟶ K

4.3.2 Radial Temperature Distribution

Radial temperature distribution for a cylindrical fuel pin rod was calculated. According to the heat transport process, the heat flow path consists of the following two steps :

(a) - Heat transfer by conduction through heat-generation fuel,gap and cladding ;

(b) - Heat transfer by convection to the coolant .

In the calculations, the thermal conductivity of the fuel (k_f) and the cladding (k_c), as well as the physical properties of the coolant (density, viscosity, specific heat) were assumed dependent of temperature. Such dependence are shown in the following equations/23/.

- Thermal Conductivity

- Oxide fuel

$$k_f = 1.10 \times 10^{-2} \times \frac{1}{t\,(0.4848 - 0.4465\,D)}$$

(Kcal/m sec °C)

- Carbide fuel /21/

$$k_f = \frac{56.2773}{t + 273} + 0.761 \times 10^{-4} (t + 273)$$

(Kcal/m sec °C)

- Cladding material

$$k_c = 0.1 \times (0.03066 + 0.3584 \times 10^{-4} t - 0.0042 \times 10^{-6} t^2)$$

(Kcal/m sec °C)

- Viscosity

$$\text{Log } \eta = 0.5108 + \frac{220.65}{t + 273} - 0.4925 \log(t + 273)$$

From the point of generation, the heat flows through fuel material, through a gap between fuel and cladding material, through cladding material to an interface with a coolant and finally through a portion of the coolant which will transport the heat from the core.

At a given power level, the temperature in the fuel depends both on the temperature gradient through the various materials and on the bulk temperature of the coolant at point considered, along the length of the fuel element under studing.

Starting with the coolant temperature, which may be considered as a reference temperature, and using known temperature gradients it is possible to determine the fuel temperature profile.

The temperature gradient is represented by Fourier heat flow equation

$$\frac{dT}{dx} = -\frac{1}{k}\frac{q}{A}$$

Fig.4.3.2 shows the cross section of a cylindrical fuel element having a center temperature t_p and surrounded by cladding of thickness c , gap and coolant fluid having temperature t_f.

In the steady-state with no heat generated in cladding or coolant and with negligible resistance to heat flow at the fuel-caldding interface, the fuel element radial temperature distribution can be calculated using following expressions :

- At cladding outer surface

$$t_{cl} = \frac{q''' \quad R^2}{2(R + c + g)\ h} + t_f$$

- At cladding inner surface

$$t_{c2} = \frac{q''' R^2}{2 k_c} \ln \frac{(R+c+g)}{R} + t_{c1}$$

- At fuel pellet outer surface

$$t_s = \frac{q''' R^2}{2 h_g} + t_{c2}$$

- At fuel pellet center

$$t_p = \frac{q''' R^2}{4 k_f} + t_s$$

Where

q''' : power density

R : fuel pellet radius

c : cladding thickness

g : gap thickness

h : heat transfer coefficient of coolant

k_f : thermal conductivity of fuel material

k_c : thermal conductivity of cladding material

TABLE 4.2.1

ENERGY BOUNDARIES OF THE CROSS SECTION SET

ENERGY LIMIT (eV)	25 GROUP	6 GROUP	3 GROUP
1.05E 07	1	1	1
6.50E 06	2		
4.00E 06	3		
2.50E 06	4		
1.40E 06	5	2	
8.00E 05	6		
4.00E 05	7		2
2.00E 05	8	3	
1.00E 05	9		
4.65E 04	10	4	
2.15E 04	11		
1.00E 04	12		3
4.65E 03	13	5	
2.15E 03	14		
1.00E 03	15		
4.65E 02	16		
2.15E 02	17	6	
1.00E 02	18		
4.65E 01	19		
2.15E 01	20		
1.00E 01	21		
4.65E 00	22		
2.15E 00	23		
1.00E 00	24		
4.65E-01	25		

TABLE 4.3.1

THERMO-PHYSICAL PROPERTIES OF SODIUM (liquid) /21/

Melting temperature	°C	97.82
Boiling temperature	°C	881.0
Melting heat	cal/g	27.08
Boiling heat	cal/g	925.6
Density	g/cc	
at 97.98 °C		0.9275
at 400 °C		0.8563
*Specific heat	cal/g °C	0.312
*Heat conductivity	kcal/m h °C	66.0
*Viscosity	kg/m sec	3.4E -04

* at 300 °C

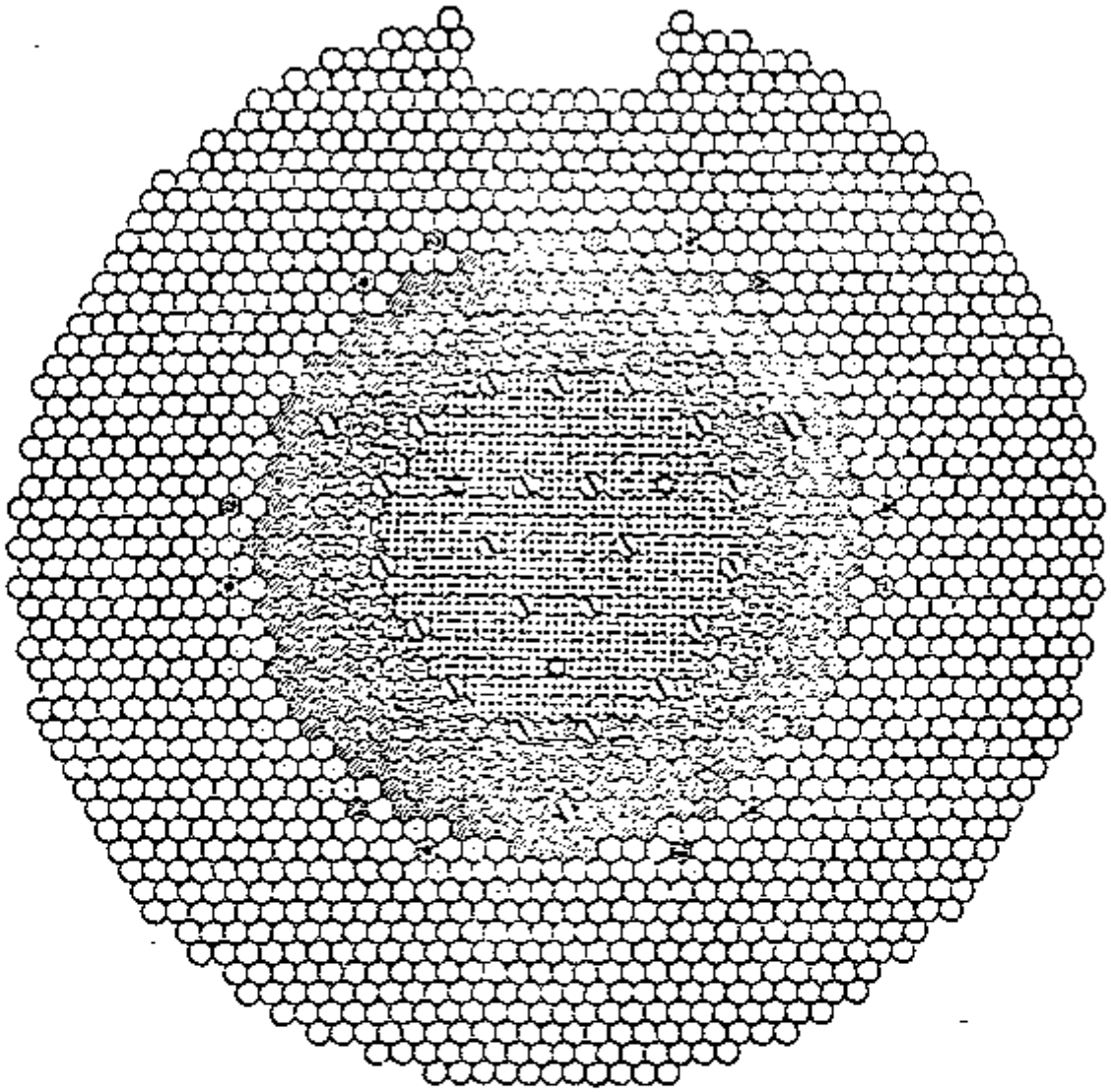

FIG 4.1.1-LMFBR HOMOGENEOUS CORE LAYOUT /13/

FIG 4.1.2

EQUIVALENT RADIUS

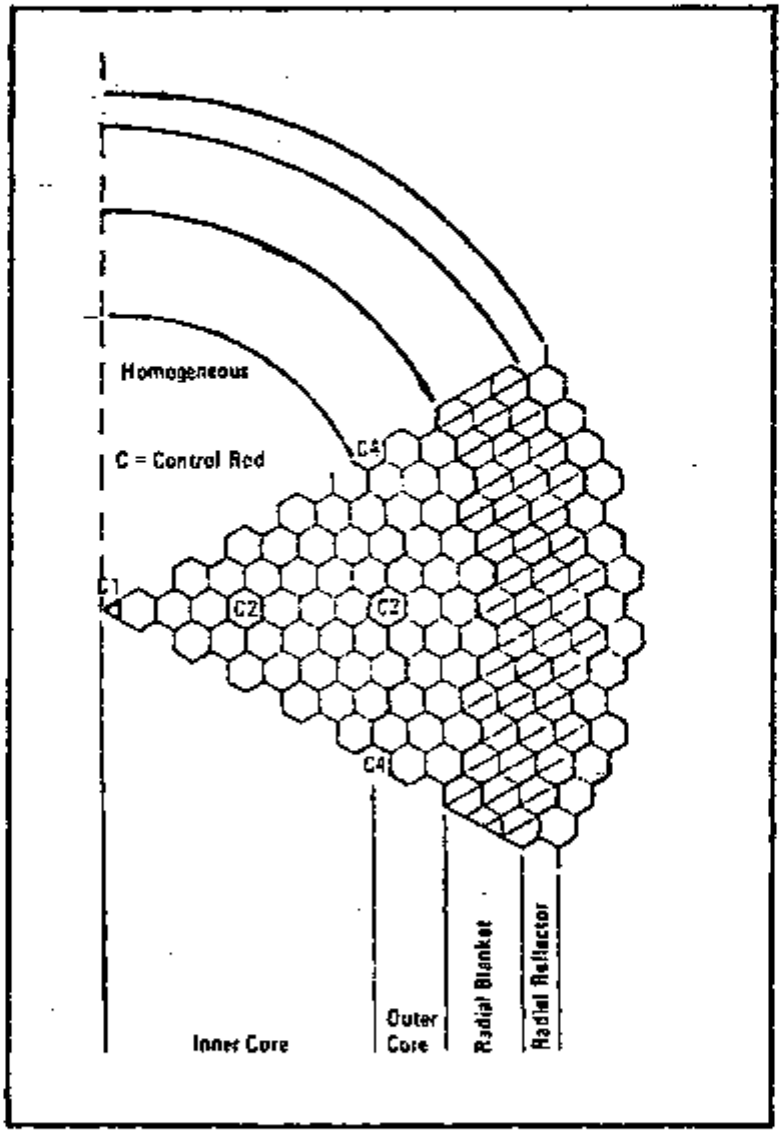

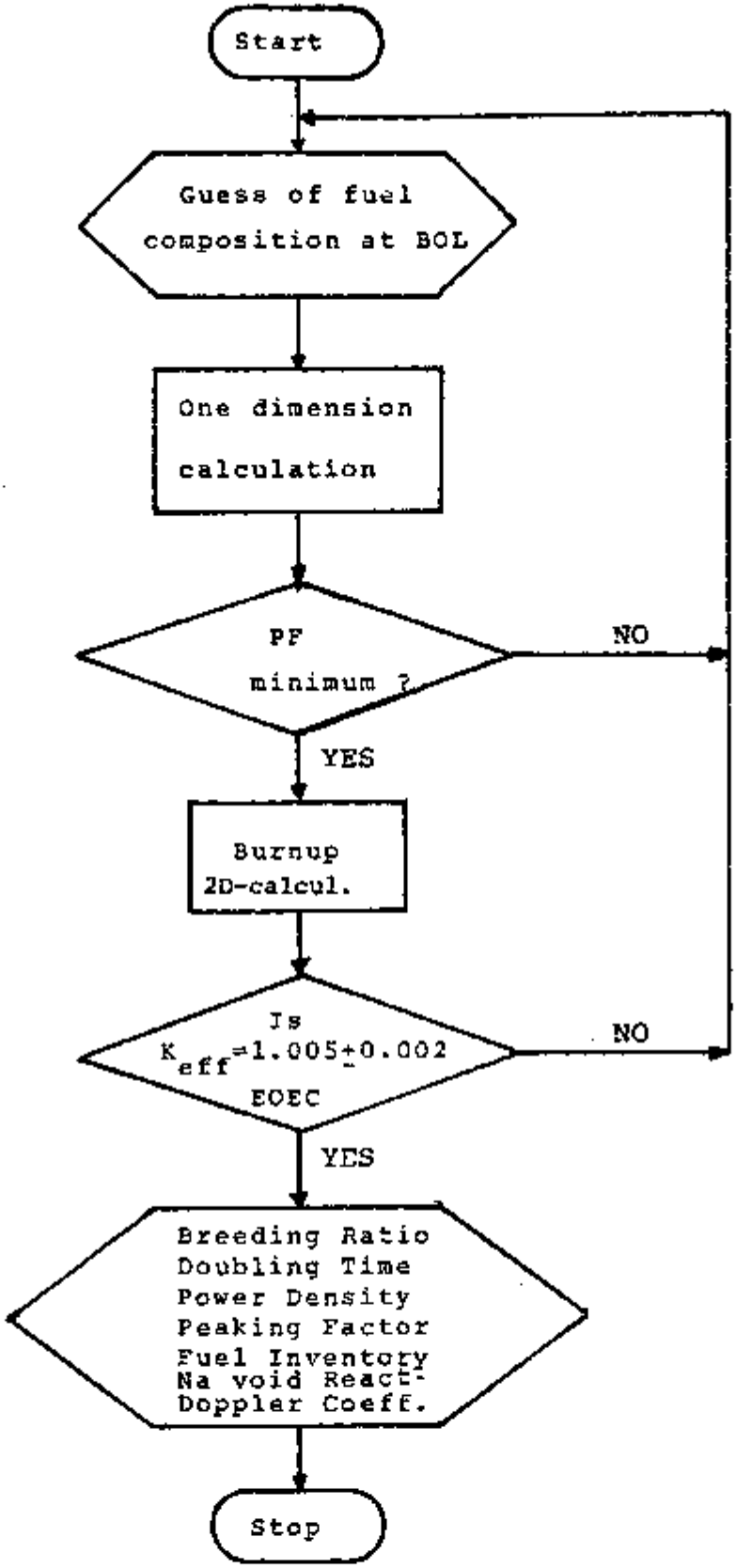

FIG 4.2.1
ITERATIVE SCHEME FOR PHYSIC PARAMETERS CALCULATION

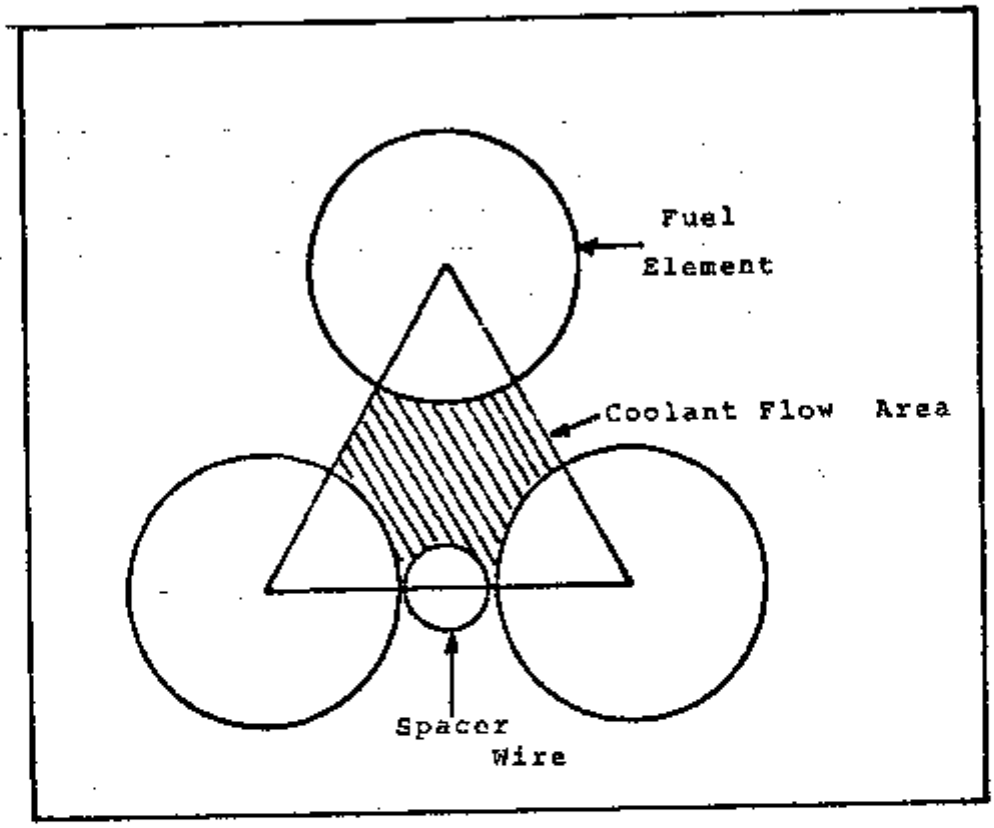

FIG . 4.3.1

TRIANGULAR PITCH WIRE-WRAPPED

ROD BUNDLE GEOMETRY

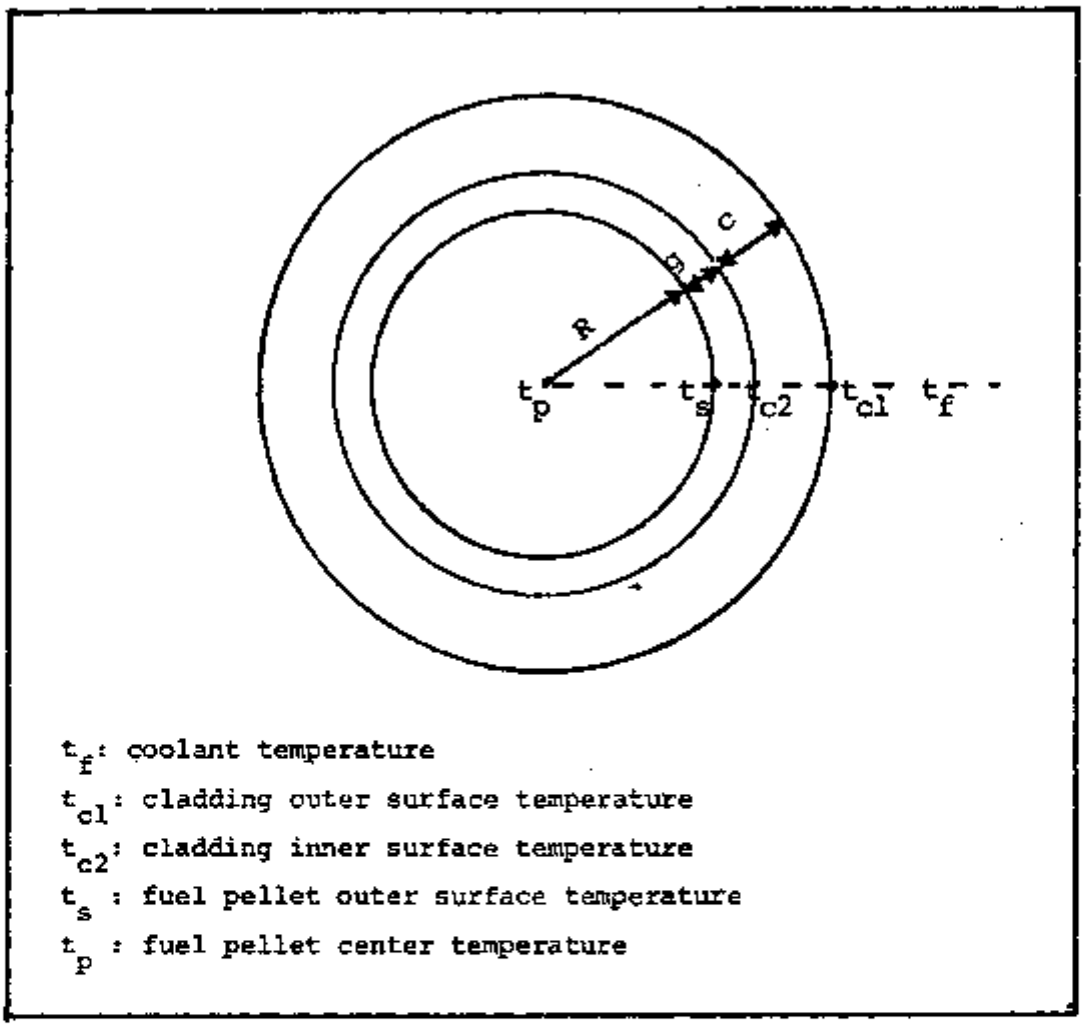

t_f: coolant temperature

t_{cl}: cladding outer surface temperature

t_{c2}: cladding inner surface temperature

t_s : fuel pellet outer surface temperature

t_p : fuel pellet center temperature

FIG . 4.3.2

CROSS SECTION OF A FUEL ELEMENT

CHAPTER 5

LMFBR OXIDE HOMOGENEOUS REACTOR

5.1 INTRODUCTION

In this chapter the performance of the reference reactor ,sodium liquid cooled oxide reactor, is calculated and analyzed. The main design parameters for this reactor were adopted from the 1200 MWe Super-Phenix /13/, the first high power commercial fast breeder presently under construciotn.

The target of this study is to achieve a core design that produces a short doubling time. A reactor doubling time around 10 years is desired, thus aiming this objective any design parameters changing were performed. The basic design parameters that can affect the reactor breeding performance are the ratio of the core height to diameter, thickness of radial and axial blanket zones, reflector material, fuel pin diameter, fuel volume fraction, fuel material, fuel isotopic composition , core volume and so on.

In this chapter the effect of the blanket thickness,cladding thickness,fuel density and plutonium isotopic composition on the breeding performance was investigated.

In next chapter an analysis of the performance of reactor fueled with advanced fuel like carbide will be done.

Many literatures refer to fuel pin diameter effect on the reactor doubling time /26,27,28/. Such studies have been shown that the fuel pin diameters ranging from 0.75 to 0.80 mm lead to the minimum doubling time for oxide fueled reactor.

In the case of reflector material, Komatsu /26/ has shown that the substitution of stainless steel by Ni produces a negligible change on reactor doubling time.

5.2 REFERENCE REACTOR

The reference homogeneous reactor considered here has 379 fuel assemblies that are divided into two enrichment zones. The fuel zone is surrounded by 3 rows of radial blanket and 2 rows of reflector assemblies. The fuel assembly structural member is a hexagonal stainless steel duct containing 271 fuel rods in a triangular array. A schematic diagram of the fuel assembly and fuel rod is shown in Fig.5.2.1. Each fuel rod is 7.02mm in diameter and has a cladding thickness of 0.70 mm. The blanket assemblies are the same hexagonal cross-section, except that they contain only 91 rods with a 15.80 mm outer diameter. The height of active core zone is 100 cm, bounded by 30 cm axial blanket cotaining depleted uranium.

5.2.1 Nuclear Characteristics

For the reactor physics analysis,one and two dimensional diffusion calcualtions were carried out using 3 energy group cross section. As mentioned above the the reference reactor design was based on a typical 1200 MWe oxide homogeneous reactor Super-Phenix. The reactor gecmetry as well as the parameters adopted for calculations are illustrated in Fig.5.2.2 and Table 5.2.1. Tables 5.2.2 and 5.2.3 list the reactor dimension and material composition.

For burnup calculation the following considerations are assumed:

- The loaded core fuel is plutonium from a light water reactor discharged fuel ;
- The fuel supplied for the blankets is depleted uranium and was assumed for this study to be 99.80 w/o U-238 and 0.20 w/o U-235 ;
- The reactor load factor is 0.82 ;
- The core fuel is irradiated at fixed location. The core presents 3 batch for refueling and the cycle length is 300 days ;
- 1/5 of radial blanket assemblies is changed each year.

The isotopic composition of the light water reactor plutonium is sensitive to the discharge exposure and is also influenced by the particular reactor spectrum.

For this study the isotopic composition of plutonium is follow:

Isotope	Weight percent (w/o)
^{239}Pu	63.0
^{240}Pu	22.0
^{241}Pu	12.0
^{242}Pu	3.0

Applying the iterative method described in Chapter 4 the fuel concentration at the beginning of life was determined and equilibrium cycle search was carried out. For this reactor the equilibrium cycle was achieved after 4 cyles as is shown in Fig. 5.2.3.

For doubling time calculation the expressions defined in Chapter 4 was utilized considering also the specifications listed in Tab.5.2.4.

The calculated nuclear characteristics at equilibirum cycle are given in Tab. 5.2.5. The total flux distribution is illustrated in Fig. 5.2.4 while the power density distributions are in Figs. 5.2.5 and 5.2.6.

As can be observed from the results this

reactor design produces a long doubling time and high sodium void reactivity. In the next sections the effect on doubling time due to design parameters modifications are analyzed.

5.2.2 Safety Considerations

A major safety concern in the design of commercial size LMFBR is the addition of positive reactivity with coolant voiding that occurs in loss of flow accident case.

Safety related parameters of common interest are sodium void reactivity and Doppler coefficient. The quantity , T (dk/dT) , is the negative Doppler change in reactivity due to the rise in the average reactor fuel temperature from its normal operating temperature at 100 per cent design power to the maximum permitted .

The Doppler feedback alone cannot necessary make a reactor subcritical but it can at least reduce a superprompt critical reactivity back to subprompt critical value. The Doppler feedback is larger in commercial sized breeder reactors than in the smaller demonstration type reactor due to the softer neutron spectrum and the lower enrichment in the large core.

For the reference oxide reactor in this work the safety studies have been performed at end-of-equilibrium cycle and the sodium void reactivity and Doppler coefficients obtained are listed in Tab.5.2.5.

For the sodium void reactivity calculation the total core voiding was assumed and the value of 0.0260 was obtained. This indicates that at EOEC the voiding of the core increases the reactivity by 2.6%.

Owing to high positive sodium void reactivity presented by homogeneous configuration, there is a strong incentive for designing large LMFBR that has a low sodium void reactivity. Many variations of the conventional homogeneous core design that will limit the sodium void worth have been identified /29,30,31,32,33,34/. These can be generally classified as follow :

- Pancake core with large axial neutron leakage ;
- Heterogeneous core, axial and radial heterogenization;
- Modular island heterogeneous core ;
- Modereted core with decreased spectral component of sodium void ;
- Annular configuration .

5.2.3 Thermal Charateristics

The temperature distribution in the maximum power channel was calculated considering the specifications listed in Table 5.2.6 .

The temperature profiles illustrated in Fig. 5.2.7 were determined in the following positions for fuel pin with maximum power density ;

(A) - coolant

(B) - outer surface of cladding

(C) - inner surface of cladding

(D) - fuel pin rod surface

(E) - fuel pin rod center

For the calculations it was assumed that the coolant inlet temperature is 395°C and that the coolant temperature rise along the core is 150 °C. To satisfy these conditions the coolant mass flow rate necessary is 40.90 Kg/sec. The radial temperature profile for the fuel pin at the position of maximum volumetric power generation is illustrated in Fig. 5.2.8 .

The thermal limits imposed for Super-Phenix reactor operation are :

- Maximum linear power : 450 W/cm
- Maximum cladding temperature : 620 °C

According to the results listed in Tab. 5.2.7 the maximum fuel temperature is around 2400 °C , therefore, below the oxide fuel melting point (2700 °C) and the maximum cladding surface temperature is 561 °C, hence below the maximum permitted.

5.3 PLUTONIUM ISOTOPIC COMPOSITION EFFECT ON BREEDING RATIO

In this section the neutronic and thermal characteristics of a reactor for the FBR-FBR fuel cycle are analyzed and compared with those of the reactor for conventional fuel cycle LWR-FBR described in Section 5.2.

The LWR - FBR fuel cycle or conventional fuel cycle is that in which the plutonium loaded in FBR core is obtained from LWR discharged fuel (see Fig. 5.3.1). In the case of the FBR - FBR fuel cycle, as shown in the flowsheet of the Fig. 5.3.2 , the reactor is fueled with plutonium which is recovered from FBR discharged fuel. The plutonium considered is the total recovered from discharged fuel from the core and blanket zones. This comparative study between two fuel system was made to verify the effect of plutonium composition on reactor breeding performance and also because although the first generation of commercial LMFBRs is fueled with plutonium obtained from LWR , a second generation shall be fueled by a LMFBR discharged fuel, as the number of fast breeders installed will increase.

Reactor Performance

The reactor design data adopted for physics parameters calculations are the same as those described in Section 5.2.1 , except in the case of the plutonium isotopic composition of the initial fuel loading .

The plutonium composition is that of LMFBR discharged plutonium with the following composition :

Isotope	Weight percent (w/o)
^{239}Pu	67.0
^{240}Pu	23.6
^{241}Pu	6.0
^{242}Pu	3.4

Such composition was determined in Section 5.2.1 and corresponds to the end-of-equilibrium cycle discharged fuel composition.

The fresh fuel concentration loaded at BOL is

Core zone	Fuel concentration (w/o)
Inner core	16.3
Outer core	20.25

Fuel concentration is defined here as the plutonium mass to total fuel mass ratio or

$$E = \frac{Pu \ (kg)}{(Pu + U) \ (kg)}$$

The fuel concentration in this case is higher in comparison with LWR-FBR system due to the lower concentration of the fissile isotope ^{241}Pu for FBR-FBR system.

The following comments are concerned with a comparative analysis for the both fuel cycles relatively to reactor performance.

(a) - Burnup (Table 5.3.1)

For the same fuel residence time the reactivity change due to burnup is 28 % higher for LWR-FBR system where the ^{241}Pu concentration is higher.

(b) - Breeding Ratio and Doubling Time (Table 5.3.2)

Small difference was verified for breeding ratio between the two cycles whereas any improvement in doubling time is verified.

(C) - Sodium Void Reactivity and Doppler Coefficient (Table 5.3.3)

No difference in Doppler coefficient was verified for the both fuel cycles since the Doppler effect is sensitive to the fertile to fissile material ratio.

On the other hand, the FBR-FBR system presents a higher sodium void reactivity resulting from the lower ^{241}Pu concentration. An addition of ^{241}Pu is seen to have influence on the sodium void effect in the negative direction because the substitution of ^{241}Pu for ^{239}Pu has a negative effect on the spectral component /35/ .

(d) - Thermal Characteristics (Table 5.3.4)

The coolant mass flow rate was determined assuming the outlet temperature is 545 °C. On the basis of the calculations it appeared that both fuel cycles show the similar thermal characteristics.

5.4 BLANKET THICKNESS EFFECT ON BREEDING RATIO (see addendum at end of this chapter)

The effect of blanket thickness change on breeding ratio is investigated in this section. The reference reactor design has an axial blanket thickness of 30.0 cm and 3 rows of fertile subassemblies as radial blanket zone. The breeding performance analysis was carried out for three different blanket thicknesses like as 1.33 , 1.66 and 2.00 times the reference blanket thickness as is specified in

Table 5.4.1

The calculations were performed using 3 energy group cross section and two dimensional computer code. The results are presented in Table 5.4.2.

Changing the blanket thickness the total breeding ratio increases (Fig.5.4.1) and doubling time decreases (Fig.5.4.2.) but these improvement are only significant up to blanket thickness ratio equal to 1.66.

The total breeding ratio improvement is due mainly to the contribution from axial breeding gain (see Fig.5.4.3). Small or no change was verified in the radial blanket breeding gain. Although the breeding performance is improved, the volume of blanket zones increase too much (Fig.5.4.4) causing an increase in total reactor plant cost.

From Tab.5.4.2 it is possible to see that increasing blanket thickness the depleted uranium inventory required is high compared with the advantage from plutonium recovered.

A more detailed economic study must be taken out analyzing the compromise between plant cost and advantage from breeding gain with blanket thickness.

5.5 CLADDING THICKNESS EFFECT ON BREEDING RATIO

One of the most effective way to decrease the doubling time of a breeder is to improve breeding gain through design changes that increases the fuel volumetric

fraction in the core. The primary design variable affecting this quantity is the cladding thickness.

In this section the effect on the doubling time due to the change in cladding thickness was evaluated. The conventional reactor presents a thick cladding, near 0.70 mm, and here it was reduced to 0.40 mm. The new reactor dimensions as well as material composition adopting a thinner cladding are listed in Tab.5.5.1 and Tab.5.5.2 respectively.

The fuel assembly number was assumed same as reference reactor keeping the total reactor power. The performance of the reactor with altered design parameters is shown in Tab. 5.5.3.

By comparison with reference reactor the following improvements were verified :

- reduction of doubling time by 38% ;
- increase in breeding gain by 33% ;
- reduction of initial fissile inventory by 7% ;
- increase in fuel fraction by 7.5 % .

As can be observed a marked improvement relatively to doubling time was verified. This result incentives to develop a new material or alloy that resists a high fast neutron flux.

5.6 FUEL DENSITY EFFECT ON BREEDING RATIO

Most cases use a fuel smear density of

80 - 85% theoretical density. In this section the effect of increasing the density to 90 %TD and the advantages from the breeding point of view were analyzed.

Overall reactor design data considered in Section 5.4 were adopted and the results are shown in Table 5.6.1.

In this case increasing fuel density by 5% reduces doubling time by 44% in comparison with that calculated for reference reactor.

5.7 SUMMARY OF THE RESULTS

The nuclear characteristics of the various modified homogeneous oxide reactor were calculated as was described in the previous sections. These results collected and summarized in Table 5.7.1 are analyzed in this section.

These data compared with those for the reference core lead the following conclusions:

- Reducing cladding thickness near 43% an improvement of 5% on breeding ratio and 33% on doubling time were verified ;
- Keeping the same core design and changing only fuel density, from 85 to 90 %TD, the breeding ratio increased 8% and doubling time reduced near 44%,
- The blanket thickness effect on breeding ratio was

observed until an increasing of 66% in reference blanket thickness.

In conclusion from the results of the present survey, it was observed that among the design parameters considered the cladding thickness change induced the largest effect on doubling time.

ADDENDUM

5.4 BLANKET THICKNESS EFFECT ON BREEDING RATIO

The effect of blanket thickness change on breeding ratio is investigated in this section. The reference reactor design has an axial blanket thickness of 30.0 cm and 3 rows of fertile subassemblies as radial blanket zone. The breeding performance analysis was carried out for three different blanket thicknesses like as 1.33, 1.66 and 2.00 times the reference blanket thickness as is specified in Table 5.4.1.

The calculations were performed using 3 energy group cross section and two dimensional computer code. The results are presented in Table 5.4.2.

Changes in blanket thickness affect the neutron flux magnitude and spectrum in blanket zones. Breeding characteristic is improved as the blanket thickness is increased due to softer neutron spectrum and smaller leakage than reference design. The total breeding ratio increase is due to the balnket zones, mainly to the contribution from axial blanket zone (see Fig.5.4.3). Small changes are verified in the radial blanket breeding gain.

Although the total breeding ratio present a small decline at blanket thickness ratio equal to 2.00 at EOEC, as can be observed in Fig.5.4.1, the saturation condition is expected to be achieved for thicker blanket. But the breeding ratio improvement or specificaly doubling time, is significant only up to blanket thickness ratio equal to

1.66 (Fig.5.4.1 and 5.4.2). Although the breeding performance is improved, the volume of blanket zones increase too much (Fig.5.4.4) causing an increase in total reactor plant cost.

From Tab.5.4.2 it is possible to see that increasing blanket thickness the depleted uranium inventory required is high compared with the advantage from plutonium recovered.

A more detailed economic study must be taken out analyzing the compromise between plant cost and advantage from breeding gain with blanket thickness.

TABLE 5.2.1

REACTOR CHARACTERISTICS

(reference reactor)

Reactor thermal power	MWth	3000
Reactor electric power	MWe	1200
Coolant		Na
core inlet temperature	°C	395
core outlet temperature	°C	545
Core Height	cm	100
Axial blanket (upper/lower)	cm	30/30
Axial reflector	cm	20
Core diameter	cm	366
Radial blanket thickness	cm	49.62
Radial reflector thickness	cm	32.89
Number of assemblies		
inner core		211
outer core		168
radial blanket		234
reflector		186
control rod		21
Fuel cycle length	day	300
Load factor		0.82
Number of refueling batches (core/radial blanket)		3/5

TABLE 5.2.1

REACTOR CHARACTERISTICS (cont.)

Fuel assembly design		
fuel material		$(Pu,U)O_2$
density	%TD	85
pins per assembly		271
pin length	cm	270
assembly length	cm	540
lattice pitch	cm	17.90
fuel pin OD	cm	0.85
fuel pellet OD	cm	0.702
cladding material		SS 316
cladding thickness	cm	0.07
wire diameter	cm	0.12
Radial blanket assembly design		
blanket material		(UO_2) dep.
pins per assembly		91
pin length	cm	195
assembly length	cm	540
lattice pitch	cm	17.90
pin OD	cm	1.58
pellet OD	cm	1.45
cladding thickness	cm	0.065
fuel density	% TD	95
wire diameter	cm	0.095
Control rod assembly		
absorber element		B_4C
pins per assembly		31
rod OD	cm	14.90
number of control assemblies		21
enrichment		90% ^{10}B

TABLE 5.2.2

REACTOR DIMENSIONS (reference reactor)

ZONE	Equivalent outer radius (cm)	Height (cm)
Inner core	135.96	100.0
Outer core	182.55	100.0
Radial blanket	232.17	
Radial reflector	265.06	
Axial blanket		30.0
Axial reflector		20.0

TABLE 5.2.3

REACTOR COMPOSITION

(reference reactor)

ZONE	Material volume fraction (%)			
	Core fuel (PuO_2+UO_2)	Sodium	S.Steel type 316	Blanket fuel (UO_2)
Core	38.41	33.53	28.06	
Radial blanket		25.40	20.30	54.40
Axial blanket		33.53	28.06	38.41
Radial reflector		14.0	86.0	
Axial reflector		33.53	66.47	

TABLE 5.2.4

INPUT DATA FOR DOUBLING TIME CALCULATION

Refueling fraction	0.33
Processing loss fraction	0.02
External cycle time	1.0 year
Fuel cycles/ year	1.0
Cycle length	300 day
Annual load factor	0.82
^{241}Pu half-life	14.7 year
Fissile material	^{235}U, ^{239}Pu, ^{241}Pu

TABLE 5.2.5

REACTOR CHARACTERISTICS -CALCULATION RESULTS
(reference reactor)

Reactor power	Mwe	1200
Core fuel		$(Pu,u)O_2$
Blanket fuel		UO_2
* Core enrichment	w/o	
inner core		15.80
outer core		19.65
Power peaking factor		1.546
Fissile inventory (^{239}Pu + ^{241}Pu)	ton	4.393
Breeding ratio		1.18
Compound system doubling time	year	39
Doppler coefficient	$\partial T(dk/dt)$	-6.8E-03
Na void reactivity	$\% \Delta k/k$	2.60
Maximum power density	W/cc	431.0
Maximum linear power	W/cm	439.3
Average discharge burnup	MWd/t	7.375E 04
Maximum discharge burnup	MWd/t	11.193E 04
Burnup swing	$\%\delta k$	2.86

Obs. * means fuel concentration

TABLE 5.2.6

REACTOR DESIGN SPECIFICATIONS

Total coolant mass flow rate	kg/sec	15750.0
Reactor power	MWth	3000.0
Coolant inlet temperature	°C	395.0
Fuel pin		
outer diameter of pin	mm	8.50
diameter of pellet	mm	7.02
cladding thickness	mm	0.70
fuel density	% TD	85.0
Pins per assembly		271
Max. power density	W/cc	431.0
Max. linear power	W/cm	439.3

TABLE 5.2.7

MAXIMUN TEMPERATURE — RADIAL DISTRIBUTION (°C)
(reference reactor)

region / cycle	Coolant	Clad inner surface	Clad outer surface	Fuel surface	Center of fuel
BOL	541.7	541.7	558.5	723.0	2379.5
BOEC	542.5	542.5	559.0	722.5	2370.0
EOEC	545.0	545.0	560.8	723.2	2365.1

* Coolant mass flow rate = 40.90 kg/sec

TABLE 5.3.1

BURNUP AND REACTIVITY CHANGE DUE BURNUP

	LWR - FBR	FBR -FBR
Burnup swing , %Δ k	2.86	2.24
Max.discharge burnup (MWd/t)	11.193E 04	11.243E 04
Aver. discharge burnup (MWd/t)	7.375E 04	7.433E 04

TABLE 5.3.2

PEAKING FACTOR, BREEDING RATIO AND DOUBLING TIME

	LWR - FBR	FBR - FBR
Peaking factor	1.546	1.555
Breeding ratio	1.189	1.191
Compound system doubling time (CSDT - year)	39	34

TABLE 5.3.3

DOPPLER COEFFICIENT AND SODIUM VOID REACTIVITY
(at EOEC)

	LWR - FBR	FBR - FBR
Doppler coefficient (T dk/dt) x 10^{+4}	-68.0	-68.0
Na void reactivity (% Δk/k)	2.60	2.73

TABLE 5.3.4

MAXIMUM LINEAR POWER AND COOLANT MASS FLOW RATE

	LWR - FBR	FBR - FBR
Maximum linear power (W/cm)	439.3	443.0
Coolant mass flow rate (Kg/sec)	40.90	41.23

TABLE 5.3.5

MAXIMUM TEMPERATURE- RADIAL DISTRIBUTION (°C) (FBR-FBR system)

region / cycle	coolant	clad outer surface	clad inner surface	fuel surface	center of fuel
BOL	542.2	542.2	559.2	726.4	2412.0
BOEC	542.1	542.1	558.7	723.8	2386.8
EOEC	545.1	545.1	561.1	726.4	2387.4

* coolant mass flow rate #41.2 Kg/sec

TABLE 5.4.1

BLANKET THICKNESS AND VOLUME

Thickness ratio	Axial blanket thickness (cm)	Radial blanket thickness (cm)	Axial blanket volume (l)	Radial blanket volume (l)
standart (1.0)	30.0	49.62	6.282	10.345
1.33	40.0	66.08	8.376	16.113
1.66	50.0	82.51	10.450	23.185
2.00	60.0	98.90	12.522	31.658

TABLE 5.4.2

DOUBLING TIME AND FUEL INVENTORY (at equilibirum cycle)

Thickness ratio	Total breeding ratio	Reactor doubling time (y)	CSDT (year)	Blanket uranium inventory (ton)	Pu discharged from blanket at EOEC (kg)
Standart (1.0)	1.18	30.1	39.2	79.336	283.20
1.33	1.22	25.5	31.5	117.390	313.08
1.66	1.23	24.9	30.6	161.390	325.28
2.00	1.23	24.7	30.2	212.460	332.67

TABLE 5.5.1

. REACTOR DIMENSIONS

(cladding thickness= 0.40 mm)

ZONE	Equivalent outer radius (cm)	Height (cm)
Inner core	129.00	100.0
Outer core	172.88	100.0
Radial blanket	219.87	
Radial reflector	251.02	
Axial blanket		30.0
Axial reflector		20.0

TABLE 5.5.2

. REACTOR COMPOSITION

(cladding thickness = 0.40 mm)

ZONE	Material volume fraction (%)			
	Core fuel (PuO_2+UO_2)	Sodium	S.steel type 316	Blanket fuel (UO_2)
Core	41.3	35.1	23.6	
Radial blanket		22.0	17.3	60.7
Axial blanket		35.1	23.6	41.3
Radial reflector		14.0	86.0	
Axial reflector		35.1	64.9	

TABLE 5.5.3

NUCLEAR CHARACTERISTICS

- RESULTS -

(cladding thickness = 0.40 mm)

Reactor power		
thermal	MWth	3.000
electrical	MWe	1.200
* Core enrichment	w/o	
inner core		14.65
outer core		18.40
Power peaking factor		1.547
Initial fissile inventory ($^{239}Pu + ^{241}Pu$)	ton	3.963
Fuel density	%TD	85
Cladding thickness	mm	0.40
Driver pin outer diameter	mm	7.90
Blanket fuel pin outer diameter	mm	15.30
Breeding ratio		1.248
Compound system doubling time	year	24
Average burnup	MWd/t	7.628E 04

Obs. * means fuel concentration

TABLE 5.6.1

NUCLEAR CHARACTERISTICS - RESULTS -

(cladding thickness= 0.40mm, fuel density=90%TD)

Reactor power		
thermal	MWth	3.000
electrical	Mwe	1.200
* Core enrichment :	w/o	
inner core		13.95
outer core		17.58
Power peaking factor		1.578
Initial fissile inventory	ton	
$(^{239}Pu + {}^{241}Pu)$		4.002
Fuel density	% TD	90
Cladding thickness	mm	0.40
Driver pin outer diameter	mm	7.90
Blanket fuel pin outer diameter	mm	15.30
Breeding ratio		1.270
Compound system doubling time	year	22
Average burnup	MWd/t	7.281E 04

Obs. * means fuel concentration

TABLE 5.6.2

SUMMARY OF NUCLEAR CHARACTERISTICS OF THE MODIFIED HOMOGENEOUS OXIDE REACTORS

	Reference reactor	Thin cladding	Hight fuel density	Blanket thick. 1.33 ST
Reactor power (MWth)	3,000	3,000	3,000	3,000
Cladding thickness (mm)	0.70	0.40	0.40	0.70
Fuel density (% TD)	85	85	90	85
* Fuel average enrichment (w/o)	17.51	16.31	15.56	17.58
Breeding ratio	1.18	1.24	1.27	1.21
Compound system doubling time (y)	39	24	22	31
Reactor doubling time (y)	30	20	19	25
BOEC fissile fuel inventory (ton)	4.869	4.515	4.581	4.901

Obs. * means fuel concentration

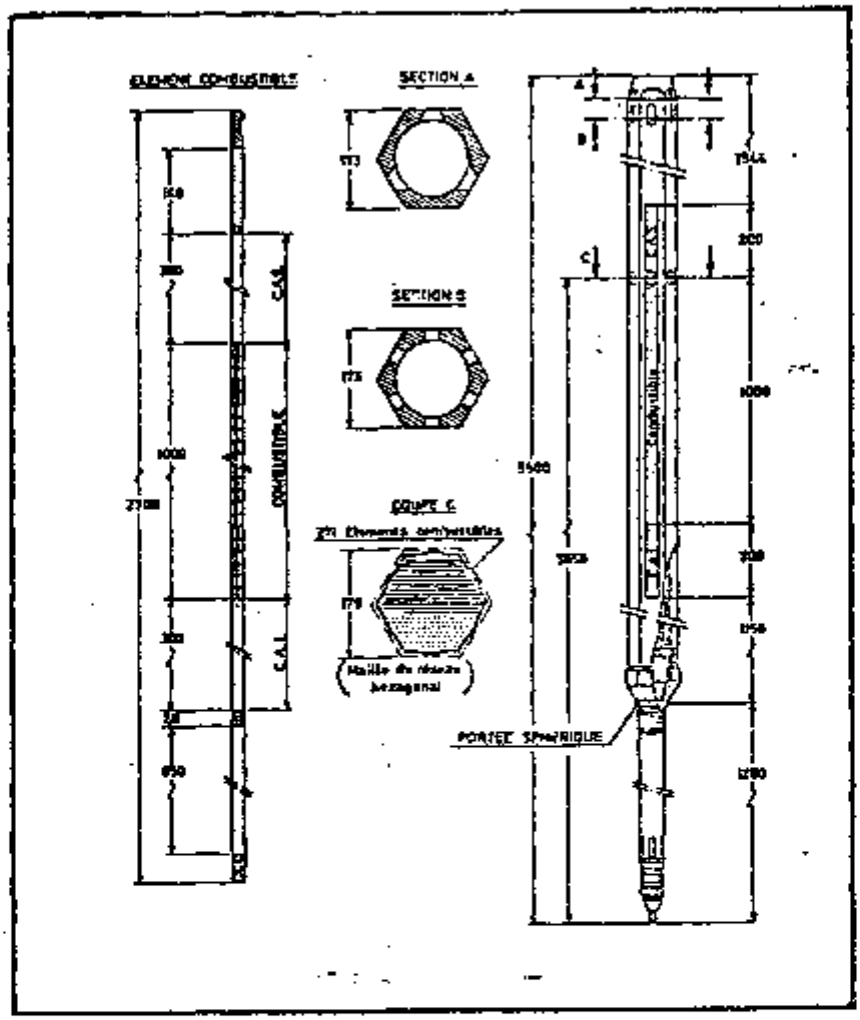

FIG .-5.2.1

DIAGRAM CF FUEL ELEMENT AND FUEL ROD

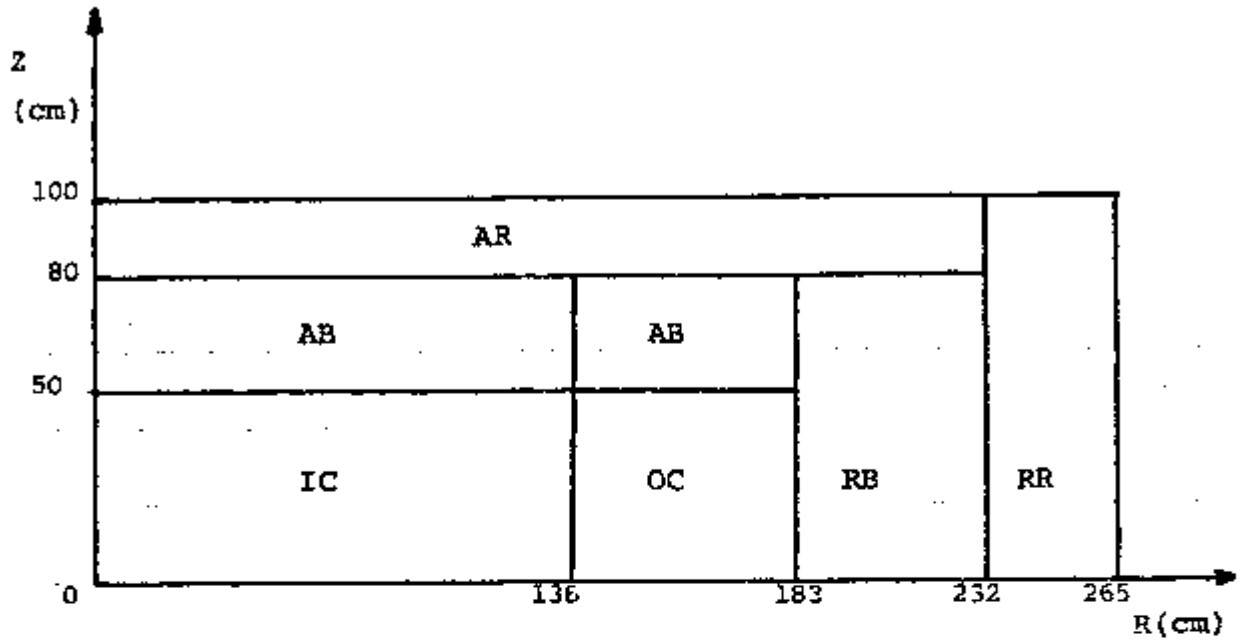

IC: Inner Core

OC: Outer Core

RB: Radial Blanket

AB: Axial Blanket

RR: Radial Reflector

AR: Axial Reflector

FIG. 5.2.2

CONFIGURATION OF REFERENCE HOMOGENEOUS REACTOR

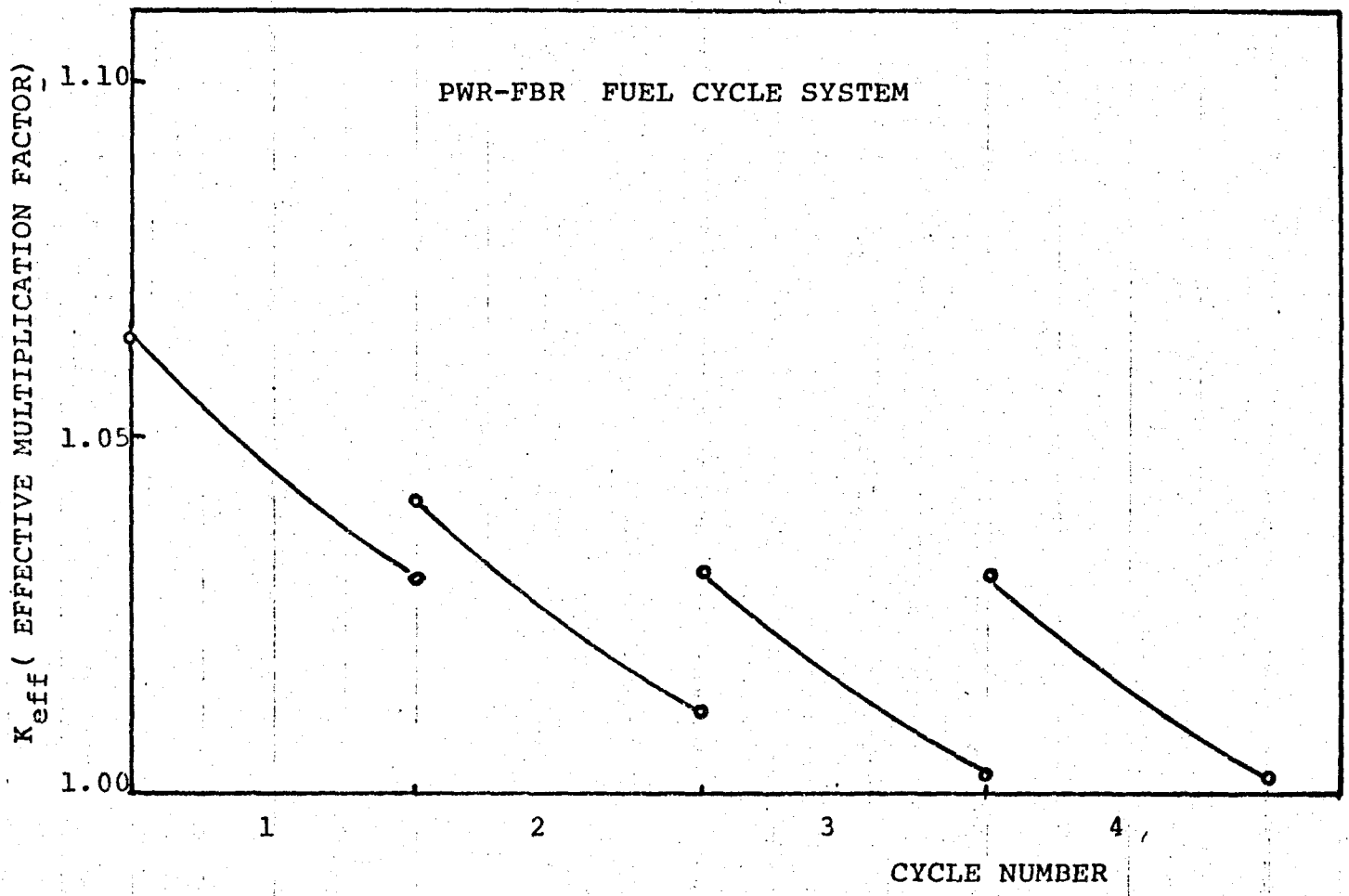

FIG. 5.2.3 EQUILIBRIUM CYCLE SEARCH

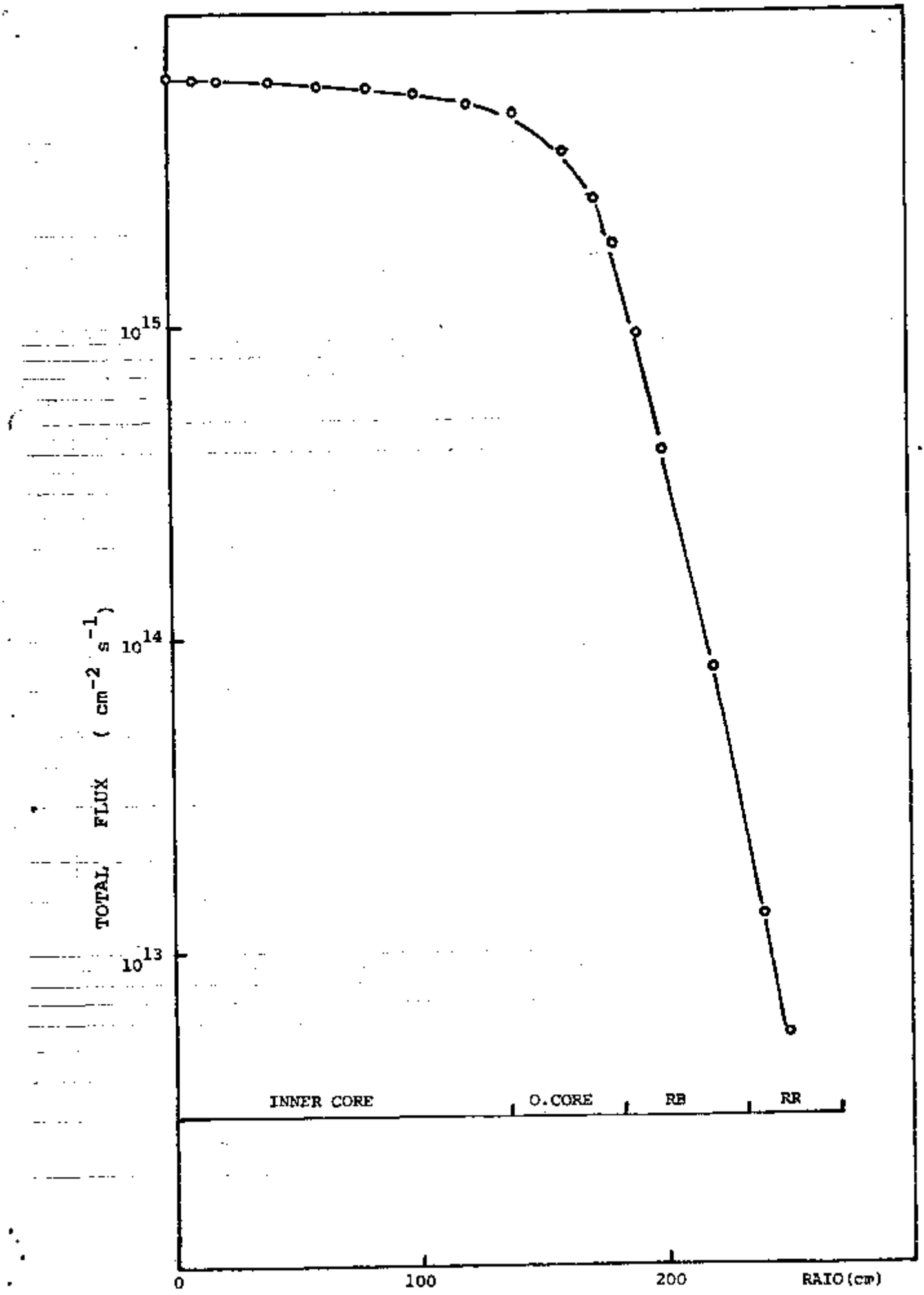

FIG 5.2.4 EOEC FLUX DISTRIBUTION FOR HOMOGENEOUS CORE

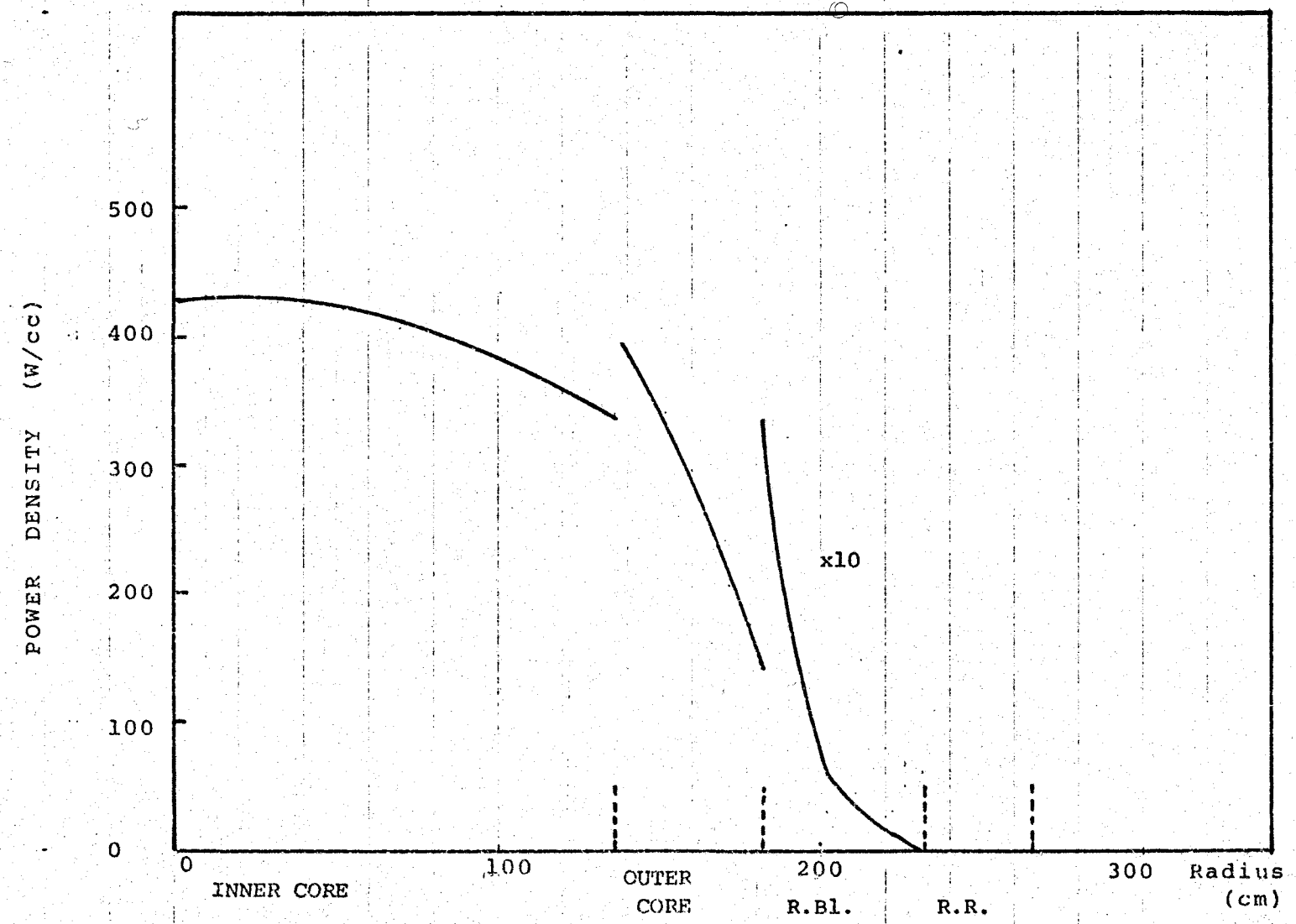

FIG 5.2.5 RADIAL POWER DISTRIBUTION AT EQUILIBRIUM CYCLE

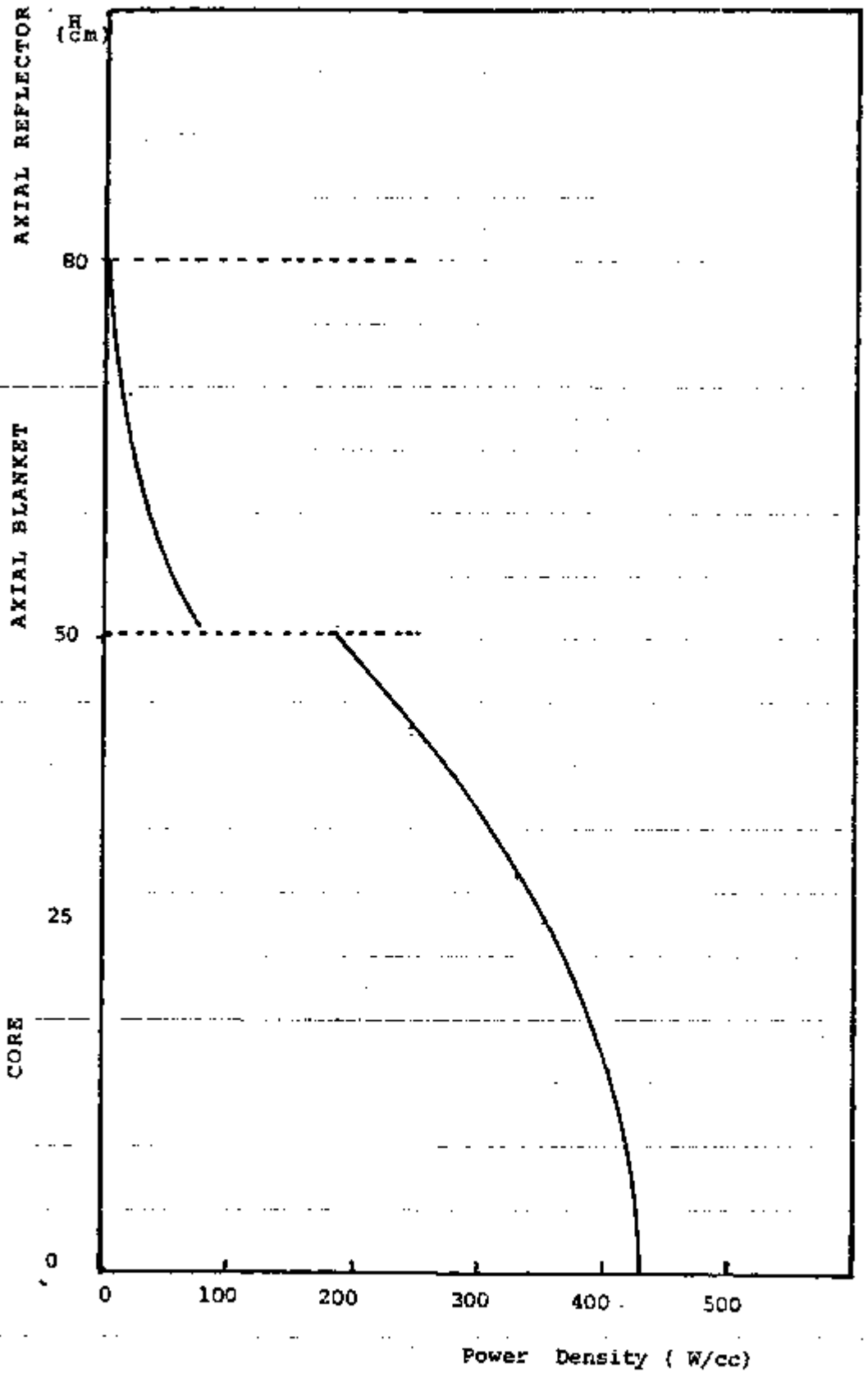

FIG 5.2.6

EQUILIBRIUM CYCLE-AXIAL POWER DISTRIBUTION

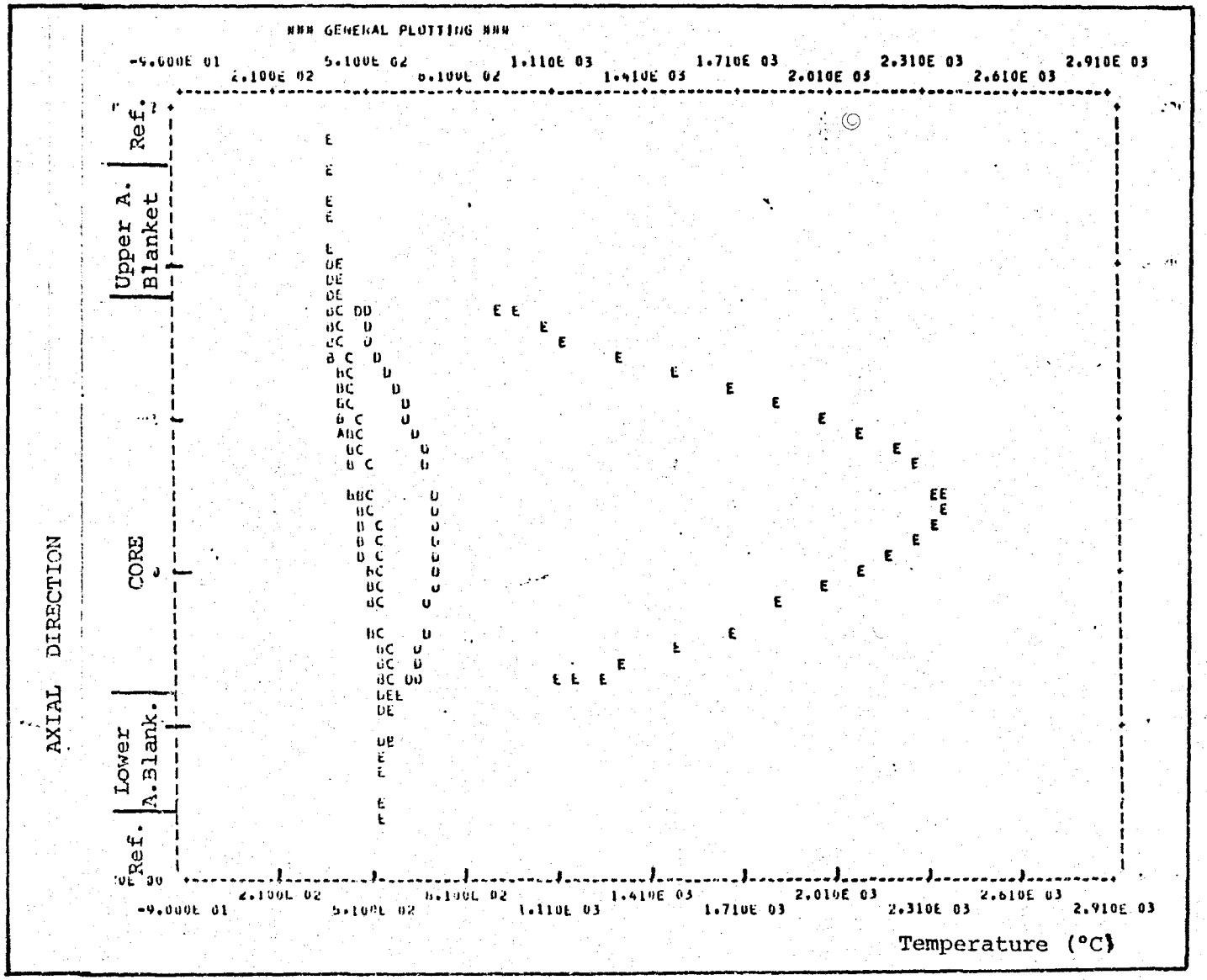

FIG. 5.2.7 AXIAL TEMPERATURE PROFILE FOR FUEL PIN AT THE POSITION OF MAXIMUM VOLUMETRIC POWER GENERATING

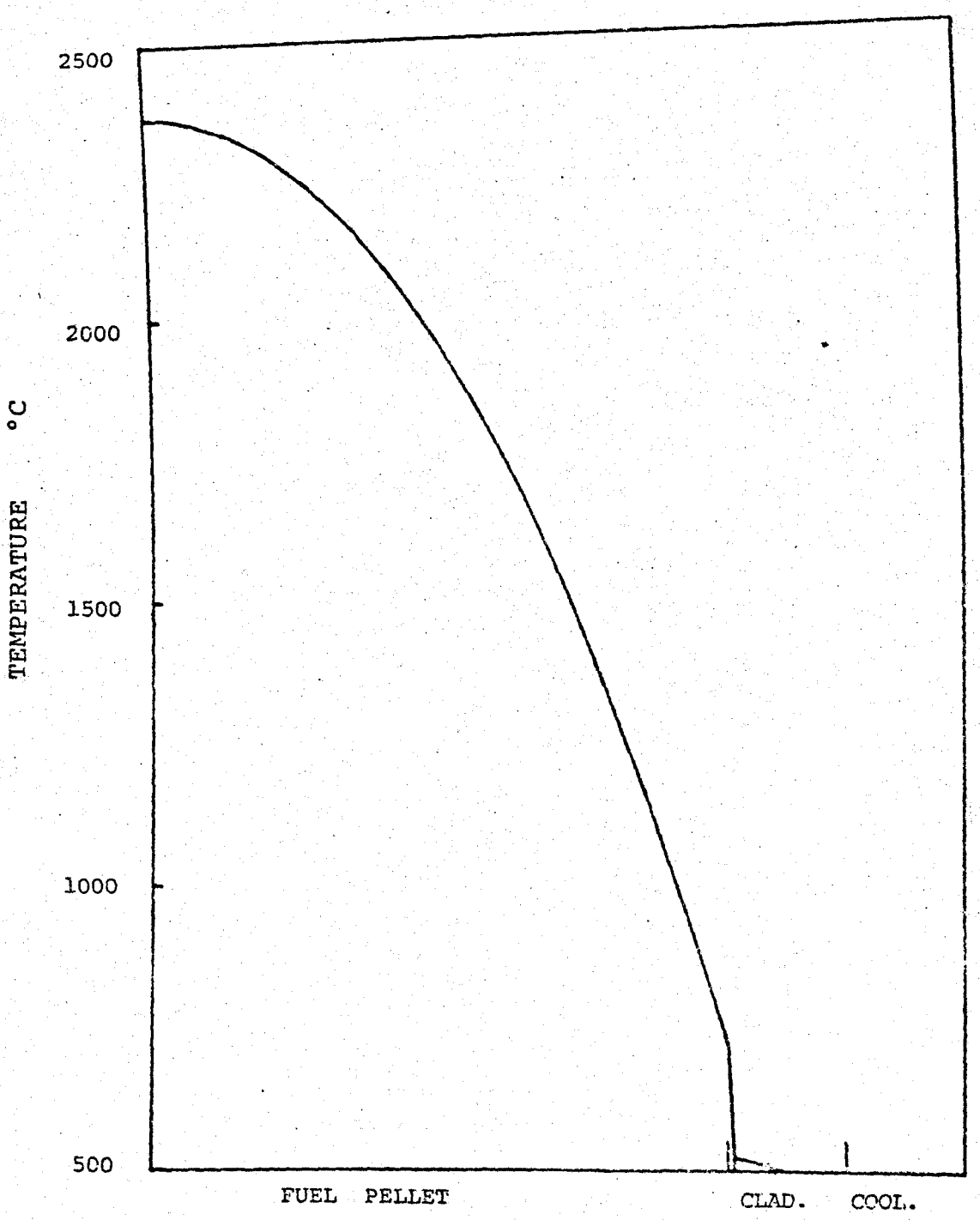

FIG 5.2.8

RADIAL TEMPERATURE PROFILE FOR FUEL PIN AT THE POSITION OF MAXIMUM VOLUMETRIC POWER GENERATING (EOEC)

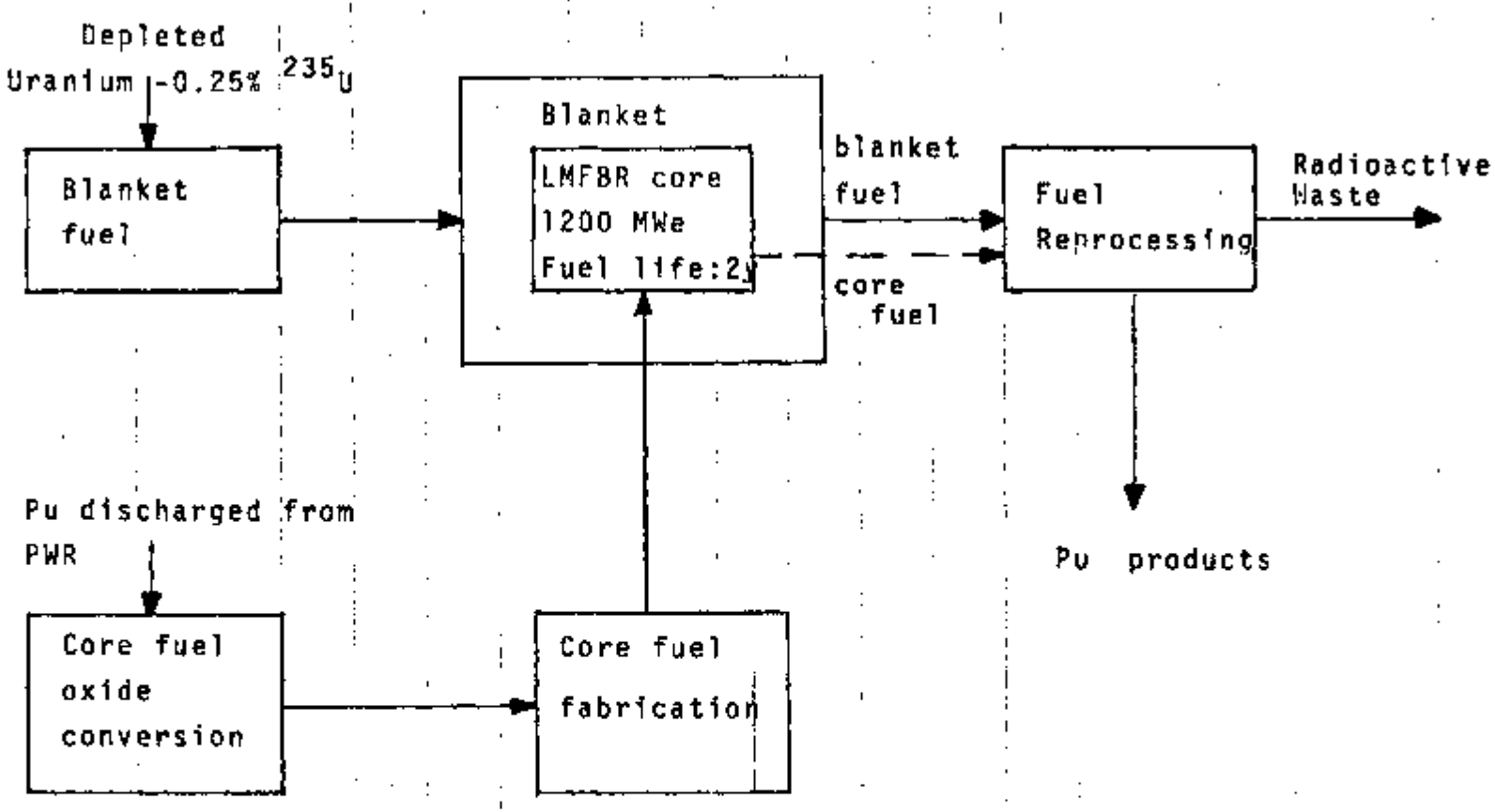

FIG 5.3.1

FUEL CYCLE FLOWSHEET FOR PLUTONIUM FUELED LMFBR

(Pu discharged from PWR)

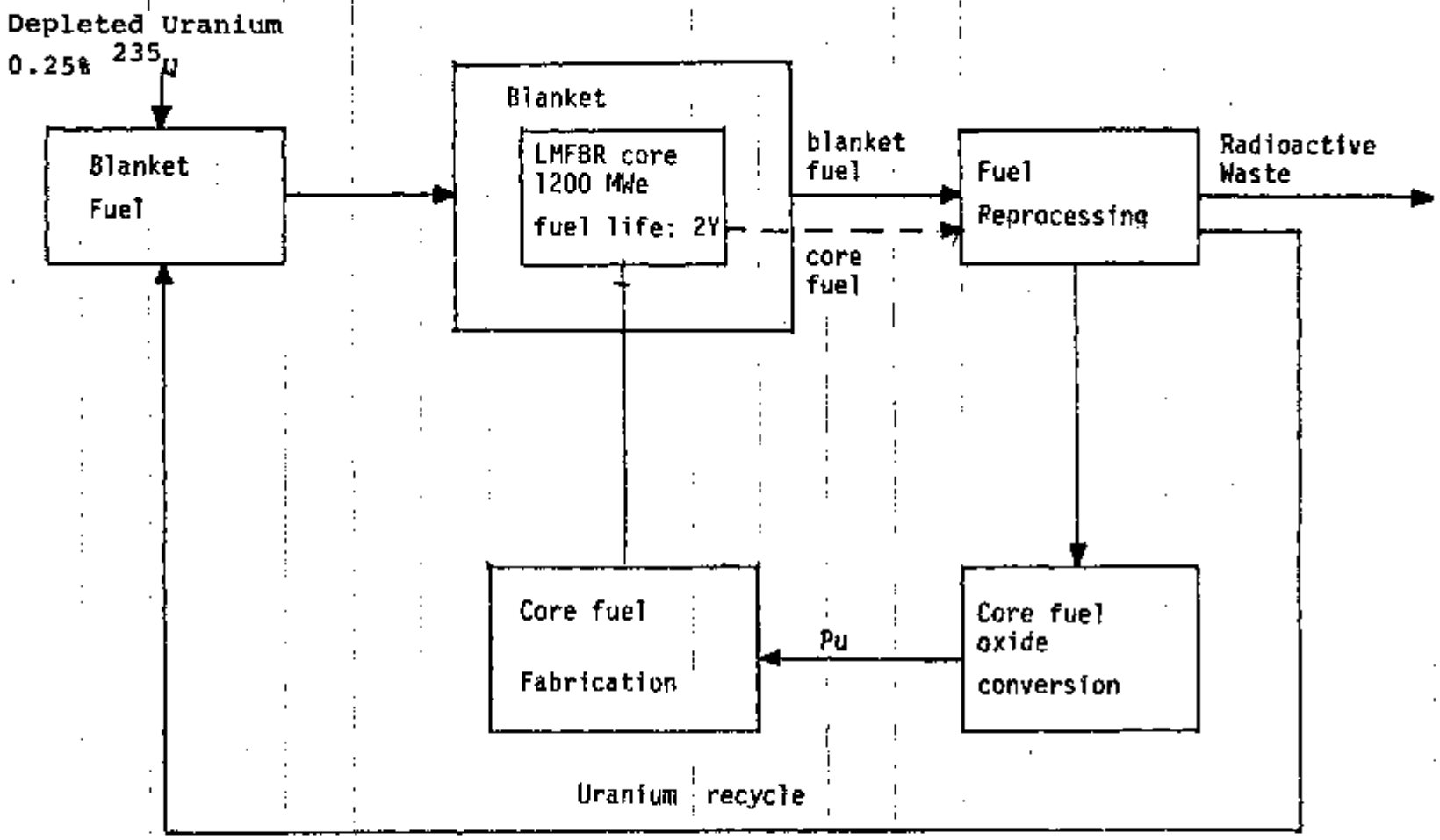

FIG 5.3.2

FUEL CYCLE FLOWSHEET FOR PLUTONIUM FUELED LMFBR

(Pu discharged from LMFBR)

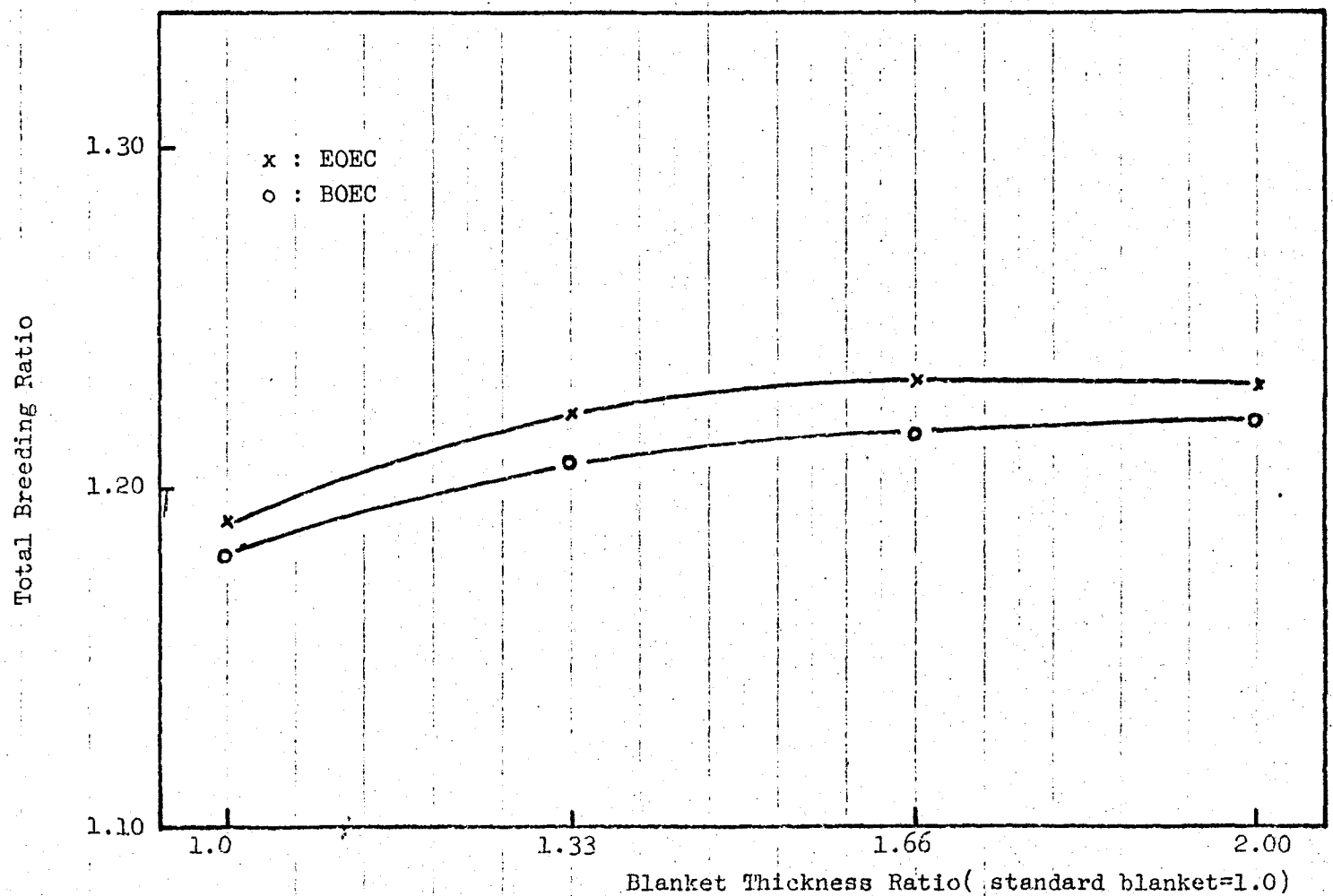

FIG.5.4.1

TOTAL BREEDING RATIO CHANGE WITH BLANKET THICKNESS

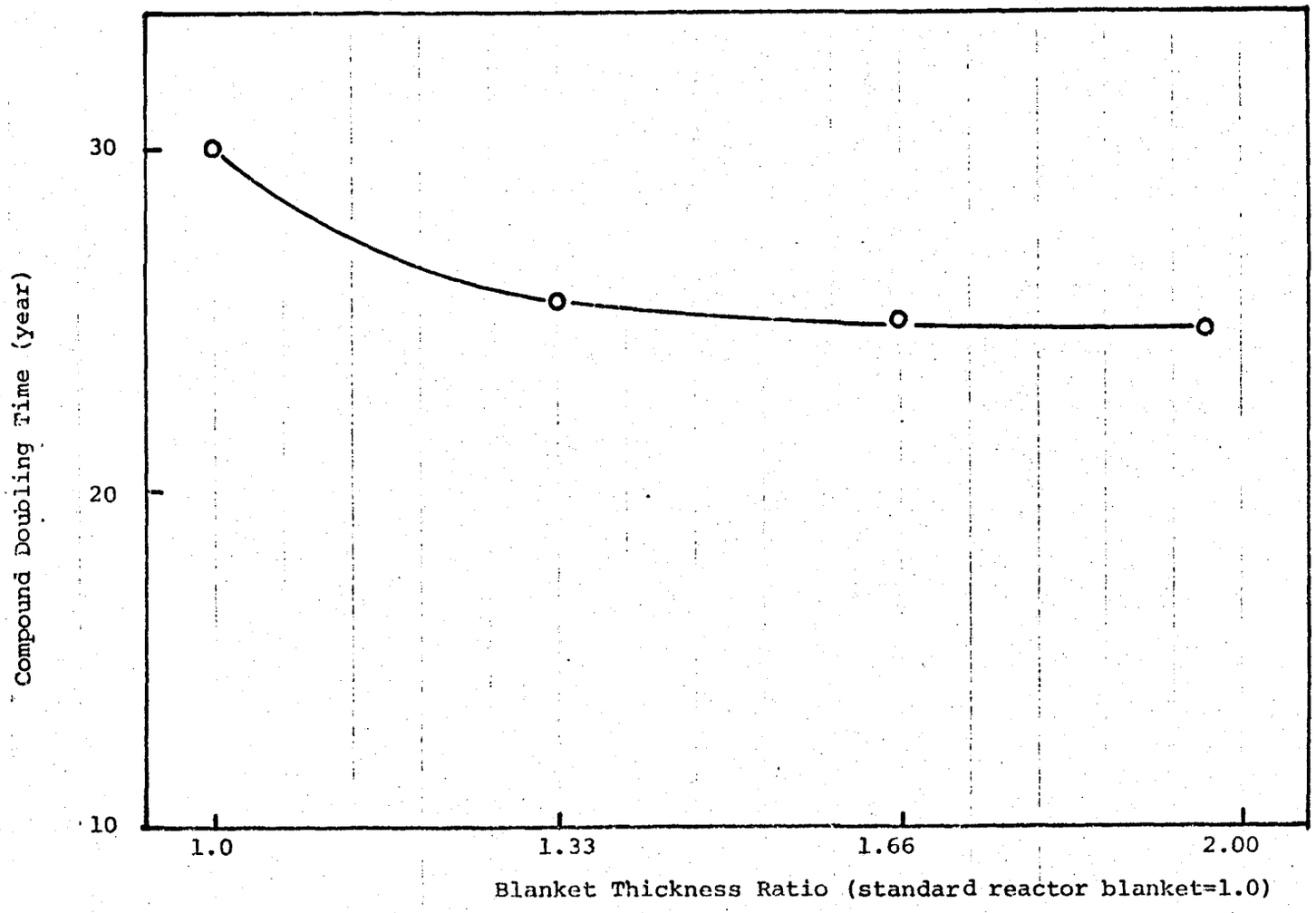

FIG 5.4.2

COMPOUND SYSTEM DOUBLING TIME VARIATION WITH BLANKET THICKNESS

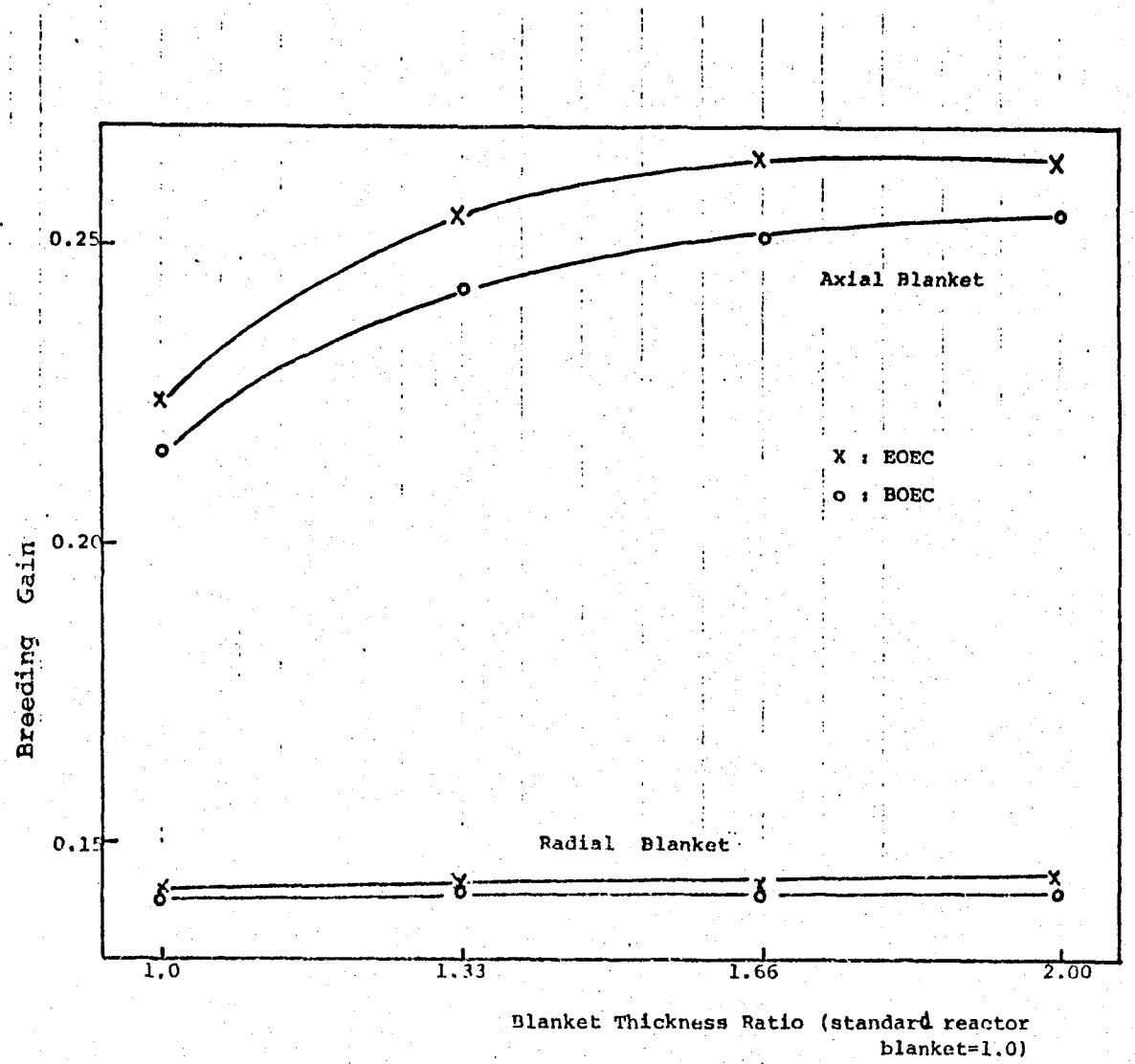

FIG 5.4.3

RADIAL AND AXIAL BREEDING GAIN CHANGE WITH BLANKET THICKNESS

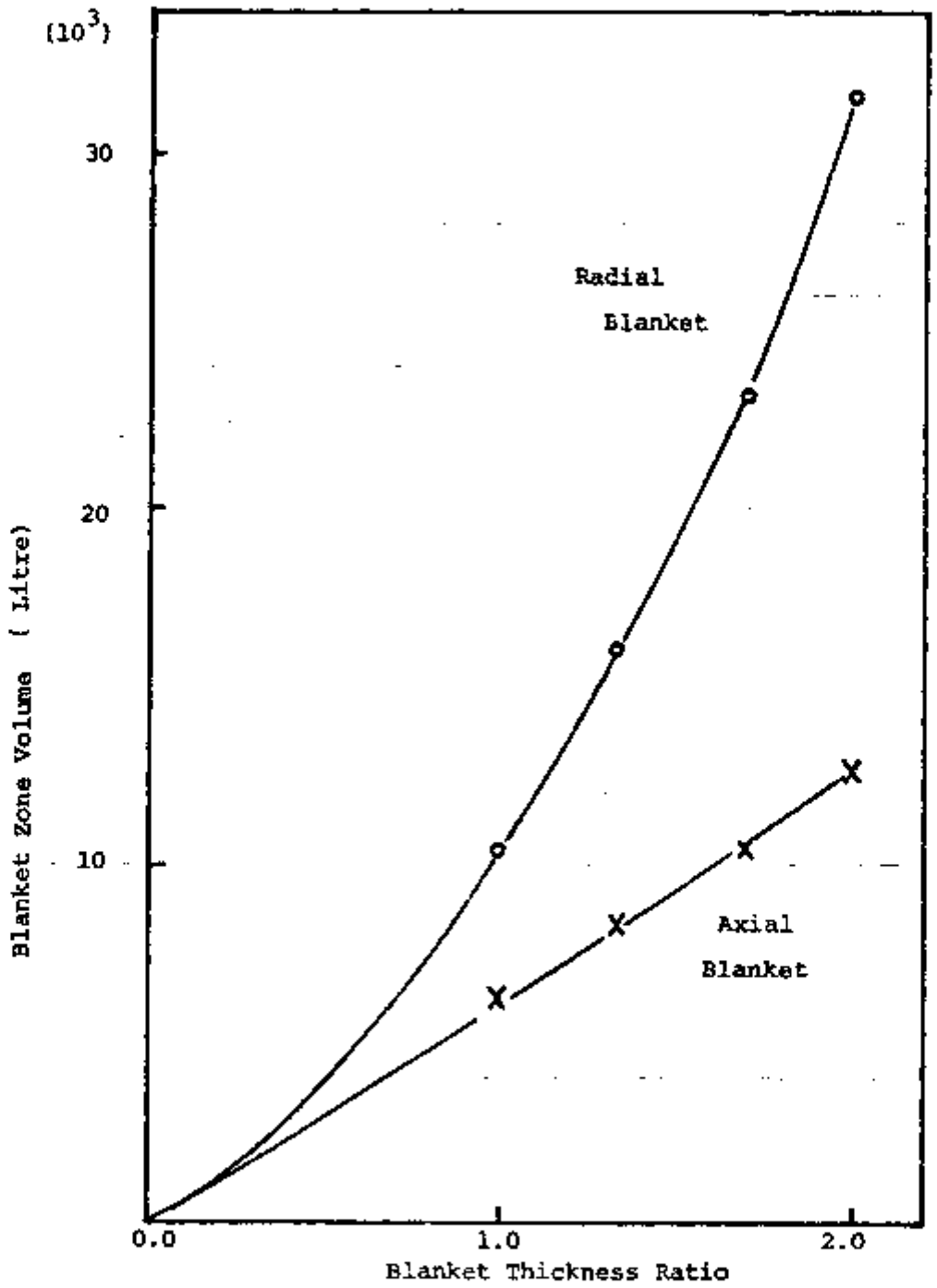

FIG 5.4.4

BLANKET VOLUME CHANGE WITH BLANKET THICKNESS

CHAPTER 6

CARBIDE FUELED HOMOGENEOUS REACTOR

6.1 INTRODUCTION

Present commercial fast breeder reactor developed or under development utilize the mixed oxide fuel $(Pu,U)O_2$. However such reactors present a long-doubling time, ranging from 20 to 30 years, even with some design parameters changes introduction.

However the modern nuclear power strategy requires fast breeder with a short doubling time, around 10 years / Chap.2/ to supply the required future energy demand. Thus recent events have lead to renowed interest in advanced fuels.

To advanced fuels are generally referred those different from oxide uranium or uranium-plutonium fuel and promissing better realization of fast reactor potential breeding capabilities. They include carbide, nitride, phosphide and, in principle, metallic fuel. In Fig.6.1.1 four spectra are plotted to exemplify the reactor core spctrum dependence with fuel type.

Main advantages of advanced fuels

compared to oxide ones are higher density, higher thermal conductivity and smaller content of neutron moderating and absorving material. An important feature of advanced fuel is a possibility to increase the breeding in the core.

Using carbide in commercial fast breeders following improvements on reactor performance can be expected:

- Higher rod power ;
- Higher breeding ratio ;
- Lower doubling time ;
- Initial plutonium inventory is smaller.

In this chapter the design characteristics and performance of plutonium-uranium carbide fuel are compared with those of plutonium-uranium oxide fuel in a large fast liquid metal cooled reactor through analytical studies of nuclear and thermal performance.

In spite of early study of carbide utilization in fast reactor, its development and use has fallen for behind development of oxide fuel utilized in water moderated reactors /36,37,38/.

Recently FBR fueled with carbide became attractive subject in many countries and most national programs are in the process of evaluating the merits of these core concepts /39,40,41,42/.

Two primary advantages for using carbide fuel in place of oxide are :

- The density of carbide is approximately 30% higher than oxide. This higher density reduces the required concentration of fissionable material improving the breeding performance ;

- The thermal conductivity of carbide is substantially higher than oxide, approximately five times, and slight variation with temperature is observed. It permits larger fuel rod diameter meaning lower fabrication cost.

A summary was made of fuel carbide properties available in the literature /26,36,38 / to supply necessary information to the calculations. These data are listed in Table 6.1.1. The coefficient of thermal conductivity of UC and UO_2 are shown in Fig.6.1.2 as function of fuel temperature.

Works are carried out in the direction of improving advanced fuel fabrication technology. At present experience in advanced fuel investigation is limited to tests in experimental reactors /43,44,45,46,47 /.

6.2 FUEL PIN DIAMETER OPTIMIZATION

The performance of plutonium-uranium carbide fueled LMFBR was analyzed and compared with the results previously obtained from the study in the case of plutonium-uranium oxide fueled reactor (Chap.5).

The main parameters of comparison are breeding ratio, specific fissile inventory, doubling time, sodium void reactivity and Doppler coefficient.

For the calculations the same cross section data library used in the oxide fuel was adopted and the methodology employed is that described in Chapter 4.

Initially using doubling time as the basis for choice, an optimum pin diameter was determined for homogeneous core. The Table 6.2.1 lists the fixed design parameters for the cores analyzed. The details of design for fuel assemblies as well as reactor dimensions are shown in Tabs. 6.2.2, 6.2.3 and 6.2.4 .

For each pin diameter burnup calculation was carried out and doubling time at equilibirum cycle was calculated. The doubling time, breeding ratio ,core volume and material composition variation with fuel pellet diameter are illustrated in Fig. 6.2.1. From this figure one may observe that the minimum doubling time occurs at fuel pellet diameter ranging from 0.85 to 0.95 cm whereas the optimum range for oxide fuel is about 0.60 to 0.70 cm /28/.

6.3 NUCLEAR CHARACTERISTICS ANALYSIS

6.3.1 Reactor Core Geometry

The design data of carbide fueled homogeneous core considered in this study are listed in Tab.6.3.1.

The reactor core contains 313 hexagonal fuel assemblies arranged in two radial core zones of different fuel enrichment. Different radial core enrichment is usually applied in order to flatten the radial flux profile.

Hexagonal fuel element contains 169 fuel pins, 10.5 mm outer diameter, with core fuel (Pu,U)C in the middle and fertile fuel (UC) at both ends. The radial blanket assembly contains 61 pins and the design for fuel rods is basically the same as that for the oxide.

The primary sodium is pumped upwards through the fuel element and heated from 395 to 545 °C. Tables 6.3.2 and 6.3.3 give the dimensions and material composition for the reactor studied.

In a carbide reactor the coolant fraction must be high. This is necessary owing to the high power density for this fuel. Otherwise, on account of high thermal conductivity a more compact core is possible generating the same total thermal power of that of oxide fuel.

6.3.2 Nuclear Performance

The calculated nuclear characteristics for carbide fueled homogeneous reactor are given in Tab. 6.3.4. On the basis of these results the following comparisons are important:

- Higher breeding ratio

oxide fuel	1.18
carbide fuel	1.42

- Shorter compound system doubling time (year)

oxide fuel	39.0
carbide fuel	15.7

- Lower fissile inventory (ton)

oxide fuel	4.607
carbide fuel	3.952

- Higher linear power (W/cm)

oxide fuel	439.3
carbide fuel	948.5

- Smaller core volume (litre)

oxide fuel	10,521
carbide fuel	8,615

- Larger pin diameter (cm)

oxide fuel	0.85
carbide fuel	1.05

- Smaller burnup swing (% Δk)

oxide fuel	2.86
carbide fuel	0.16

The Fig. 6.3.1 shows the radial power density distribution at mid-core plane at BOEC.

6.3.3 Cladding Thickness Effect on Breeding Ratio

It is recognized that there is a potential advantage in breeding from decreasing the cladding thickness and the benefits of using thin can are quantified in this section.

The cladding thickness of 0.45 mm was assumed and new core dimensions as well as the material composition were determined and listed in Tab. 6.3.5 and Tab. 6.3.6 , respectively.

An increase in the fuel volume fraction is verified in consequence of thin cladding, thus a low fuel concentration is required. The calculated characteristics are listed in Table 6.3.7 . A significant improvement on breeding performance was observed and a reactor doubling time around 10 years was achieved.

6.4 SAFETY CHARACTERISTICS

In this section the sodium void and Doppler effects in carbide fueled homogeneous reactor are analyzed and the differences in these two safety parameters for oxide and carbide reactors are discussed. Table 6.4.1 gives the sodium void reactivity and Doppler coefficients

for the two reactors.

Sodium Void Reactivity

Sodium void reactivities were calculated by eigenvalue differences assuming total reactor voiding. Carbide reactor presents higher sodium void reactivity than of the oxide reactor at all reactor life. The increase in sodium void reactivity with burnup are also greater for carbide fuel.

The reasons for these differences are:

- Carbide reactor has a higher heavy-metal concentration;
- Carbide reactor presents a greater sodium volume fraction.

Sodium void effect increases with burnup due to high plutonium isotope production. As can be observed at beginning of life (BOL) the sodium void reactivity is low for both fuels.

Doppler Coefficient

The primary negative feedback needed for reactor stability is derived from the Doppler effect. This effect is influenced by neutron spectrum, fertile-to-fissile ratio and heavy metal concentration.

The carbide reactor considered has a higher fertile-to- fissile ratio and heavy metal concentration,

but its spectrum is harder than oxide reactor as illustrated in Fig. 6.4.1. Consequently the Doppler coefficient of the carbide reactor is less negative.

Another difference between these two fuels is the Doppler coefficient behaviour with burnup. While the Doppler coefficient of the oxide reactor remains unchanged with burnup that of the carbide reactor is greatly reduced. This effect shows how the fertile-to-fissile ratio in the carbide reactor changes with burnup.

To evaluate the Doppler effect is important to know the fuel temperature adopted for the determination.

Doppler effect is defined as change in reactivity due to the rise in average reactor fuel temperature and it is determined by direct eigenvalue calculations.

In this study the temperatures considered are :

- for oxide fuel 1000 ⟶ 2100 K
- for carbide fuel 1000 ⟶ 1800 K

These temperature ranges were assumed based on the normal operating temperature and the maximum permitted for either fuels.

The Doppler effect is sensitive to the temperature changes and to verify this dependence Doppler coefficients were calculated for three different temperatures,

at BOEC, for carbide fuel and the results are described below:

Temperature range (K)	Doppler coefficient
1000 ⟶ 1400	-0.0035
1000 ⟶ 1800	-0.0059
1000 ⟶ 2100	-0.0078

If the same temperatures were taken for carbide and oxide reactors the Doppler coefficient for two reactor are comparable at the beginning of reactor life.

6.5 THERMAL CHARACTERISTICS

If fuel melting point is a temperature limit in reactor design, carbide will have a lower peak temperature than oxide. Melting point of the mixed carbide is approximately 2400 °C. However since PuC,in particular, enters to the vapor phase before the melting point is reached, limitation of the fuel center temperature to a maximum of about 1800 °C is feasible for technical reasons /36/.

Despite a low permitted temperature for carbide fuel, the high thermal conductivity allows one to

design large diameter fuel pin. To keep the fuel integrity, temperature distributions in a fuel pin were calculated using the expressions described in Chapter 4. The sodium outlet temperature was set 545 °C and with power density obtained from nuclear calculations the maximum teperatures achieved at each point of fuel pin were determined and listed in Table 6.5.1. The fuel pin taken is that located at point where the power generation is maximum into the reactor core. Fig.6.51 shows the radial teperature profile for this fuel pin.

From the results it was found that the temperature at center of fuel and cladding surface do not exceed the limiting temperature.

6.6 RESULTS

Comparison of the plutonium-uranium carbide cores with the plutonium-uranium oxide cores shows that the breeding performance of the former is superior . With the carbide fueled homogeneous reactor a breeding ratio of 1.49 and a doubling time of 11.8 years result, while the best oxide values are 1.27 amd 19 years ,respectively.

Otherwise, the sodium void reactivity is larger and Doppler coefficient has a less negative value for carbide fuel.

To make good use of the carbide fuel

breeding performance and to ensure a low positive sodium void reactivity a carbide fueled heterogeneous configuration is recommended.

TABLE 6.1.1 PROPERTIES OF CARBIDE AND OXIDE FUELS /36/

Characteristics \ Fuel Type	OXIDE			CARBIDE		
	UO_2	PuO_2	$(Pu,U)O_2$	UC	PuC	(Pu,U)C
Melting point (°C)	2730	2300	2700	2400	1850	2270
100% theoretical density (g/cc)	10.96	11.46	10.87	13.63	13.62	13.60
Percentage of elements as (O,N,C,..) (w/o)	11.8			4.80		
Thermal conductivity (W/cm)						
at 500 °C	0.047			0.16		
1500 °C	0.025			0.17		
1000 °C			0.027			0.177

TABLE 6.2.1

FIXED DESIGN PARAMETERS

Total reactor power (MWth)	3000
Core height (cm)	100.0
Thickness of each axial blanket (cm)	30.0
Thickness of each axial reflector (cm)	20.0
Radial blanket thickness (row)	3
Fuel pellet density (%TD)	95/95
Maximum burnup (MWd/T)	1.0×10^5

TABLE 6.2.2 CORE FUEL PIN AND ASSEMBLY DESIGNS

Fuel pin OD (mm)	8.0	8.5	9.5	10.5	11.5
Fuel pin pitch to diameter	1.16	1.15	1.14	1.12	1.11
Number of fuel pins per assembly	169	169	169	169	169
Assembly pitch (mm)	139.70	146.20	159.30	172.50	185.60
Volume ratio					
fuel	0.32	0.35	0.39	0.42	0.45
structure	0.30	0.29	0.27	0.26	0.24
sodium=	0.38	0.36	0.34	0.32	0.31
Cycle lenght (day)	292	237	292	330	325
Cycle number	2	3	3	3	4

TABLE 6.2.3 BLANKET FUEL PIN AND ASSEMBLY DESIGNS

Fuel pin OD (mm)	14.4	15.2	16.9	18.5	20.0
Fuel pin pitch to diameter ratio	1.07	1.07	1.06	1.05	1.05
Number of fuel pins per assembly	61	61	61	61	61
Assembly pitch (mm)	139.70	146.20	159.30	172.50	185.60
Volume ratio :					
fuel	0.49	0.50	0.53	0.55	0.56
sodium	0.23	0.22	0.20	0.19	0.18
structure	0.28	0.28	0.27	0.26	0.26

TABLE 6.2.4 REACTOR DIMENSIONS

Pin OD (mm) / Equivalent outer radius (mm)	8.0	8.5	9.5	10.5	11.5
Inner Core	106.0	112.0	121.0	132.0	142.0
Outer Core	143.0	149.0	163.0	176.0	190.0
Radial Blanket	182.0	190.0	207.0	224.0	241.0
Radial Reflector	207.0	217.0	236.0	256.0	275.0

TABLE 6.3.1

REACTOR CHARACTERISTICS

(carbide fuel)

Reactor thermal power	MWth	3.000
Reactor electrical power	MWe	1.200
Coolant		Na
core inlet temperature	°C	395
core outlet temperature	°C	545
Core height	cm	100.0
Axial blanket (upper/lower)	cm	30.0/30.0
Axial reflector	cm	20.0
Core diameter	cm	331.0
Radial blanket	row	3
Radial reflector	row	2
Number of assemblies		
inner core		169
outer core		144
radial blanket		216
reflector		176
Fuel cycle lenght	day	255
Load factor		0.70
Number of refueling batches (core/radial blanket)		3/5

TABLE 6.3.1

REACTOR CHARACTERISTICS (cont.)

Fuel assembly design		
fuel material		(Pu,U)C
density	% TD	85
pins per assembly		169
lattice pitch	cm	17.83
fuel pin OD	cm	1.05
fuel pellet OD	cm	0.902
cladding material		SS 316
cladding thickness	cm	0.07
wire diameter	cm	0.12
Radial blanket assembly design		
blanket material		(UC) dep.
pis per assembly		61
pin OD	cm	1.85
pellet od	cm	1.72
cladding thickness	cm	0.065
fuel density	% TD	95
wire diameter	cm	0.095

TABLE 6.3.2

REACTOR DIMENSIONS

(' carbide fuel)

ZONE	Equivalent outer radius (cm)	Height (cm)
Inner core	121.7	100.0
Outer core	165.6	100.0
Radial blanket	215.3	
Radial reflector	248.5	
Axial blanekt		30.0
Axial reflector		20.0

TABLE 6.3.3

REACTOR MATERIAL COMPOSITION

(carbide fuel)

ZONE	Material volume fraction			
	Core fuel (Pu,U)C	Sodium	S.steel type 316	Blanket fuel $(UC)_{dep}$
Core	0.39	0.37	0.24	
Radial blanket		0.31	0.18	0.51
Axial blanket		0.37	0.24	0.39
Radial reflector		0.14	0.86	
Axial reflector		0.37	0.63	

TABLE 6.3.4

REACTOR NUCLEAR CHARACTERISTICS -RESULTS-

(carbide fueled homogeneous reactor)

* Core fuel enrichment	w/o	
inner core		11.75
outer core		14.75
Blanket fuel enrichment		
$^{238}_{U}$	w/o	99.8
$^{235}_{U}$		0.2
Fuel density	% TD	85
Cladding thickness	mm	0.70
Driver pin outer diameter	mm	10.50
Blanket fuel pin outer diameter	mm	18.50
Power peaking factor		1.566
Initial fissile plutonium inventory	ton	3.705
Breeding ratio		1.42
Compound system doubling time	year	15.7
Reactor doubling time	year	14.3
Average burnup	MWd/t	5.812E 04

* means fuel concentration

TABLE 6.3.5

REACTOR DIMENSIONS

(carbide fuel, cladding thickness= 0.45mm)

ZONE	Equivalent outer radius (cm)	Height (cm)
Inner core	117.7	100.0
Outer core	160.2	100.0
Radial blanket	208.3	
Radial reflector	240.5	
Axial blanket		30.0
Axial reflector		20.0

TABLE 6.3.6

REACTOR MATERIAL COMPOSITION

(carbide fuel, cladding thickness=0.45mm)

Z O N E	MAterial volume fraction			
	Core fuel (P,U)C	Sodium	S.Steel type 316	Blanket fuel $(UC)_{dep}$
Core	0.42	0.38	0.20	
Radial blanket		0.29	0.17	0.54
Axial blanket		0.38	0.20	0.42
Radial reflector		0.14	0.86	
Axial reflector		0.38	0.62	

. TABLE 6.3.7

· REACTOR NUCLEAR CHARACTERISTICS

- RESULTS-

(carbide fuel, cladding thickness= 0.45mm)

* Fuel enrichment	w/o	
inner core		11.0
outer core		13.55
Fuel density	% TD	85
Cladding thickness	mm	0.45
Driver pin outer diameter	mm	10.00
Blanket fuel pin outer diameter	mm	18.00
Power peaking factor		1.634
Initial plutonium inventory (^{239}Pu + ^{241}Pu)	ton	3.441
Breeding ratio		1.49
Compound system doubling time	year	12.80
Reactor doubling time	year	11.80
Average burnup	MWd/t	5.797E 04

Obs. * means fuel concentration

TABLE 6.4.1

SODIUM VOID REACTIVITIES AND DOPPLER COEFFICIENTS FOR OXIDE AND CARBIDE FUELED REACTORS

O X I D E F U E L			
	BOL	BOEC	EOEC
Sodium void reactivity, total core , Δk	0.0199	0.0238	0.0261
Doppler coefficient total core ,T $\frac{dk}{dt} \times 10^4$	- 92.0	- 68.0	- 68.0
C A R B I D E F U E L			
	BOL	BOEC	EOEC
Sodium void reactivity total core ,Δk	0.0224	0.0260	0.0306
Doppler coefficient total core, T $\frac{dk}{dt} \times 10^4$	- 64.0	- 59.0	- 42.0

Obs: Isothermal Doppler for sodium in core:

1000 ⟶ 2100 K for oxide and 1000 ⟶ 1800 K for carbide

TABLE 6.5.1

MAXIMUM TEMPERATURE - RADIAL DISTRIBUTION (°C)

region / cycle	Coolant	Clad inner surface	Clad outer surface	Fuel surface	Center of fuel
BOEC *(47.22)	545.0	545.0	574.8	840.2	1250.9
EOEC *(52.21)	545.0	545.0	578.6	868.6	1309.4

Obs: (*) - Coolant mass flow rate (Kg/sec) nccessary.

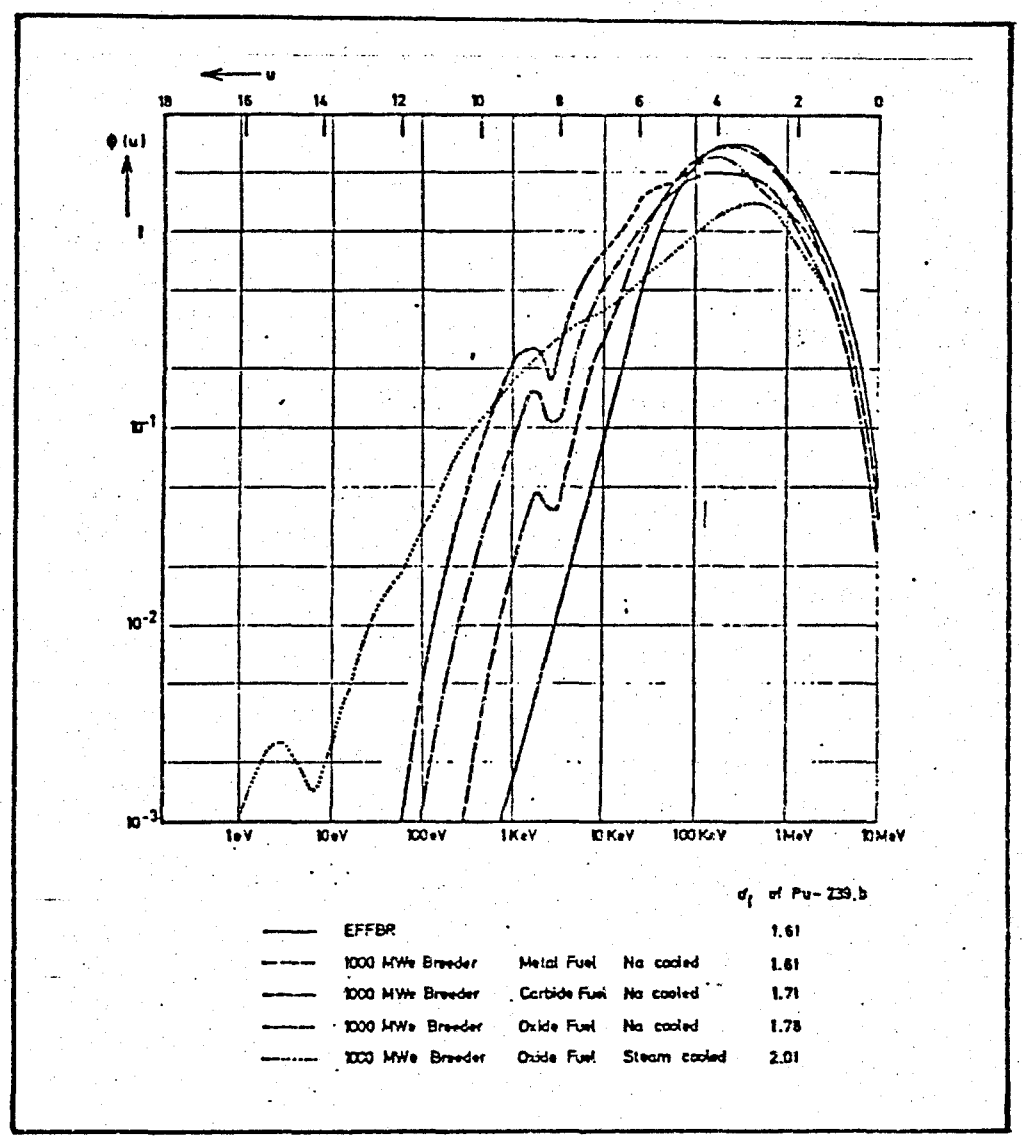

FIG 6.1.1

NEUTRON FLUX SPECTRA OF FAST REACTORS /10/

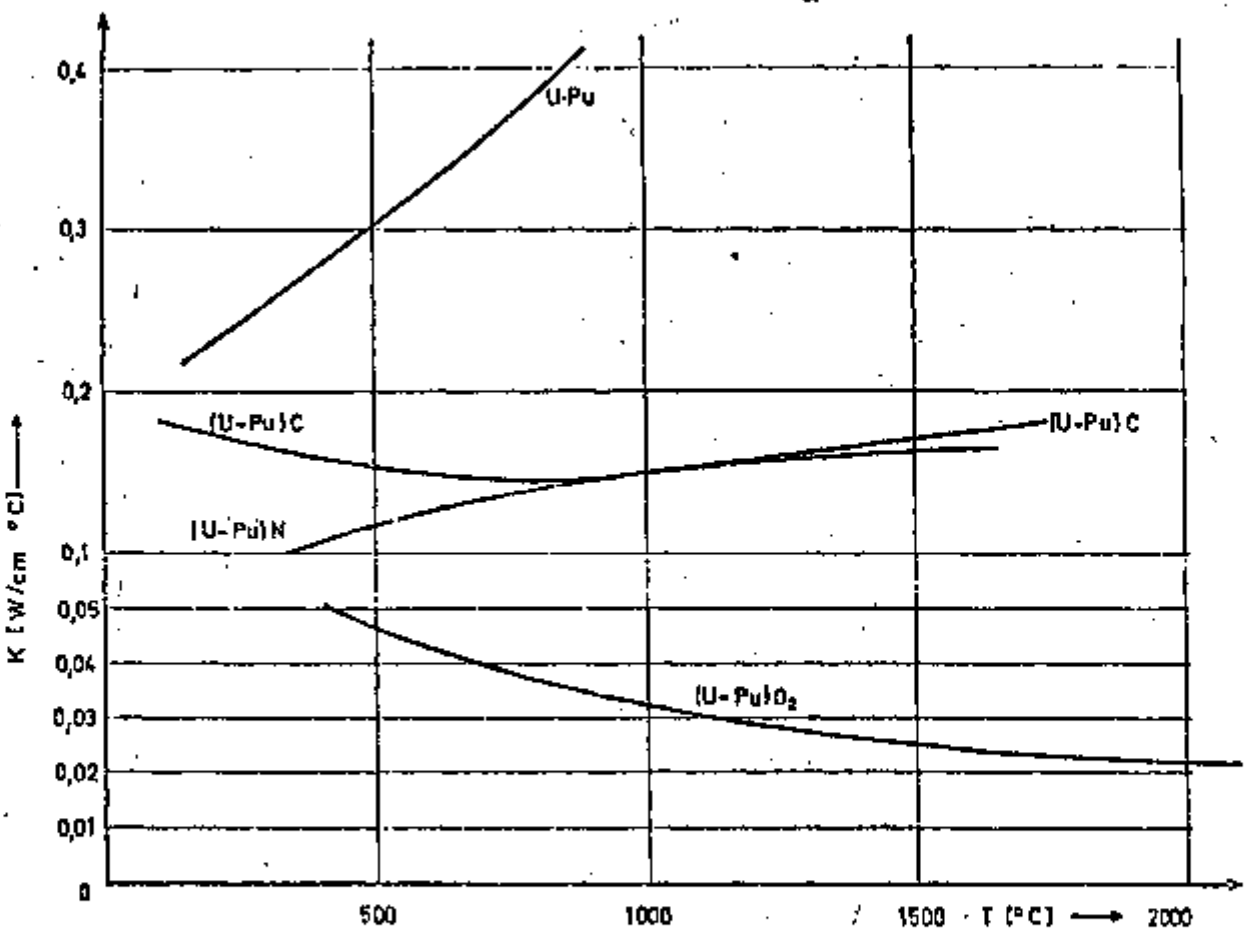

FIG 6.1.2 : Heat Conductivity of Mixed Oxide-Nitride-Carbide and Metal Fuel (Ceramic Density 95 % th. D., Pu Content 20 Weight-%). /63/

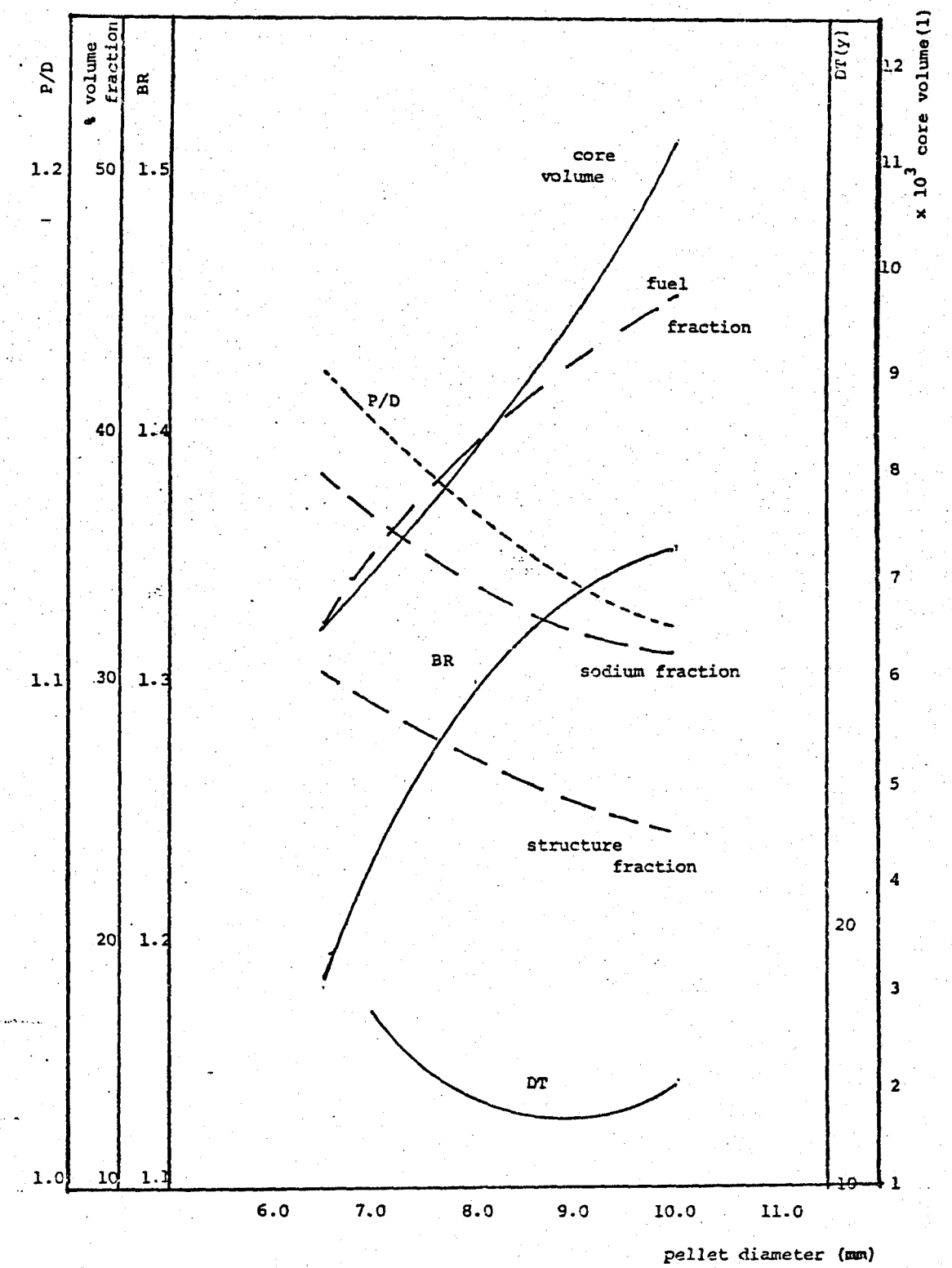

FIG . 6.2.1

RDT, BR AND MATERIAL COMPOSITION AS FUNCTION OF PELLET DIAMETER (Carbide fuel).

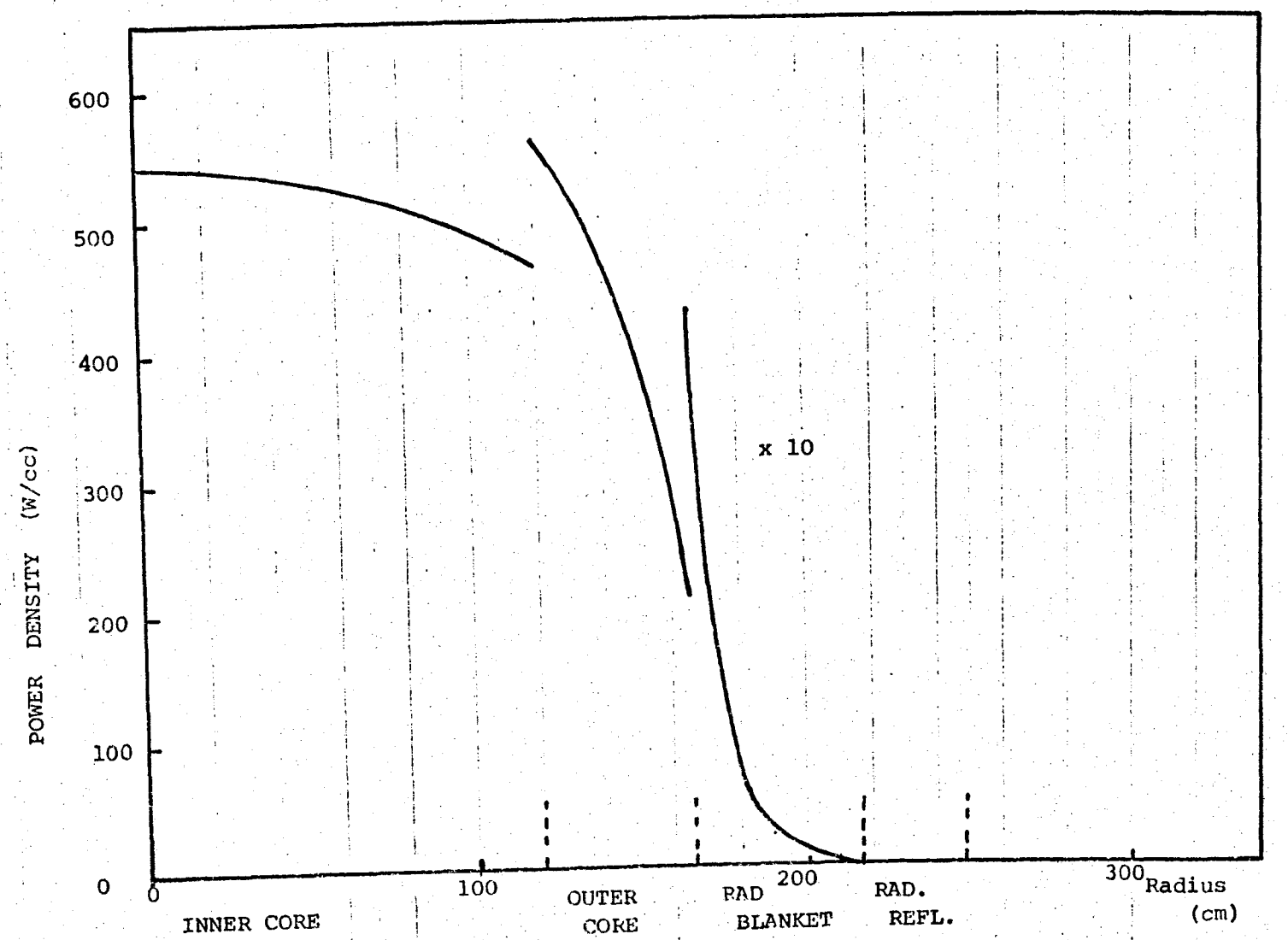

FIG 6.3.1
RADIAL POWER DISTRIBUTION AT BOL

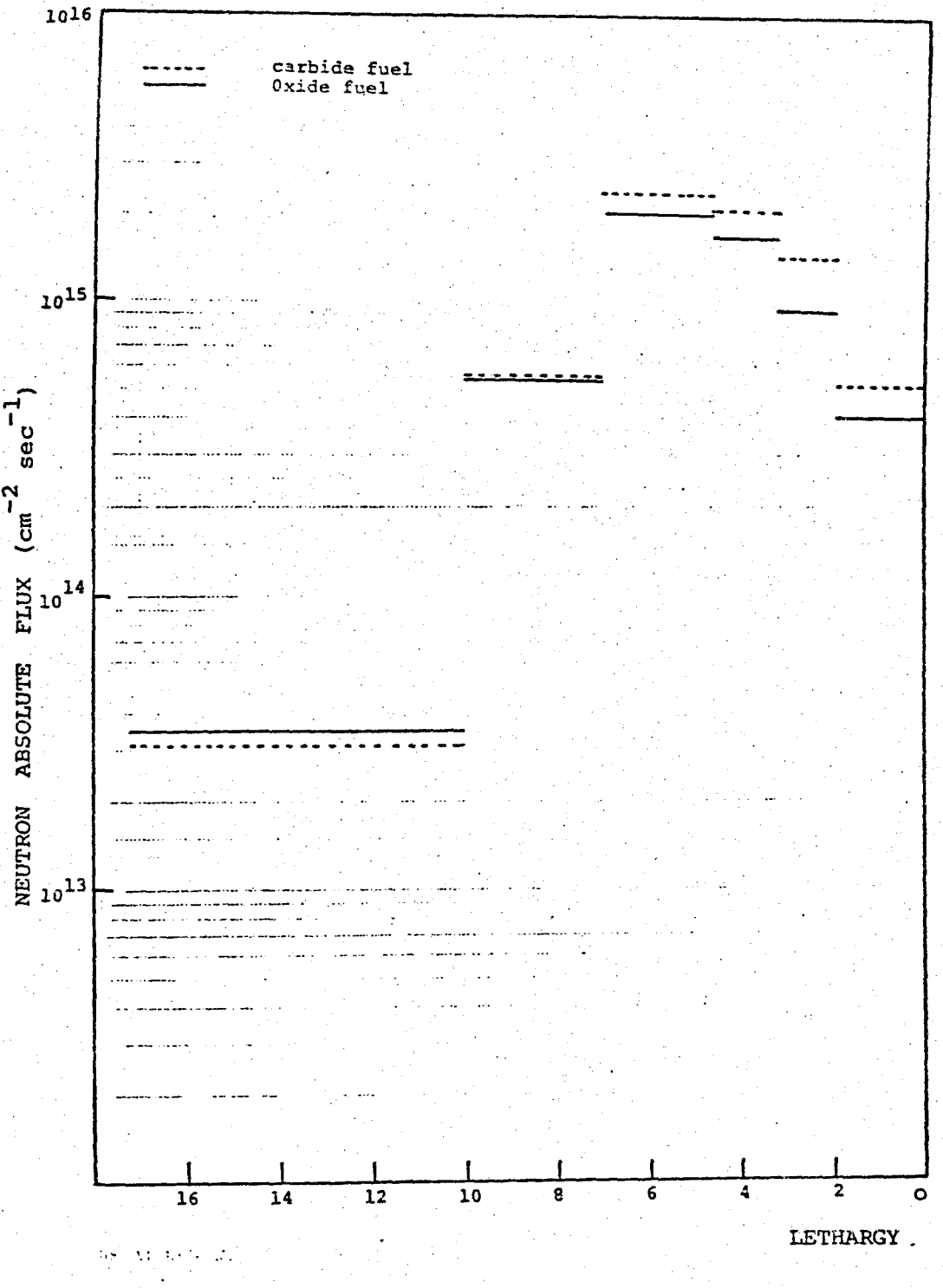

FIG 6.4.1
NEUTRON SPECTRA FOR CARBIDE AND OXIDE CORE
(EOEC)

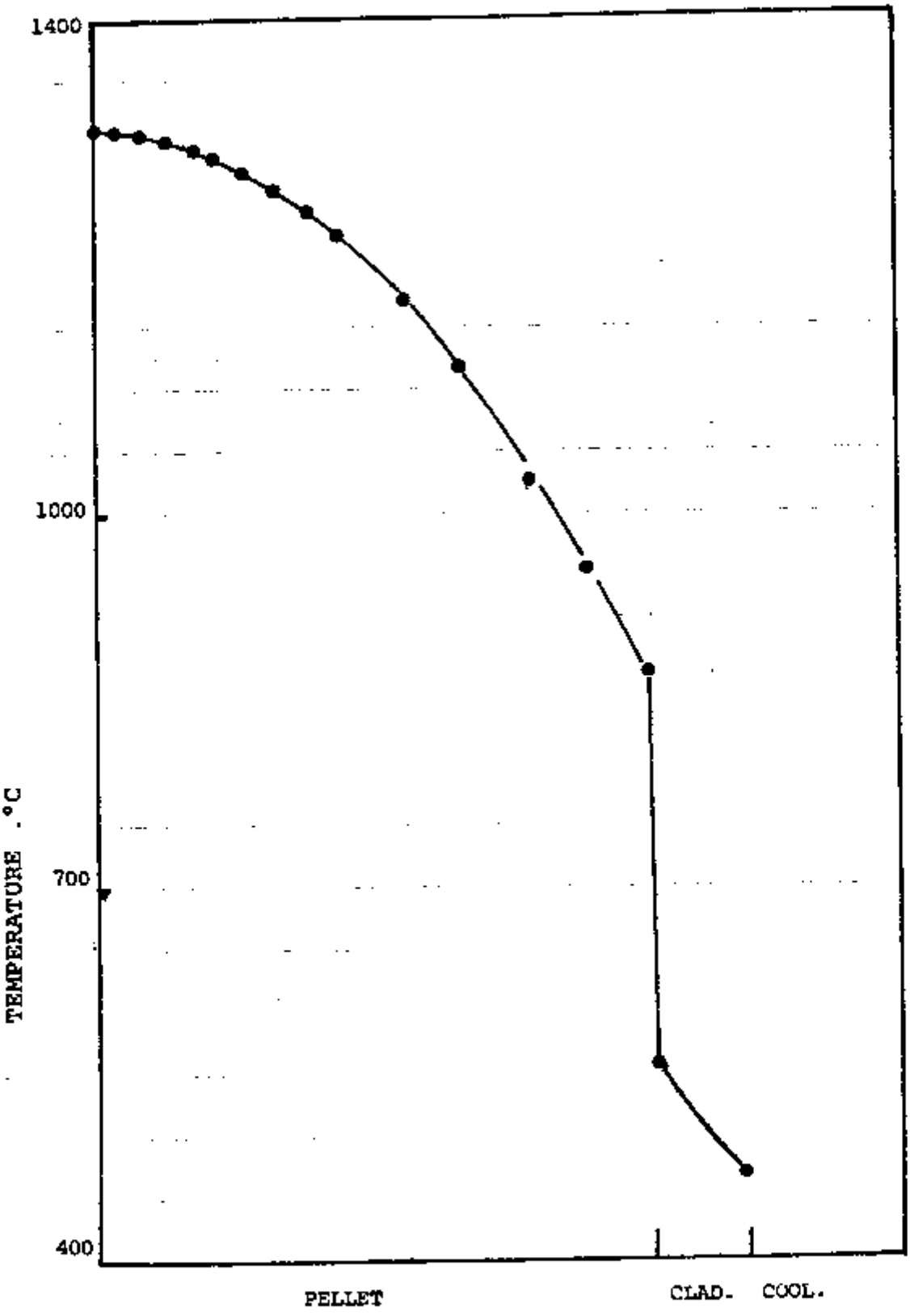

FIG 6.5.1 PROFILE OF FUEL PIN TEMPERATURE

CHAPTER 7

HETERGOGENEOUS REACTORS

7.1 INTRODUCTION

One of the primary motivations of developing the heterogenoeus core configuration of a LMFBR is its increased breeding ratio, reduced sodium void reactivity worth and reduced hypothetical disruptive accident energies.

It is known that there is not a just one heterogeneous reactor but a great variety of heterogeneous cores depending on the arrangement of the internal blankets assemblies into the core zone. We can mention the heterogeneous core with the axial internal blankets (the axial heterogeneous core) /29,30/; the heterogeneous cores with the radial internal blankets (the radial heterogeneous core) /48,49,50,51/ and the modular island core /31,56/ .

A systematic methods for designing heterogeneous configuration having a low value of sodium void reactivity is presented in the ref. /48/ and its conclusion is that among several core configurations the heterogeneous that consist of sucessive radial core and blanket zones

(radial heterogeneous core) are very promissing .

The arrangement of the internal blanket assemblies in the core is of great significance to the performance of the reactor. A basic characteristics of heterogeneous cores is then the degree of neutronic coupling between different core zones. As the thickness of the internal blanket zones increases the neutronic coupling among the core zones decreases and this increases the sensitivity of the power distribution.

The comparative studies /51,53,56,57/ between heterogeneous and homogeneous configurations have shown the higher breeding performance and lower positive sodium void reactivity for the former core. Several experiments for sodium void and physics properties measurements have been made in experimental reactors such as ZPPR and Masurca /54,55/.

Many studies were divulged in the international conferences as those held in Chicago /58/, London /60/ ,France /59/ and IDAHO /61/ where the safety and economic aspects of heterogeneous configurations were discussed.

Biley /22/ suggests that the relative tightly coupled (no more than two-row blanket width) radial heterogeneous cores with optimum fuel pin design provide a better balance between the nonenergetics core disruption safety feature and the economic performance.

The heterogeneous core concept is being widely investigated since last years and the applicability of this concept for large commercial reactors is being evaluated currently by various laboratories. In spite of the advantages presented by heterogeneous configuration it has not a defined plane to date its introduction into the planned reactors. The breeder program in the world has been concentrated on the mixed uranium-plutonium oxide fuel.

In this chapter , in order to evaluate the carbide fueled radial heterogeneous core performance, the characteristics of three configurations were investigated, and the results compared with those of oxide fuel.

7.2 CARBIDE FUEL

7.2.1 Reactor Configurations

The reactor configurations analyzed in this chapter are shown in Fig. 7.2.1, where the case (2-1) and case (3-1) are tightly coupled configurations while case (2-2) is loosely coupled.

The optimum pin diameter determined for homogeneous reactor was utilized in all heterogeneous calculations. In addition the internal and radial blanket assemblies are identical in design. The core height and the fuel assemblies design were fixed for all the configurations considered but for the case (2-2) two pin designs were

selected, one conventional with 0.70 mm cladding thickness and other with 0.40mm .

Cases (2-1) and (3-1) have same internal blanket volume ratio of 18% while case (2-2) has higher volume ratio, approximately 28%. In all the configurations the refueling of the core zones and internal blanket assemlies is performed each year with 1/3 of the assemblies eplaced. The radial blanket has a fuel cycle length of 5 years.

7.2.2 Nuclear Characteristics

The calculational method and the cross section data employed for the nuclear characteristics calculations were the same those utilized in homogeneous core.

The generation of the equilibrium cycle was performed by the two dimensional R-Z geometry three group burnup calculations. The plutonium loaded is that from LWR.

The R-Z configurations of the heterogeneous cores for the parametric study are shown in Figs. 7.2.2, 7.2.3 and 7.2.4 and the performance characteristics at EOEC analyzed for three cores are given in Table 7.2.1. Comparisons are made with those of the oxide heterogeneous reactor. The data of oxide fuel heterogeneous reactor used for the comparative study were taken from the work developed by Konomura /22/.

An analysis of the results obtained resulted in the following conclusions:

- Breeding Ratio

Small or no difference was seen in breeding ratio for the three heterogeneous configurations considered but when compared with homogeneous configuration an increase of 3.5% was verified. This gain in breeding is primarily the result of the introduction of the greater fertile mass of the blanket assemblies ant its effect on the neutron importance. The neutron spectrum in the heterogeneous design has higher average energy that tends to improve breeding performance.

On the other hand when compared with oxide heterogeneous reactor a substantially increase in breeding ratio is observed emphasizing the good nuclear properties of the carbide fuel.

- Reactor Doubling Time

In spite of the high breeding ratio, the reactor doubling time is larger in heterogeneous core because high fissile inventory required to makes reactor critical.

But 16 years of the carbide compared with 32.7 years to the oxide represent a significant reduction, near 50% in doubling time.

- Burnup Swing

Generally the reactivity change with burnup is smaller in heterogeneous than homogeneous core for tha same fuel pin diameter. The degree of neutronic coupling in a radial heterogeneous configuration affects the burnup swing. For the same pin diameter the burnup swing is smaller in tightly coupled core as can be observed in Table 7.2.1. For the same core configuration using oxide fuel results a higher burnup reactivity due smaller fuel pin diamenter.

Changing fuel cladding thickness the breeding ratio will increase due to fuel volume fraction increasing. The configuration (2-2) was choosen considering its low positive sodium void reactivity value, and assuming a cladding thickness of 0.40 mm the calculations were performed. As illustrated in Tab. 7.7.2 a brreding ratio of 1.52 and reactor doubling time of 13.0 years were achieved for this case.

The power distribution in heterogeneous design is very sensitive to enrichment distribution and to the thickness of the internal blanket. The flux distribution for the three cases are illustrated in Figs. 7.2.5 , 7.2.6 and 7.2.7 .

7.2.3 Safety Characteristics

Sodium void reactivity and Doppler coefficient were calculated at ECEC as inherent reactor safety related parameters and listed in Table 7.2.3.

The sodium void reactivity is smaller in the heterogeneous core than in a homgeneous core by rougly a factor of two. All the sodium void reactivities have been calculated determined from direct k_{eff} calculations for the voided and unvoided reactor. Both fuel and blanket (axial and internal) zones were considered voided.

The sodium void decrease for the radial heterogeneous core is mainly caused by the increment of the leakage neutron from the core into the internal blanket. Thus sodium void reactivity depends on the size of the core zones and the thickness of the internal blankets. For thicker internal blanket the sodium void is reduced as was observed for the case (2-2).

Doppler coefficient value for the homogeneous and heterogeneous configurations are given in Table 7.2.3. The Doppler coefficient at core zone is smaller for heterogeneous core due its high fissile enrichment. For heterogeneous reactor an additional Doppler feedback is verified from internal blanket zones, thus considering total core small difference is observed between heterogeneous and homogeneous configurations.

7.2.4 Results

Three heterogeneous core configurations have been analyzed. The nuclear characteristics are quite equal for all the cases but the sodium void reactivity is lower in the loosely coupled case.

The breeding ratio increased near 3.5% and doubling time reduced approximately 12% relatively to the homogeneous core.

The fissile inventory of heterogeneous core is 30 to 50 % higher than of the homogeneous design and for the same residence time average and peak burnup are lower in heterogeneous design. Comparing the burnup swing for same fuel pin diameter, it found that the burnup swing is smaller for heterogeneous case and this reduction depends on the neutronic coupling. For the tightly coupled configuration the burnup swing is smaller than that for loosely core.

When compared with oxide fuel heterogeneous configuration a significant improvement on breeding performance was verified. For the same configuration an increase of 16% is attained for breeding ratio and reactor doubling time is near 16 years shorter.

For heterogeneous configuration the degree of neutronic coupling affects the sodium void reactivity and it is lower for loosely coupled core. The reduction in sodium void reactivity relatively to the homogeneous is 30 to 60 %.

Although the thick internal blanket zone induces a low sodium void reactivity, great decoupling reduces core performance. Consequently, to design heterogeneous core the compromise between sodium void effect and core performance must be analyzed.

From the results of the present study we conclude that the configuration (2-2) with thin cladding, 0.40 mm thickness , can offer a short doubling time of 13.0 years and low positive sodium void reactivity.

7.3 SUMMARY OF CARBIDE FUEL DEVELOPMENT PROGRAMS

In chapters 6 and 7 of this work the good performance of carbide fuel was demonstrated. The high heavy metal density of carbide allows a better breeding ratio than with oxide fuel, and in additon, the good thermal conductivity permits a hig linear power, in consequence a shorted soubling time is achieved.

However , in order to use carbide fuel to improve on the oxide fuel economics a number of difficulties must be overcome.

The main areas of required development are:

1 - Development of fabrication techniques

For fabrication of mixed carbide fuel, various procedures exist /36,43,45/ but a real fabrication

route on an industrial scale is not yet developed. The fabrication process of carbide requires a special facilities for handling the fuel in low oxigen and low moisture atmosphere.

Therefore a comparison of fabrication between mixed oxide and mixed carbide is not possible today, taking into account the fact that the state of technology reached in mixed oxide fabrication is much more advanced.

2 - Cladding material development

As oposite to the oxide fuel, the compatibility of carbide fuel with cladding material like as stainless steel constitutes a serious problem in the design of a fuel element. A new material like vanadium alloy is considered /38/ .

3 - Demonstration of high exposure -high temperature irradiation.

Demonstration of the satisfactory behaviour of (Pu,U)C fuel is required for exposure of approximately 100,000 MWD/t. The fuel swelling and creep must be investigated.

4 - Fuel reprocessing technology

Reprocessing for (Pu,U)C fuel still has to be developed.

The irradiation experiments performed for the carbide fuel in experimental reactors as Rapsodie and DFR and EBR-II, were planned to investigate the behaviour of fuel pin, the fuel swelling, fission-gas release, fuel/cladding compatibility. Several programs for the carbide fuel development are in evolution.

Since 1968 a research program has been performed in Germany /45/. The main objectives of this program are : development of a suitable fuel fabrication process; basic research to obtain specific material data for irradiation creep and swelling of (Pu,U)C ; planning,design, construction and performance of irradiation experiments; post-irradiation examination and evaluation data. Introduction of carbide fuel into SNR /43/ are also being considered.

The objective of French irradiation program /40/ is to determine the satisfactory behaviour of carbide fuel under high exposure. They hope to substitute mixed carbide for mixed oxide as Rapsodie driver fuel.

Up to now He bonded and Na bonded fuel and fuel rod concepts are actively tested in experimenal programs /40,42,43/. For a number of carbide fuel burnup up to 70,000 MWD/t have already be obtained without failure /42/. The experimental results showed also that the carbide

fuel swell more than oxide and that the degree of swelling depend very much on the fuel center temperature /40/.

Irradiation testing of mixed carbide fuel however lags considerably behind that of oxide. The urgent need for an accelerated carbide fuel testing program is clear.

TABLE 7.2.1

HETEROGENEOUS REACTOR NEUTRONIC CHARACTERISTICS - RESULTS --

	Case (2-1) Carbide	Case (3-1) Carbide	Case (2 - 2) Carbide	Case (2 - 2) Oxide
K_{eff} (EOEC)	1.005	1.005	1.004	1.001
*Enrichment (w/o)	13.9/15.85/15.85	15.47/15.85/15.81	16.05/18.9/18.09	20.7/23.7/23.1
Fissile plutonium initial inventory (ton)	5.320	6.079	5.293	6.960
Breeding ratio	1.47	1.48	1.47	1.26
Reactor doubling time (y)	15.5	17.2	15.4	32.7
CSDT (year)	17.3	19.6	17.1	40.9
Peaking factor	1.543	1.536	1.570	1.632
Maximum burnup $_4$ (Mwd/t)10^4	8.545	7.191	9.430	
Na void reactivity (%Δ k)	1.81	1.67	0.98	0.93
Doppler coef(T $\frac{dk}{dT}$) x 10^4	-70.0	-74.0	-73.0	-112.0
Burnup swing (%Δk)	0.78	0.72	2.06	3.09
Inner blanket volume ratio	0.18	0.18	0.28	0.28
Core outer radius (cm)	199.0	214.0	199.0	224.0

Obs.* means fuel concentration

TABLE 7.2.2

REACTOR NUCLEAR CHARACTERISTICS

CASE (2-2) - RESULTS -

(cladding thickness=0.45mm)

*Fuel enrichment	w/o	15.1/17.66/17.01
Fuel density	% TD	85
Cladding thickness	mm	0.45
Driver pin outer diameter	mm	10.0
Blanket pin outer diamenter	mm	18.0
Internal blanket volume ratio		0.28
Fissile plutonium initial inventory	ton	5.017
Breeding ratio		1.53
Reactor doubling time	year	13.0
CSDT	year	14.5
Peaking factor		1.68
Maximum burnup	MWd/ton	9.103E 04
Core outer radius	cm	192.0
Fuel volume fraction		0.42
Na void reactivity (10^{-2})		1.09
Doppler coefficient ($T \frac{dk}{dt}$) X 10^{4}		-71.0

Obs. * means fuel concentration

TABLE 7.2.3

DOPPLER COEFFICIENTS AND NA VOID REACTIVITIES AT EOEC

	CARBIDE				OXIDE	
	HETEROGENEOUS			HOMOGENEOUS	HETEROG.	HOMOG.
	(2 - 1)	(3 - 1)	(2 - 2)		(2 - 2)	
Doppler coefficient						
Core	-0.0058	-0.0062	-0.0061	-0.0073	-0.0087	-0.0096
Core + AB+IB	-0.0070	-0.0074	-0.0073	-0.0078	-0.0112	-0.0103
Na void reactivity						
Core + IB	0.0181	0.0167	0.0098		0.0093	
Core + AB + IB	0.0236	0.0224	0.0144	0.0306		0.0260

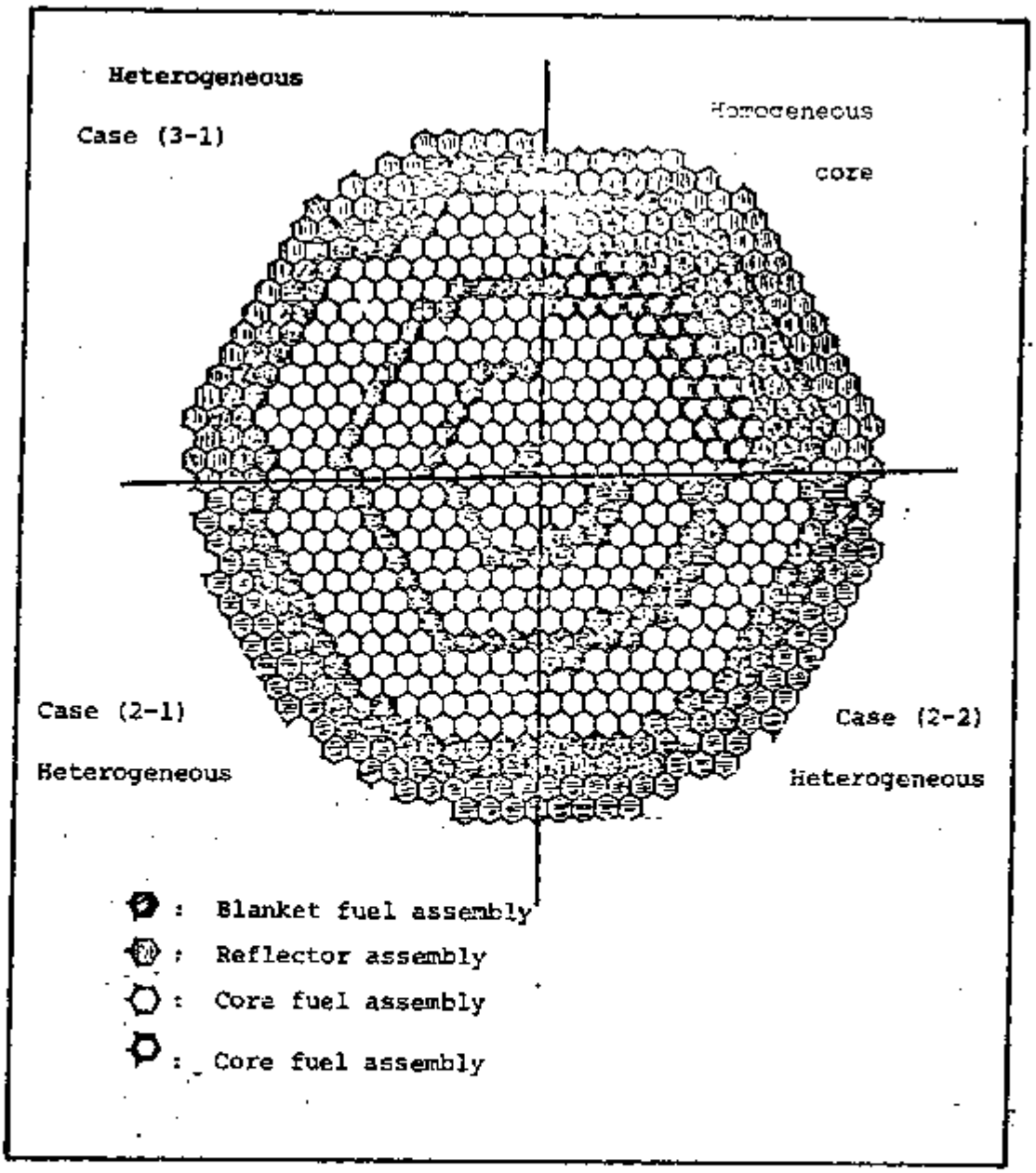

FIG 7.2.1

CARBIDE FUELED LMFBR CORE LAYOUT CONSIDERED

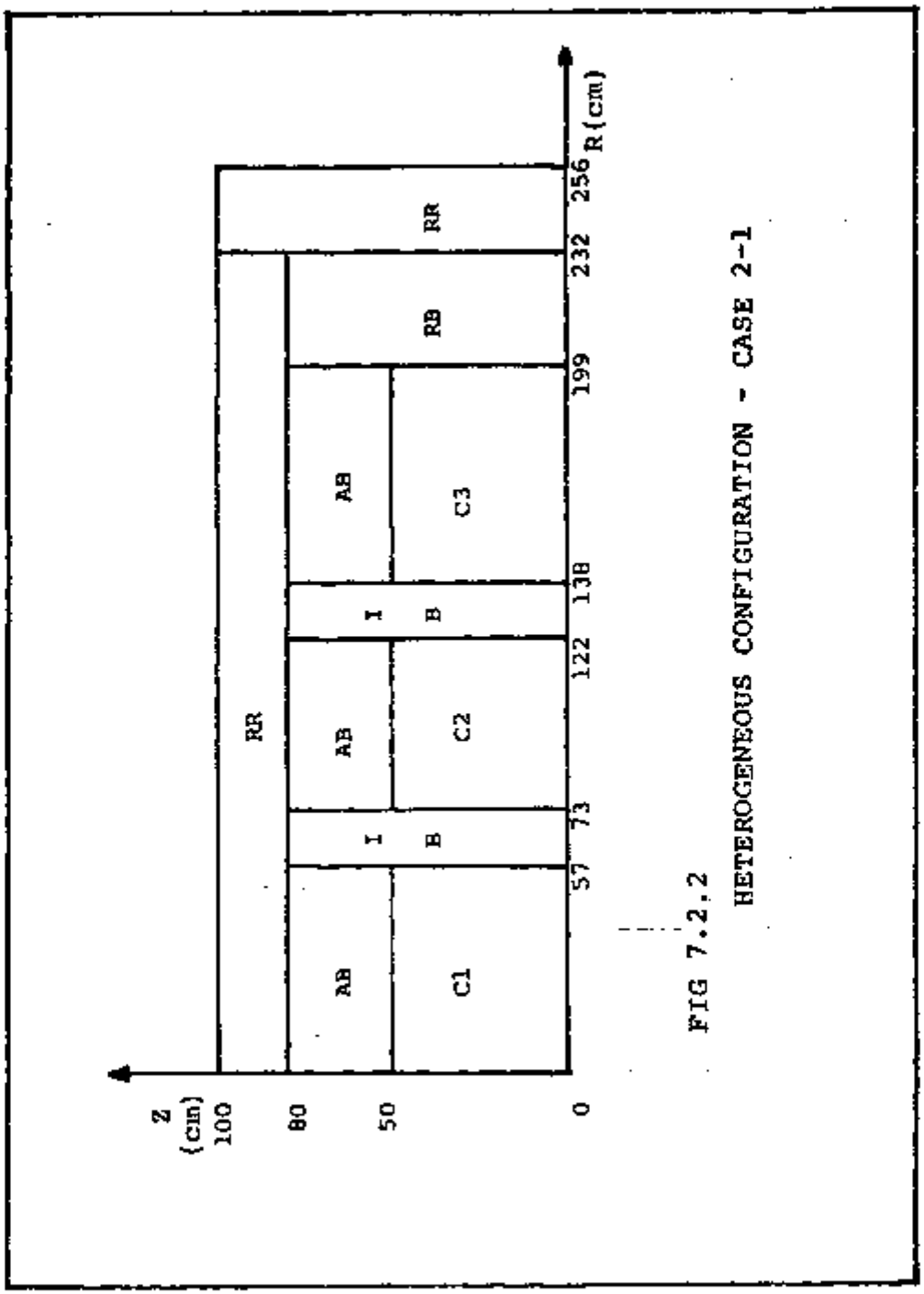

FIG 7.2.2
HETEROGENEOUS CONFIGURATION - CASE 2-1

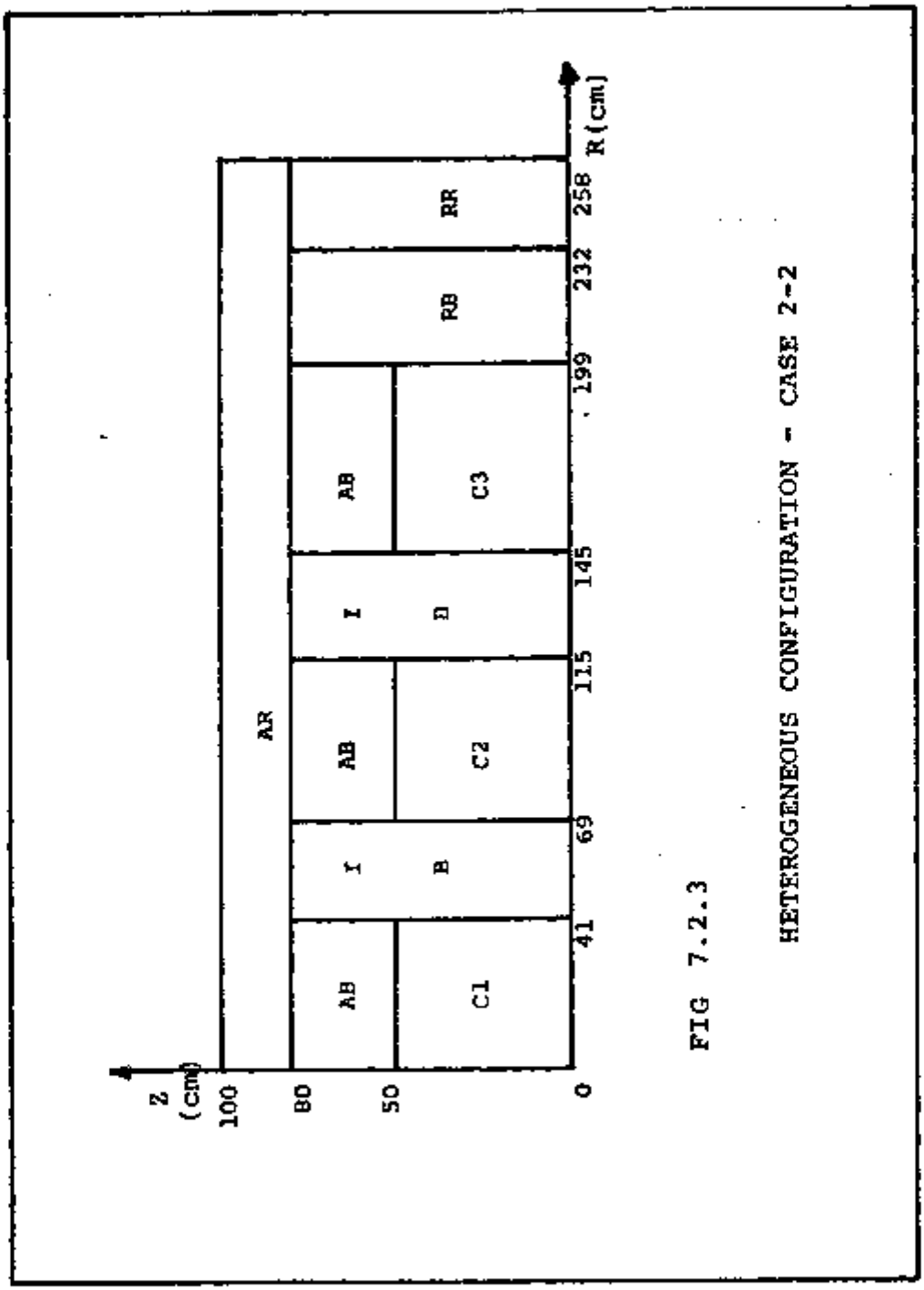

FIG 7.2.3 HETEROGENEOUS CONFIGURATION - CASE 2-2

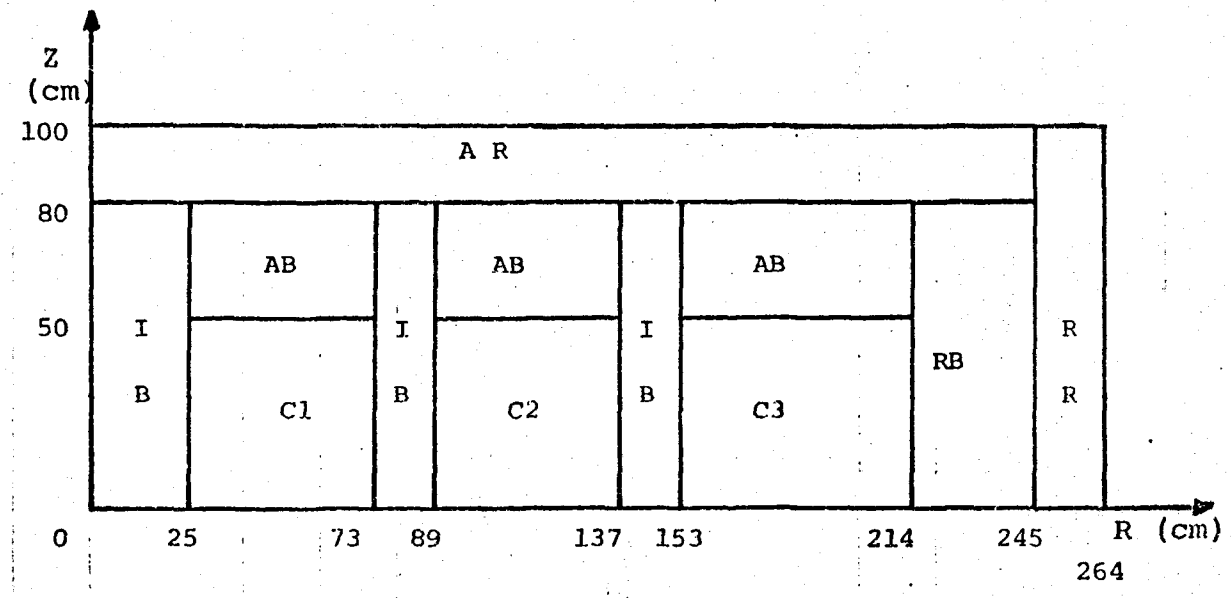

FIG 7.2.4

HETEROGENEOUS CONFIGURATION - CASE 3-1

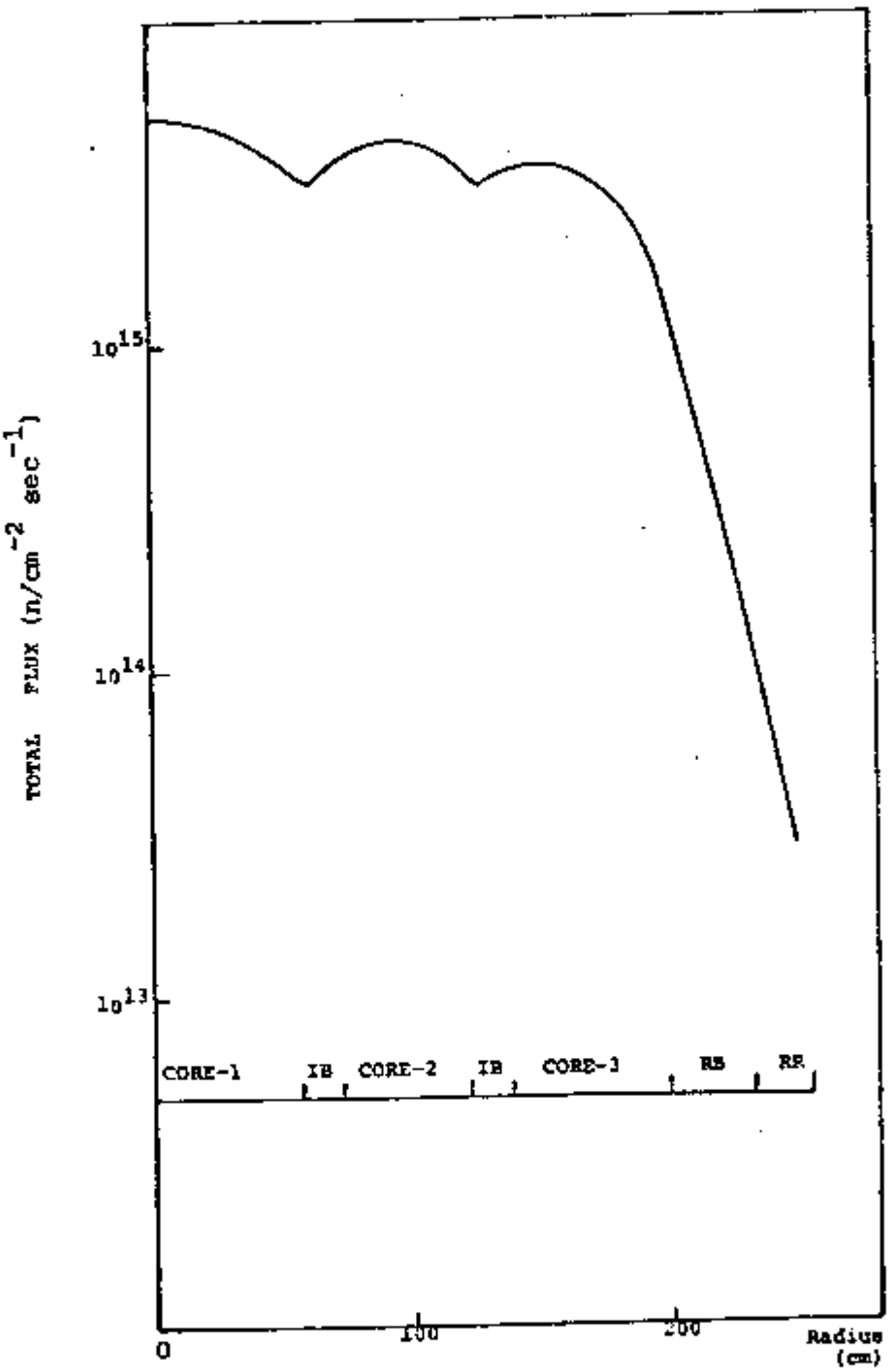

FIG 7.2.5.
EOEC FLUX DISTRIBUTION FOR HETEROGENEOUS CORE
(case 2-1)

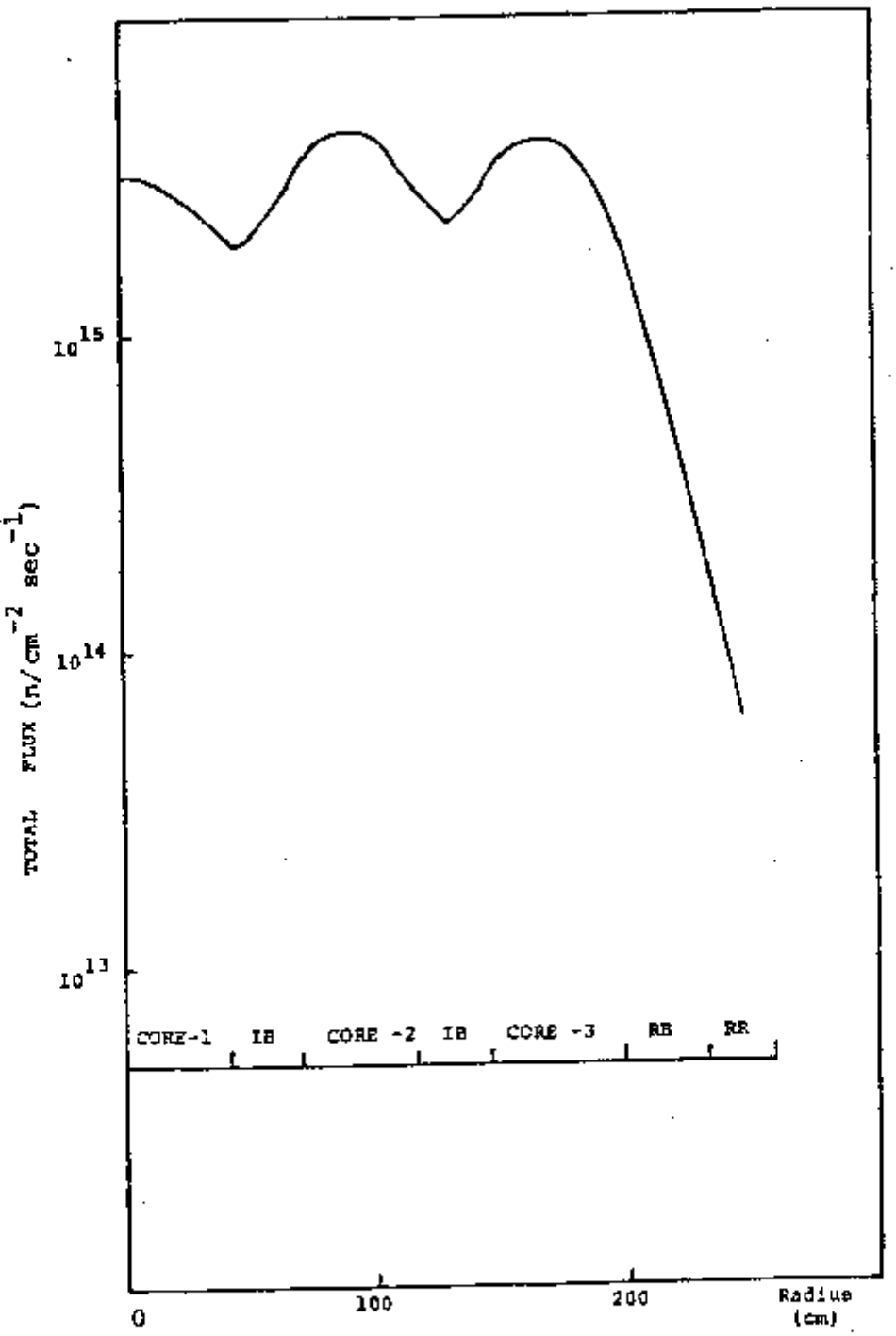

FIG 7.2.6

EOEC FLUX DISTRIBUTION FOR HETEROGENEOUS CORE

(case 2-2)

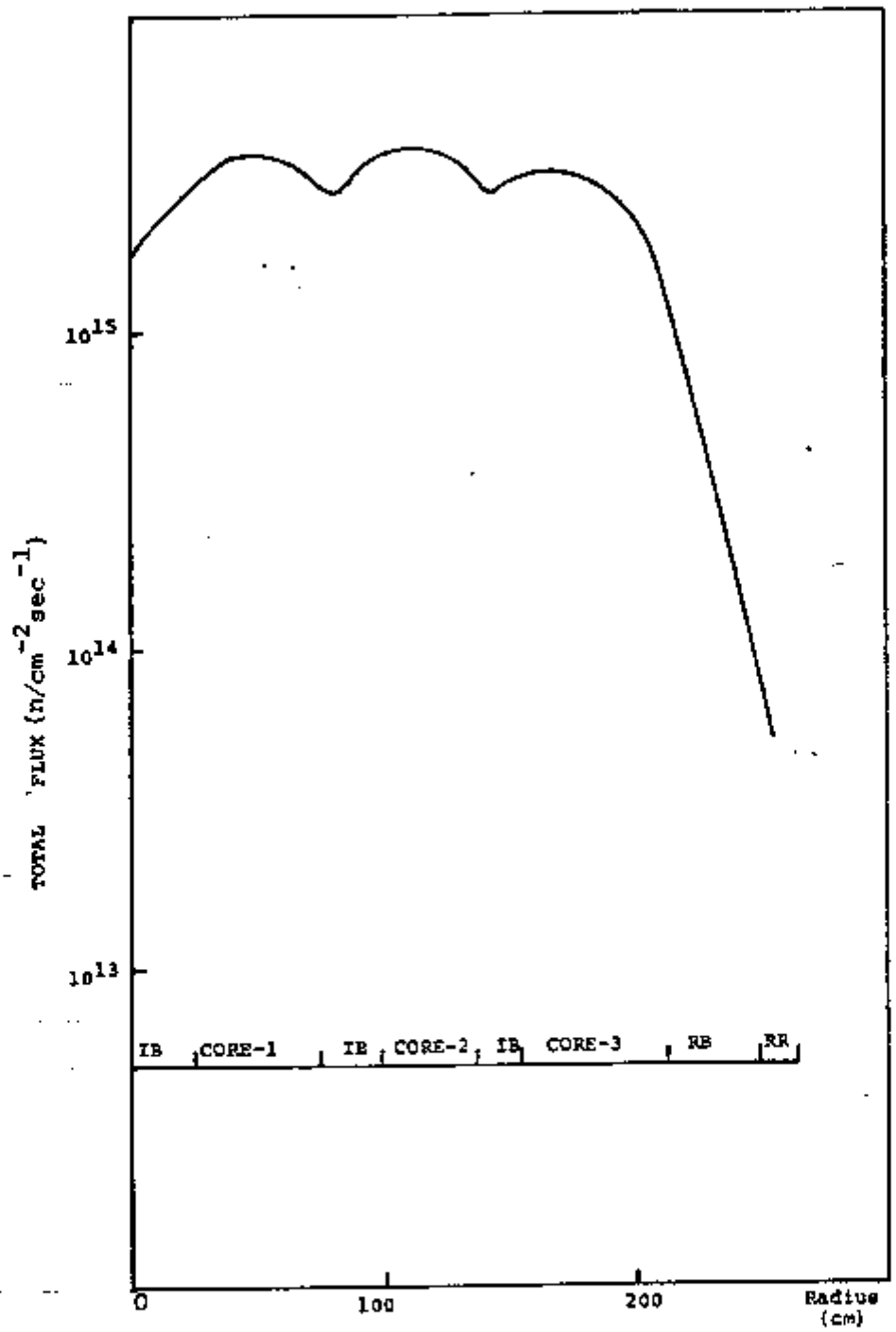

FIG 7.2.7

FLUX DISTRIBUTION FOR HETEROGENEOUS CORE AT EOEC (case 3-1)

CHAPTER 8

ANALYSIS OF IMPROVEMENT IN BREEDING PERFORMANCE OF HETEROGENEOUS CONFIGURATION CORE

8.1 INTRODUCTION

For the same power, core height and fuel pin design, the heterogeneous configuration presents a higher fertile inventory, a larger breeding performance and smaller sodium void reactivity than the homogeneous one. This improvement in breeding ratio can be attributed to the increased fertile material inventory and the spectral variation due to the internal blanket zone .

The purpose this study is to analyze the changes in breeding ratio that result from introduction of the blanket assemblies into the core zone.

8.2 NEUTRON SPECTRUM AND FERTILE MATERIAL INVENTORY EFFECT ON BREEDING RATIO

8.2.1 Methodology

The conventional breeding ratio may be written, in terms of neutron balance as :

$$BR = \frac{(\nu - 1) - \alpha - P - L + (\nu' - 1)\delta}{1 + \alpha}$$

Where

α = capture to fission rate ratio for the fissile material

ν = average number os neutron per fissile fission

ν' = average number of neutrons per fertile fission

δ = fertile to fissile fission rate

η = neutron production to absorption rate

P = parasitic capture to fissile fission rate ratio

L = leakage to fissile fission rate ratio

If only Pu-239 and U-238 are considered we have the following new expression for B.R.

$$B.R. = \eta^{239} - 1 + \eta^{238} \left(1 - \frac{1}{\nu^{238}} \right) \frac{\Sigma_a^{238}}{\Sigma_a^{239}} - \text{losses}$$

Where losses include neutron leakage and parasitic capture.

The breeding ratio depends on η , ν , ν', σ_a , σ_f and these data vary with spectrum and fuel composition. Fig.8.2.1 shows the variation of η with energy for

U-233 ,U-235 and Pu-239. One may be note that a low energies η is approximately constant for U-233 and U-235 and beyond 10 keV η increases and particularly for the case of Pu-239, raises to comparatively large values.

In this study the change in breeding ratio with respect to the differences in fertile inventory and neutron spectrum between equivalent homogeneous and heterogeneous cores were analyzed. Also breeding ratio for several neutron spectra were calculated to verify the effect of the spectrum on B.R. The analysis were made through the reaction rate calculation.

The calculations were performed using a one dimension diffusion theory code and the buckling values used to account for leakage were obtained from two dimension calculation.

8.2.2 Fertile Material Inventory

Usually in the heterogeneous reactors the internal and radial blanket assemblies are identical in design, and the fuel volume fraction is higher than of the core zone.

On purpose of analyze the effect of the fertile material inventory on the breeding ratio two fuel pin diameters were taken and for each pin size ,two sets of material volume fraction have been considered in the internal blanket zones as are shown inTable 8.2.1.

Where

DV means that internal blanket zones have a larger fuel volume fraction than core zones.

SV means that core and internal blanket zones have the same fuel volume fraction.

Breeding ratio, breeding ratio changes, fissile and fertile specific inventories calculates are shown in Tabs. 8.2.2 and 8.2.3 . The results show that the heterogenizations effect is larger for the small fuel pin diameter than for large one and the effects of fertile inventory and neutron spectrum are included in the breeding ratio changes verified. Also these effects are smaller for case SV than for case DV once the fetile inventory diminishes and spectrum change is smaller for the former case.

8.2.3 Neutron Spectrum

The effect of neutron spectrum on breeding ratio for heterogeneous configuration was verified through a moderator introduction in the core zone .

The heterogeneous core has a harder neutron spectrum in the core region than the homogeneous configuration and this difference induces changes in the ratio of the reaction rate of the isotopes.

A moderator was introduced to soft the

heterogeneous core spectrum and the breeding ratio was determined for each spectrum. Hydrogen was choosen as moderator due to its high moderation capacity , but this element has also high absorption cross section that can affect the results. Then the Hydrogen cross section data was altered to avoid the parasitic effect , only the elastic and inelastic scattering were considered.

As a measure of spectrum softness with moderator fraction , the fraction of the neutron flux for energies > 100 keV is listed in Tab. 8.2.5 for case DV and pin OD= 10.5 mm. Tab. 8.2.4 shows the fast neutron fraction for the different core configurations.

From the Tab. 8.2.5 it appeared that when the moderator fraction is equal to 0.0025 the heterogeneous core fast neutron flux is near that of the homogeneous core. The reaction rate changes for Pu-239 , Pu-240, Pu-241,Pu-242 and U -238 with moderator are illustrated in Figs. 8.2.2, 8.2.3 and 8.2.4. Spectral hardening in core region improves total bredding ratio due to:

- Reduction in the rate of the parasitic absorption in isotopes of plutonium (Fig.8.2.4);
- Increase in the fission rate of U-238 in the internal blanket zone (Figs.8.2.1 and 8.2.3). Fig 8.2.1 shows fertile material fission cross section dependence with neutron energy.

8.3 RESULTS

The heterogenization does not improve significantly the breeding ratio when the core and internal blanket zones have the same fuel volume fraction. For cases SV and DV and pin OD=10.50 the effect of each component,i.e ,fertile, inventory and neutron spcetrum, was verified and the results are:

	Breeding change (%)	
Effec	SV	DV
fertile inventory	2.40	3.50
spectral	0.50	0.60
total	2.90	4.10

One may see that the fertile inventory effect contributes more to the breeding ratio improvement for heterogeneous configuration.

TABLE 8.2.1

INTERNAL BLANKET MATERIAL VOLUME FRACTION

Material	Pin Outer Diameter (mm)			
	8.50		10.50	
	SV	DV	SV	DV
Fuel	0.35	0.50	0.39	0.51
Structure	0.29	0.22	0.24	0.18
Coolant (Na)	0.36	0.28	0.37	0.31

TABLE 8.2.2

BREEDING RATIO CHANGES WITH FERTILE MATERIAL INVENTORY

Configuration	Fuel Pin Outer Diameter (mm)			
	8.50		10.50	
	BR	BR	BR	BR
Homogeneous	1.105	----	1.222	---
Heterogeneous				
DV	1.172	0.061	1.272	0.041
SV	1.139	0.031	1.257	0.029

Obs: DV- Internal blanket zones have a larger fuel volume fraction than the core zone.
SV- Core and internal blanket zones have the same fuel volume fraction.

TABLE 8.2.3 SPECIFIC FUEL INVENTORY AND BR FOR DIFFERENT PIN DIAMETERS

	Fuel Pin Outer Diameter 8.50 mm			Fuel Pin Outer Diameter 10.50 mm		
	Homogeneous	DV	SV	Homogeneous	DV	SV
Enrichment (av),%	15.09	17.02	16.62	13.20	15.20	14.80
Specific fissile inventory,kg/MW	1.029	1.241	1.210	1.242	1.726	1.693
Specific fertile inventory, kg/MW	7.943	10.797	10.084	11.110	17.383	16.439
Core breeding ratio	0.952	0.800	0.823	1.072	0.889	0.911
Internal blanket breeding ratio	---	0.243	0.190	---	0.233	0.207
Total breeding ratio	1.105	1.172	1.139	1.222	1.272	1.257

Obs: DV- Internal blanket zones have a larger fuel volume fraction than the core zone;
SV- Core and internal blanket zones have the same fuel volume fraction.

TABLE 8.2.4

NEUTRON FLUX FRACTION (%) FOR ENERGIES > 100 keV

Configuration	Pin OD= 8.50 mm		Pin OD= 10.5 mm	
	Core	Internal blanket	Core	Internal blanket
Homogeneous	68.5	---	68.5	---
Heterogeneous				
DV	69.3	65.0	69.7	63.0
SV	68.1	64.7	69.4	62.6

Obs. DV: Internal blanket zones have a larger fuel volume fraction than the core zone ;
SV: Core and internal blanket zones have the same fuel volume fraction.

TABLE 8.2.5

NEUTRON FLUX FRACTION (%) FOR ENERGIES >100 keV AND BREEDING RATIO

(Pin OD=10.50mm, heterogeneous,case DV)

Moderator fraction	Core	Internal blanket	B.R.
0.000	69.7	63.0	1.272
0.0025	68.5	62.3	1.265
0.005	67.3	61.5	1.258
0.010	64.9	60.0	1.241
0.015	62.5	58.5	1.222
0.020	60.3	56.9	1.202

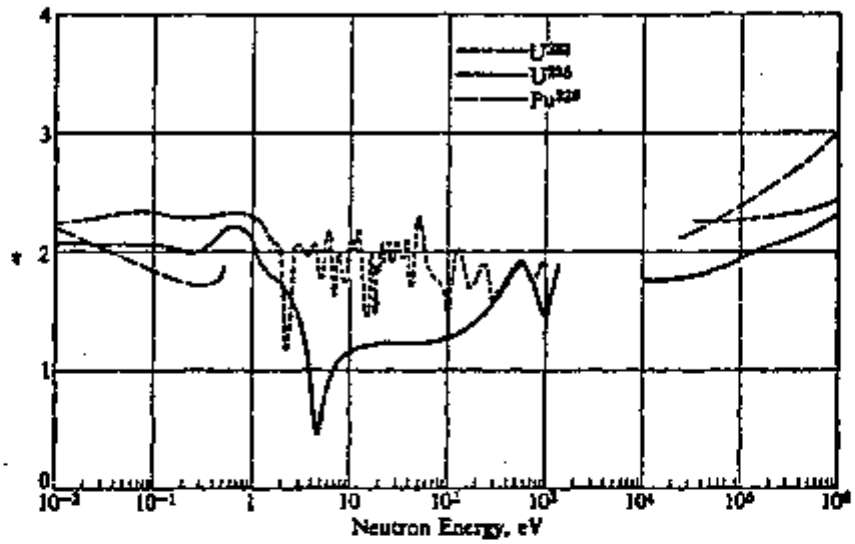

Fig. 8.1.1 /64/

. Variation of ν with energy for U^{233}, U^{235}, and Pu^{239}. The U^{235} curve has been smoothed in the eV region. [From BNL-325, Second Edition (1958 plus supplements).]

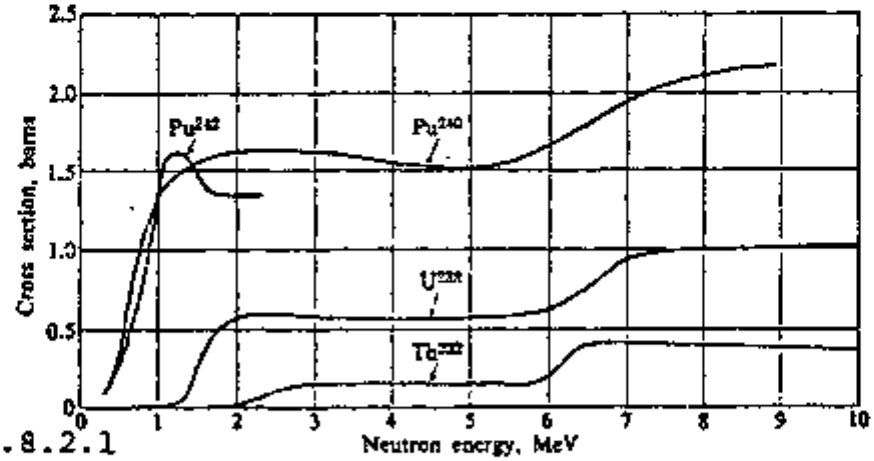

Fig.8.2.1

/64/ . The fission cross sections of Th^{232}, U^{238}, Pu^{240}, and Pu^{242}. [From BNL-325, Second Edition (1958).]

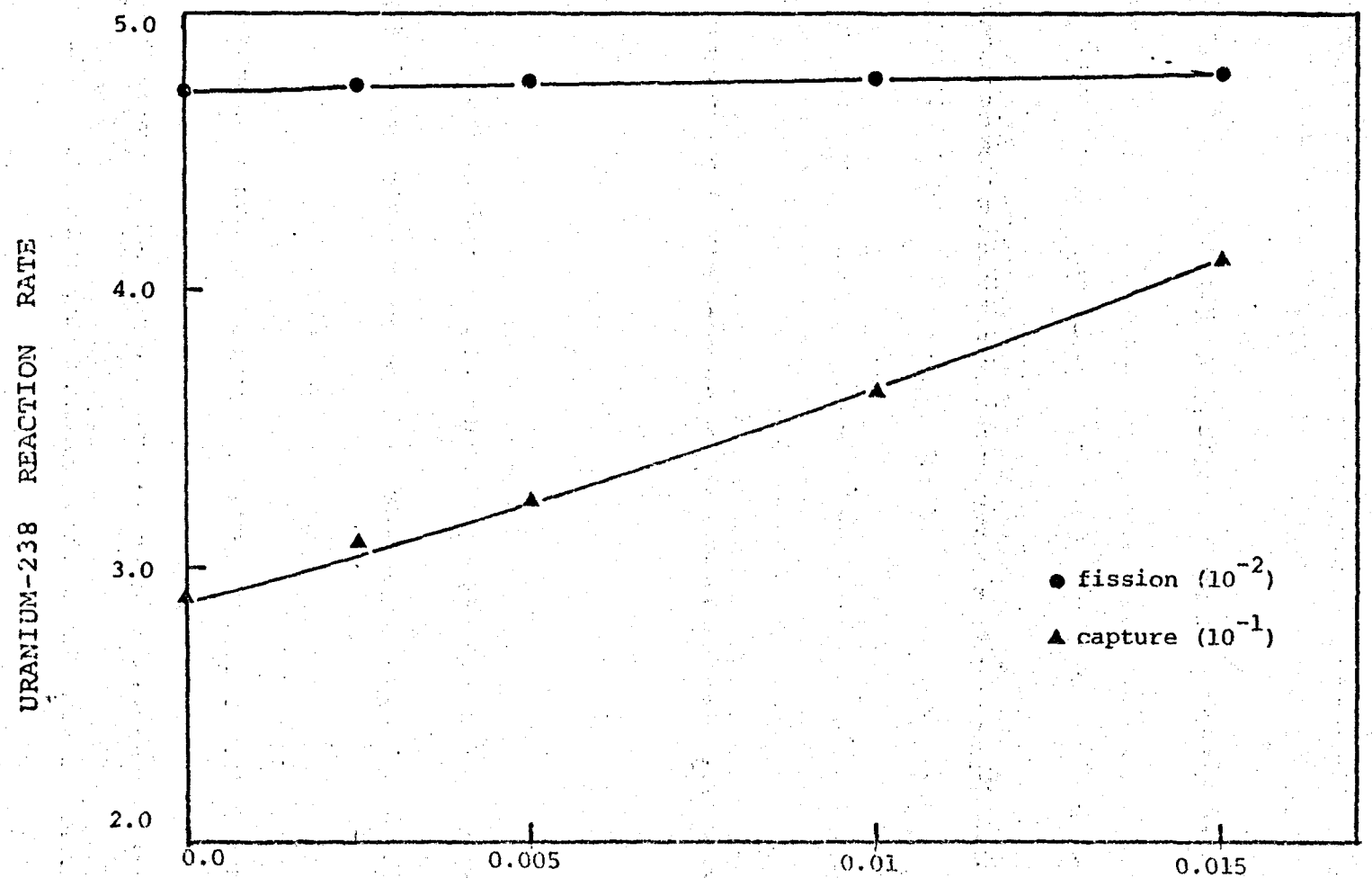

FIG 8.2.2

URANIUM-238 REACTION RATE vs. MODERATOR VOLUME RATIO

FOR THE PIN OD=10.50mm AT CORE ZONE.

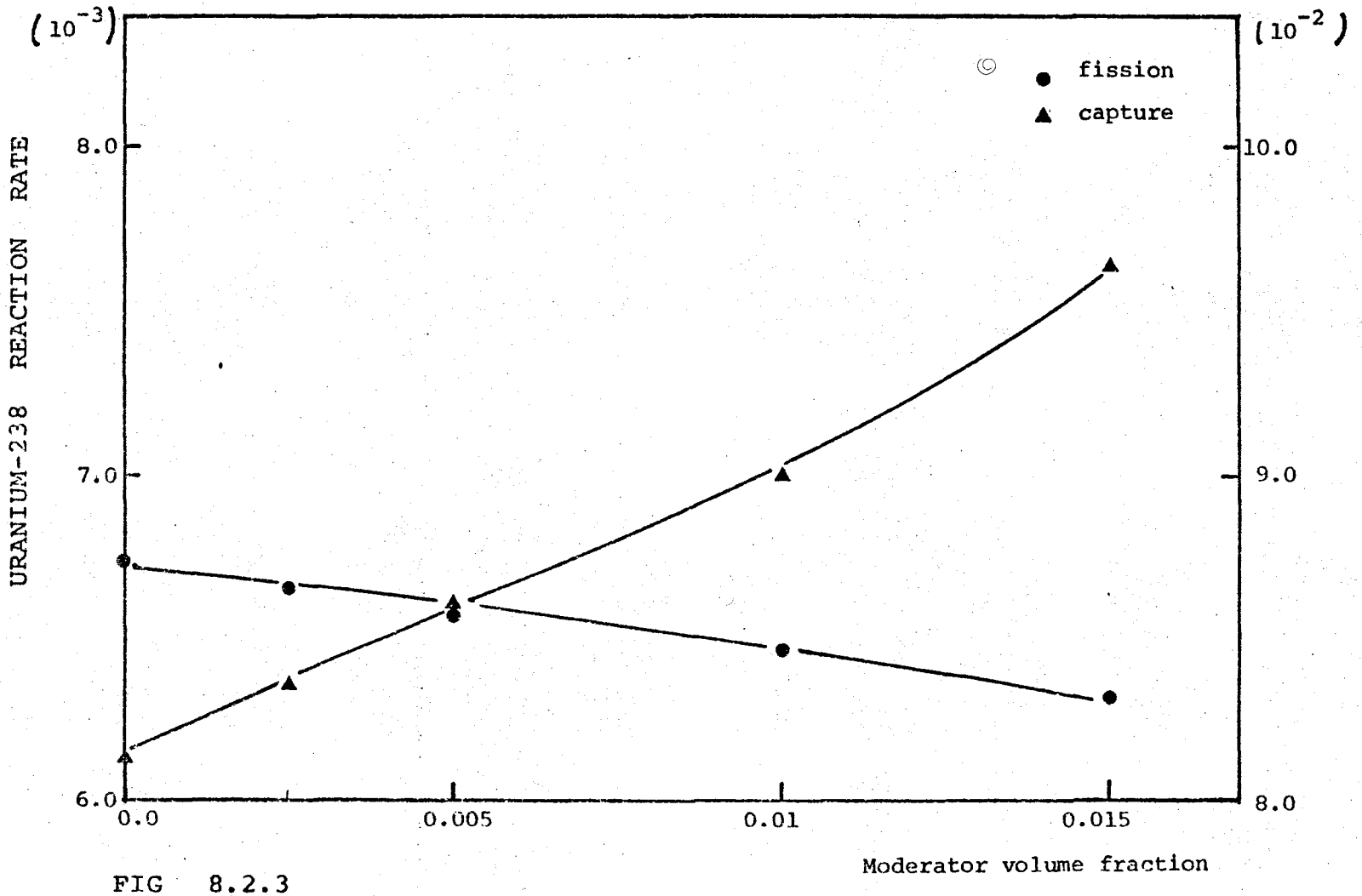

FIG 8.2.3

URANIUM-238 REACTION RATE vs. MODERATOR VOLUME FRACTION FOR THE PIN OD=10.50 mm AT INTERNAL BLANKET ZONE.

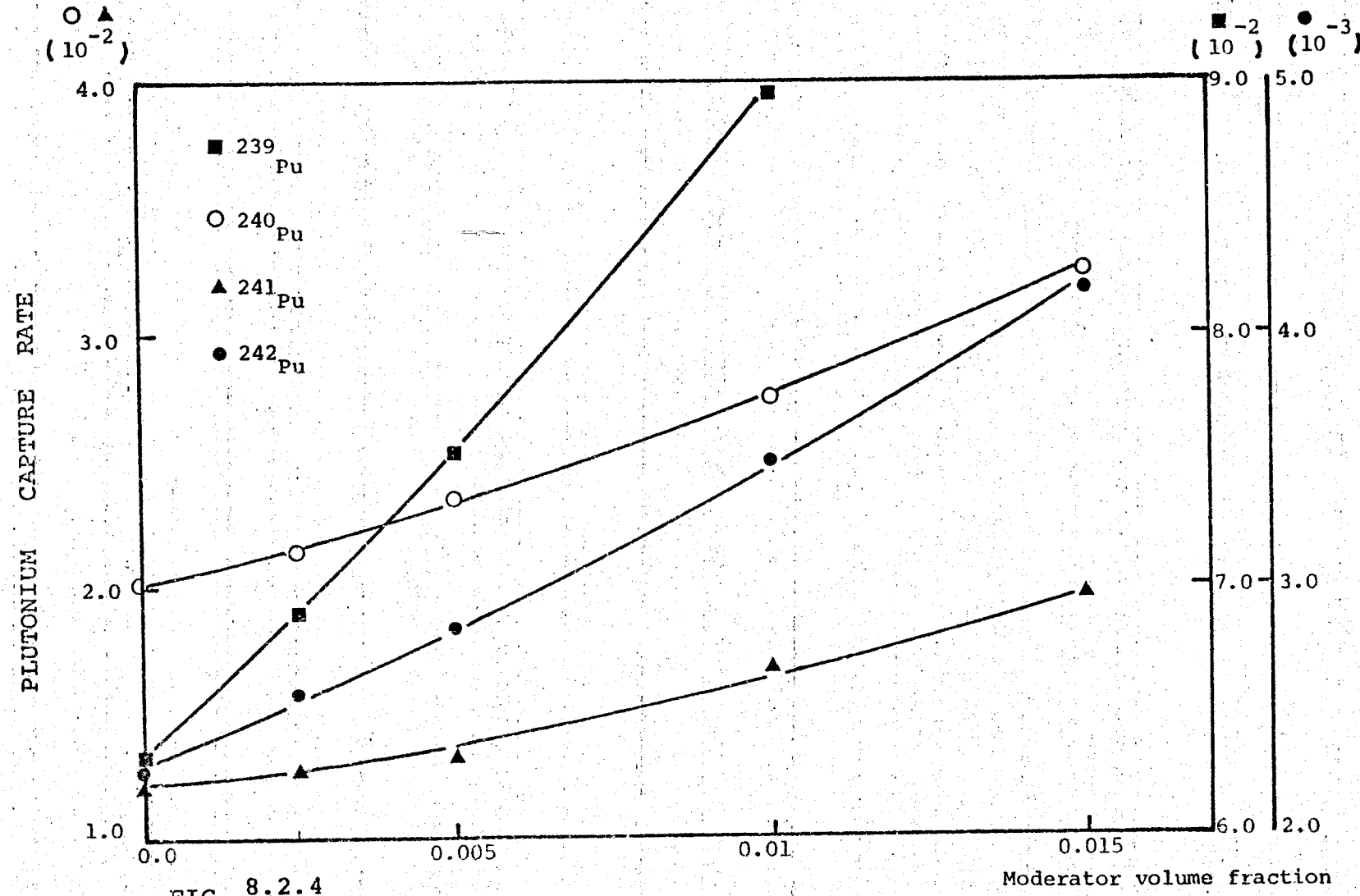

FIG 8.2.4

PLUTONIUM CAPTURE RATE vs. MODERATOR VOLUME FRACTION

FOR PIN OD=10.50 mm .

CHAPTER 9

CONCLUSIONS

In the preceding chapters a variety of specific conclusions have been reached concerning the breeding performance of the several fast breeder core configurations.

A major conclusions of this work are summarized below:

1 - Oxide Fueled Homogeneous Reactor

Calculations were performed to verify the effect of the several basic parameters on breeding ratio. The reactor doubling time and breeding ratio of the modified cores were compared with those of the reference reactor (based on Super Phenix design) and we can conclude:

- The blanket thickness effect on breeding ratio was identified until an increase of 2 rows of fertile assemblies in the reference radial blanket. Further increase in thickness causes negligible changes.

- Cladding thickness change from 0.70 to 0.40 mm resulted in a considerable improvement in doubling time, achieving a value of 20 years that corresponds a reduction of 33% .

- Increasing fuel density from 85 to 90 %TD for the thin cladding case , the doubling time reduced from 20 to 19 years.

From these results it is concluded that, among design parameters considered, the cladding thickness change induces the most impacts on doubling time in consequence of the fuel volume fraction increase.

2 - Carbide Fueled Homogeneous Reactor

Comparisons between oxide and carbide fuels show that the breeding performance is improved significantly for carbide fuel. With this fuel a breeding ratio of 1.49 and reactor doubling time of 11.8 years are achieved while the best oxide values are 1.27 and 19 years respectively .

In regard to safety parameters, carbide fueled homogeneous reactor presents a high pisitive sodium void reactivity ($8.0). Thus to make good use of the carbide fuel breeding performance ensuring a low positive sodium void reactivity a heterogeneous configurations are favorably recommended.

3 - Carbide Fueled Heterogeneous Reactor

Among the heterogeneous configurations analyzed the loosely coupled core presents a lower sodium

void reactivity (case (2-2)) without penalizing the breeding performance. For this case the doubling time achieved was 13.0 years and maximum sodium void reactivity is approximately $2.90 .

Finally collecting the results from the core design studies performed to improve the reactor doubling time, we shall find a relation between reactor doubling time (RDT) and core configuration as listed in Table 9.1 .

The carbide fuel in fast breeder reactor offers the promise of significant improvement in the reactor performance. But in order to evaluate the future potential of carbide, the characteristics of this fuel must be investigated in depth and the several problems listed in Chapter 7 must be overcome. Because of the lack of experience with carbide fuel an accelerated testing program is required.

TABLE 9.1

REACTOR DOUBLING TIME vs. CORE DESIGN PARAMETERS

Parameters \ RDT (year)	Reference reactor 30	30	25	19	15	13	12
Sodium void reactivity	High	Low	High	High	High	Low	High
Fuel	$(Pu,U)O_2$	$(PU,U)O_2$	$(Pu,U)O_2$	$(Pu,U)O_2$	(Pu,U)C	(Pu,U)C	(Pu,U)C
Configuration	Homog.	Heterog.	Homog.	Homog,	Homog.	Heterog.	Homog.
Fuel pellet diameter (mm)	7.00	7.00	7.00	7.00	9.00	9.00	9.00
Cladding thickness (mm)	0.70	0.70	0.70	0.40	0.70	0.45	0.45
Fuel density (%TD)	85	85	85	90	85	85	85
Blanket thickness	reference (Fig.5.2.2)	reference	1.33 times reference	reference	reference	reference	reference

REFERENCES

1. " World Energy Resources 1985 - 2020. Nuclear Resources ", the fuel report to the Conservation Commission of the World Energy Conference- 1977.

2. " Uranium Resources, Production and Demand ", a joint report by the OECD Nuclear Energy Agency and the International Atomic Energy Agency, December-1979.

3. " Nuclear Fuel Cycle Requirements and Supply Considerations, Through the Long-term",OECD Nuclear Energy Agency, February- 1978.

4. Nuclear Engineering International, vol. 25, 307 December- 1980.

5. " Energy: Global Prospects, 1985-2000", report of the Workshop on Alternative Energy Strategies (WASS), Mac Graw-Hill Book Companhy, 1977 .

6. MIIDA, J. et al., "Nuclear Power Programmes and Medium-Term Projections in the OECD Area", IAEA. Proceeding of the International Conference on Nuclear Power and its Fuel Cycle, held in Salzburg,Austria, 2-13 May 1977, Vienna

7. RAHLBERG, R.C., " Alternative cycle and Fast Breeders, a Look of the Future". Nuclear Engineering International, vol. 24, 292 , November - 1979 .

8. BANERJEE, S. and TAMM, H. , "Uranium Requirements for Fuel Cycles in Expanding Nuclear Power Systems". Trans. Amer. Nucl. Soc. , vol. 26, 1977 .

9. LEPINE, J. and MUGNIOT, J.C. , " Uranium Requirements and Fast Breeder Reactors". BNES.

Proceeding of the Conference on the Optimization of Sodium Cooled Fast Reactor, London, November 28, 1977 .

10. HAFELE , W. et al., " Fusion and Fission Fast Breeder Reactors", International Institute for Applied System Analysis, RR-77-8, 1978 .

11. Nuclar Engineering International , vol. 25 , 302, July/August 1980- Supplement .

12. " Status and Prospects of Thermal Breeding Preliminary Report", IAEA Proceeding on the International Conference on Nuclear Power and its Fuel Cycle, held in Salzburg, Austria, 2-13 May- 1977.

13. " La Centrale à Neutrons Rápides de Creys-Malville (Super-Phénix)". Bulletin d' Informations Scientifiques et Techniques - Commissariat a l' Énergie Atomique, 227, Janvier-Fevrier - 1978 .

14. MORILLE, J.M. et al., " Physics and Safety Aspects of Preliminary SNR-2 Core Design", BNES. Proceeding of the Conference on the Optimization of Sodium Cooled Fast Reactors, London, November 28, 1977

15. GATLY, J.A. and BRUNDLEY, K.W. , " CDTR Fuel Design Optimization ", BNES. Ibid.

16. IKAWA, K., " Two Dimensional Multigroup Diffusion Burnup Code APOLLO for Fast Breeder Long Term Burnup Analysis ". JAERI-M- 5886 , 1974 (In Japanese) .

17. IKAWA,K., "ANDROMEDA, a One-Dimensional Diffusion Theory Burnup Code ". JAERI-M- 4808 , 1972

18. HARDIE, R.W. et al., " A Comprehensive Expression for the Doubling Time of Fast Breeder Reactors".
Nuclear Technology, vol. 26 , May - 1975 .

19. BARTHOLD , W.P. and CHANG , Y.I. , " Breeding Ratio and Doubling Time Definitions used for Advanced Fuels Performance Characterization".
Trans. Amer. Nucl. Soc., vol. 26 , 1977 .

20. WYCKOFF, H.L. and GREEBLER , P. ," Definitions of Breeding Ratio and Doubling Time ".
Nuclar Technology, vol.21 , March - 1974 .

21. 三木良平 "高速増殖炉", 日刊工業新聞社 1972.

22. KONOMURA, M., Department of Nuclear Engineering, University of Tokyo. Master Thesis - 1980 (In Japanese).

23. MIYAMOTO, Y., " Temperature Analysis for the Fuel Subassembly of Sodium Cooled FBR (code FATEC- 2ROD)".
JAERI-M- 5119 , 1973

24. Tang ,Y.S. et al. , " Thermal Analysis of Liquid Metal Fast Breeder Reactors ".
American Nuclear Society - 1977 .

25. GOLDEN , G.H. et al., " Thermophysical Properties of Sodium".
ANL- 7323 - 1967 .

26. KOMATSU, I. et al., " A Study of the Breeding Characteristics of Fast Breeder Reactor ".
SJ 201-7517 , 1975 . (In Japanese)

27. TURSKY , R.B. and BARTHOLD, W.P. ," Optimum Pin Diameter for 1200 MWe Oxide LMFBRs using VW316SS as Structural Material ".
Trans. Amer. Nucl. Soc., vol.23, 1976 .

28. ORECHWA , Y. , et al. , "Pin Diameter Optimization in 1200 MWe Heterogeneous vs Homogeneous LMFBRs". Trans. Amer. Nucl.Soc., vol 26. 1977 .

29. DRISCOLL, J.A. et al. , " Safety and Breeding-Related Aspects of Fast Reactor Core ". CONF 761001 , 1976 .

30. NASER , J.A. et al., " LMFBR Heterogneous Core with Axial Internal Blankets ". Trans. Amer. Nucl.Soc., vol. 26 , 1977 .

31. SEHGAL ,B.R. et al., " Low Sodium Void Coefficient LMFBR Cores ". CONF 761001 - 1976 .

32. BAILEY ,H,S. and LU ,Y.S., " Nuclear Performance of LMFBR Designed to preclude Energetic HCDA". Trans. Amer. Nucl. Soc., vol. 26 , 1977 .

33. WEHMAN ,U. ," Safety Aspects in Nuclear Core Design of LMFBR ", CONF 701001 - 1977 .

34. CAMPBELL, G. ," Studies of Low Sodium Void Reactivity Cores ". NEARCP -A- 302 . - 1977

35. HUMMEL , H.H. and OKRENT, D. , " Reactivity Coefficients in large Fast Power Reactors". American Nuclear Society, Hindsdale , Illinois 1970.

36. KUMMER, K. and THUMMLER,F., " Carbide Fuel for Fast Breeder Reactors" . KFK - 1111 - 1969 .

37. " Carbide Fuel Development ". United State Atomic Energy Commission - NDA-2140-2 , 1959 .

38. HORST, K.M. and HUTCHINS, B.A. , " Comparative Study of PuC-UC and PuO_2_UO_2 as Fast Reactor Fuel". GEAP-3880 (Part I) - 1962 .

39. HANDA, M. ," Strategies in Development of Advanced Fuels for LMFBR". JAERI-M- 6851 , 1976 (In Japanese) .

40. LALLEMET , R. et al., " Carbide Fuel Element for Fast Reactors - Research and Development Program ". Trans. Amer. Nucl. Soc., vol.20 - 1975 .

41. STRATTON ,K.W. and BISCHOFF, K. , " The Mixed Carbide Fuel Program at EIR ". Trans. Amer. Nucl.Soc., vol.20 - 1975.

42. STRASSER ,A. and MONTEGOMERY ,M., " Carbide Fuel Development - A summary Report". Trans. Amer. Nucl Soc., vol.16 - 1973 .

43. KARSTEN ,G., " Strategy, Desing basis and Results of the Carbide Program for SNR". Nuclear Techonology , vol. 28 , February - 1976 .

44. VITII ,J.A. et al. , " Design of Prototype Carbide Subassemblies and an evaluation of Proof-Testing Plan in the FFTF ". Nuclear Technology , vol.26 , August - 1975 .

45. DIENST ,W. et al. ," Advances in Carbide Fuel Element Development for Application to Fst Reactors". IAEA. Proceeding of the International Conference on Nuclear Power and its Fuel Cycle , held in Salzburg, Austria, May-2-13 , 1977 .

46. BLANK, H. et al., " Behaviour of Advanced Fast Breeder Fuel at High Power Density ". Ibid , vol 3.

47. BOARD, J. et al., " Optimization and Analysis of Factors Influencing the Performance of Carbide Fuels". IAEA.
Proceeding of Symposium on Fuel and Fuel Elements for Fast Reactors , held in Brussels , 1973.

48. TZANOS, C.P. , and BARTHOLD. W.P. , " Design Considerations for Large Heterogeneous Liquid Metal Fast Breeder Reactors ".
Nuclear Technology, vol. 36, Mid-December 1977

49. CABRILLAT, J.C., " Optimization des Cours Rapides de Puissance de Type Heterogene radial: Etudes Parametriques".
IAEA-SM-244/26 1977 .

50. JEYU.,J. et al. ," Études Neutroniques de Cours de 1500 MWe Incident du Conteste Economique et Energètique". Colloque International sur la Physique des Reacteurs à Neutrons Ràpides - 1977 (IAEA/SM - 244/15) .

51. BARTHOLD, W.P. and BEITEL ,J.C. , " Performance Characteristics of Homogeneous versus Heterogeneous Liquid Metal Fast Breeder Reactors ".
Nuclear Technology , vol.44 , June - 1979 .

52. Su ,S.F. et al . , " Configuation Optimization of High Performance 1000 MWe Oxide Heterogeneous Core" .
Trans. Amer. Nucl. Soc., vol.34 , June 1980.

53. BARTHOLD , W.P. et al ., " Potential and Limitations of the Heterogeneous Reactor Concept".
NEACRP -L- 182 , 1977 .

54. LINEBERRY , M.J. et al., " Physics Study of a Heterogeneous Liquid- Metal Fast Breeder Reactor".
Nuclear Technology , vol.44 , June 1979 .

55. BOUGET ,Y.H. et al., " Physics Performances of Heterogeneous Fast Reactor Concept Studied in Masurca".
Nuclear Technology , vol. 36 , Mid- December ,1977 .

56. SHIH ,T.A. and TEMME ,M.I. ," An SAS3D Analysis of Unprotected Loss-of-Flow Transients for 1200 MWe Liquid-Metal Fast Breeder Reactor Homogeneous and Heterogeneous Core Design".
Nuclear Technology . vol.44, Mid-December-1978 .

57. CABRILLAT ,J.C.," Preliminary Neutronic Studies of the Compatibility Problem between Heterogeneous and Homogeneous Core ".
NEACRP-A- 429, Septermber 1980.

58. International Meeting on Fast Reactor Safety and Related Physics - Chicago- Illinois
October 5-8 - 1976 .

59. Colloque International sur la Physique des Reacteurs a Neutrons Rapides -Aix-in-Provence - FRance - 24-28 Septembre - 1979 .

60. International Conference on the Optimization of Sodium Cooled Fast Reactors British Nuclear Energy Society- London November 28 - 1977 .

61. NEACRP - Annual Meeting - Idaho - Sptember 22-24, 1980 .

62. " Present Status and Future Prospect on R & D on Carbide and Nitride Fuel ". Journal of Japan Atomic Energy Society, vol. 16 1974 (In Japanese).

63. " Lectures on Fast Reactor " - Karl Witz

64. Lamarsh, J.R. , " Introduction to Nuclear Reactor Theory ". Addison-Wesley Publishing Companhy.Inc., 1972.

65. Sayles,C.W. et al.," The Effect of Fuel Rod Diameter on the Doubling Time for Sodium-Bonded-Mixed-Carbide Fueled LMFBR". Trans.Amer. Nucl.Soc., vol.21, -1975

66. Orechwa,Y. et al., " Breeding Potential of 2000 MWe LMFBRs using Carbide and Nitride Fuel". Trans. Amer. Nucl. Soc.,vol 21 - 1975.

67. Noys,R.C. et al., " Optimum Pin Diameter for LMFBR Carbide Fuels". Nuclear Technology, vol.26- August 1975.

ACKNOWLEDGEMENTS

The author wishes to express her sincere gratitude to Prof. Shigehiro An for his excellent guindace and encouragement through out the course of present study. She is also very much indebted to Prof. Yasumasa Togo, Ass. Prof. Yoshiaki Oka and Ass. Prof. Shunsuke Kondo for many valuable advices and suggestions on various occasions.

She acknowledges the pacience of Ass.Prof. Hiroaki Wakabayashi in the correction of the manuscript. Especial thanks are due to Mr. Mamoru Konomura for the help with computer programs as well as helpful discussions.

It is a pleasure to thank her friends of the laboratory for their helps and ecouragement during her stay at the laboratory , especially to Miss Tomoko Tokunaga and Miss Yukiko Nakata.

Finally her gratitude is extended to all those who permitted her to execute this work and to Brazilian Nuclear Energy Commission and Istituto de Pesquisas Energeticas e Nucleares for the support and help.

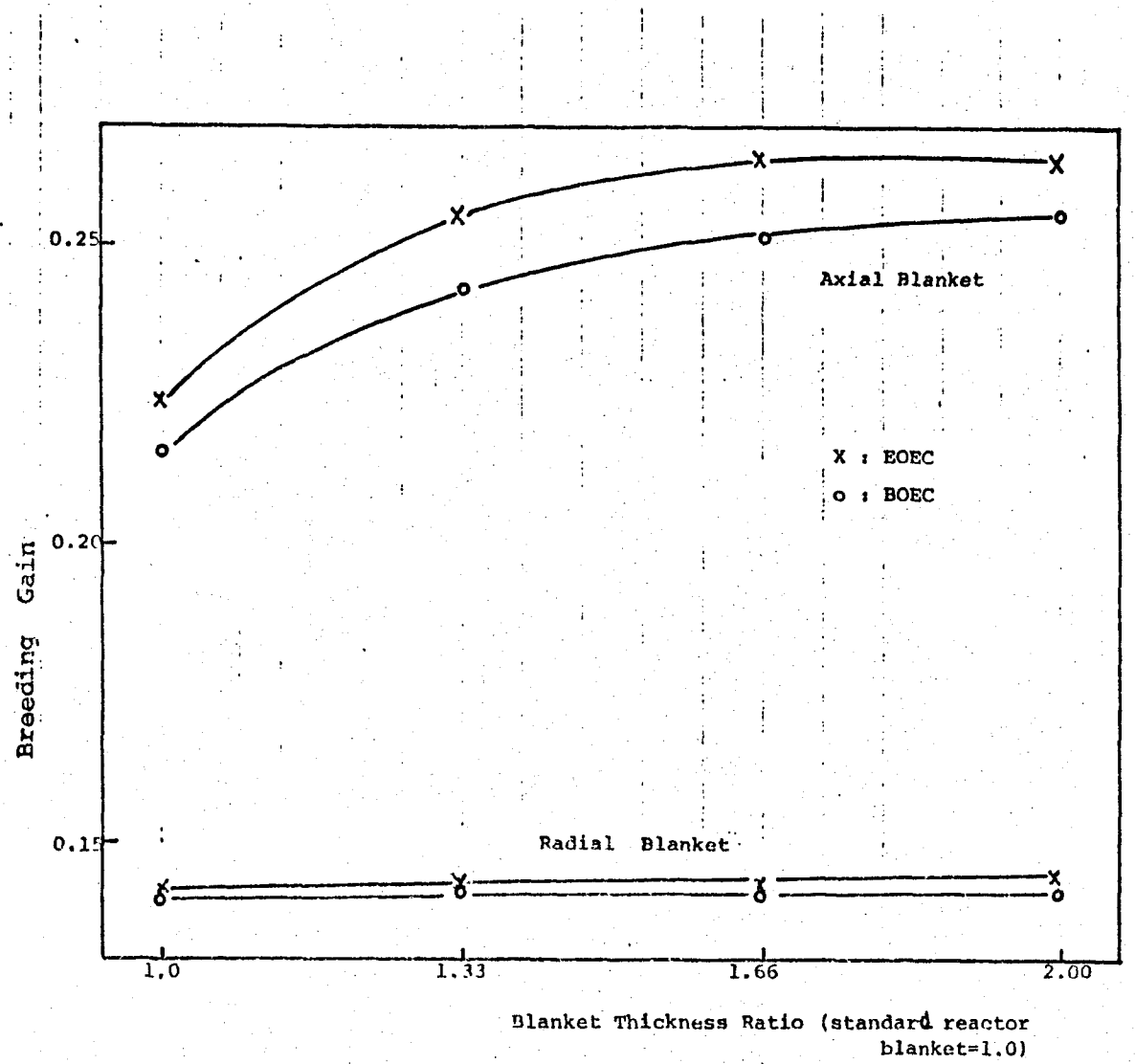

FIG 5.4.3

RADIAL AND AXIAL BREEDING GAIN CHANGE WITH BLANKET THICKNESS